

Making cultured meat in a Petri dish: optimisation of the extracellular matrix for 3D skeletal muscle tissue engineering

!CONFIDENTIAL! - MSc Thesis Project

O.R. Ibsen¹, dr. Ruud Out, dr. Duong Nguyen and prof.dr.ir. H.H. Weinans

¹MSc Biomedical Engineering | Faculty of Mechanical, Maritime and Materials Engineering (3ME)
Delft University of Technology, The Netherlands
e-mail: o.r.ibsen@student.tudelft.nl

February 2020

ABSTRACT

Context. In times where human kind is facing serious challenges due to global warming, scarcity of natural resources and inequality, to continue producing food, especially meat, as it is now done, does not seem sustainable. For people that want to continue enjoying their delicious piece of steak, the manner in which meat is sourced will need to be redesigned. One of the disruptive initiatives in this field is in vitro cultured meat. For the cultivation of muscle tissue, one needs cells, chemical factors and the appropriate biomaterials that function as a scaffold. Meatable B.V. is a food-technology startup that is a pioneer in the cultivation of steak-like meat using induced pluripotent stem cells.

Aims. The aim of the study is to optimise the extracellular matrix (i.e. scaffold) mimicry of natural biomaterials to serve as a scaffold for 3D skeletal muscle tissue engineering, using iPSCs. The supplementary aim of this study is to determine the feasibility of the optimised scaffold as a proof of concept for cultured meat.

Methods. The proof of concept model (Model A) was created in collaboration with researchers from the Loughborough University who demonstrated a scalable model for 3D human skeletal muscle tissue engineering. Their strategy was to use a hard plastic mould to confine and provide initial support for the viscoelastic hydrogel (matrigel and rat tail collagen) encapsulated with cells (C2C12 myoblasts). For the optimisation of the extracellular matrix for iPSCs for the production of cultured meat, this model was copied and repeated with different edible scaffold alternatives. The best alternative biomaterial (Model B) was further optimised in large scale tissue moulds and compared to the proof of concept model and meat. Lastly, Model C was created by seeding iPSCs in Model B. The qualitative and quantitative comparisons were based on different analytical parameters.

Results. The hydrogel scaffolds of both models A and B were highly comparable in terms of permeability, scaffold compaction by cell activity and cell alignment. The improved model (B) resulted in a higher cell proliferation as seen by cell development and cell density. The stiffness of model A was half the stiffness of Model B, and the stiffness of Model B was more comparable with the higher stiffness of beef steak (factor 5 difference). Nevertheless, when the improved model was seeded with pre-differentiated iPSCs (Model C) instead of C2C12 myoblasts, the results were clearly less successful than the first models and were not comparable with beef steak.

Conclusions. This research describes the successful improvements of an existing 3D in-vitro skeletal tissue engineering method, as prototype model for cultured meat, that was for the first time seeded with iPSCs. Model B should be set as the basis model to optimise for the culture of iPSCs. The bovine collagen model with C2C12s was not comparable to steak, but a longer culture period could result in more comparable tissue. The main reason for the limitations of Model C was the maturation of iPSCs, which could be improved in different ways. In addition, there remain certain requirements to be met for the hydrogel scaffold, mainly connected with current developments for recombinant animal-free materials. It can still be concluded that the less successful Model C was a step in the right direction to becoming a feasible model for the culture of in vitro meat.

Key words. Cultured meat – extracellular matrix – skeletal muscle tissue engineering – scaffold biomaterials – bovine collagen scaffold – C2C12 myoblasts – induced pluripotent stem cells (iPSC) – skeletal muscle physiology – bioengineering

1. Introduction

1.1. Cultured meat

Meat is a success story. Over the past decades, worldwide production and consumption has grown 4 to 5 fold. Where a stagnation in consumption can be seen in countries such as the United States of America, there is an almost exponential growth observed in China [21]. This growth is only expected to continue, in line with the growth in human population. That people find meat delicious and healthy contributes to its deep embedding in various cultures. However, the agriculture and meat industry is facing some enormous challenges.

One third of arable land is used to feed and raise livestock [33]. One kilogram of beef requires 15.000 litres of water [28]. And on top of that 15% of the total greenhouse gas emission is caused by livestock farming [35]. Usable arable land is shrinking due to the effects of global warming and the increasing growth of cities, and a sacrifice of valuable natural habitats is following [53]. Human kind depends on planet earth's resilience, but underestimate this in the manner in which natural resources and biodiversity are managed.

The industrialisation of livestock produces an enormous output of food for the world. However, the manner in which animals are bred, kept and fed, has serious downsides for these animals,

as well as for humankind. More than 70% of all antibiotics are used for livestock, which impacts on human health by increasing the risk of human antibiotic resistance [23]. Scandals in the intensive animal farming industry enforce the debate on moral and ethical issues of intensive animal farming, which is gaining a higher priority on different political agendas.

In times where humankind is facing serious challenges due to global warming, scarcity of natural resources and inequality, to continue producing food, especially meat, as it is now done, does not seem sustainable. Switching to a plant or insect based diet can be regarded as one solution. It does however seem that people want to continue enjoying their delicious piece of lamb rack or steak [58]. To still the world's growing appetite for meat will be a challenge. It follows that there is a need to redesign the way in which meat is sourced. The steak is the end goal, but the process that currently takes place to provide this does not necessarily need to be the starting point. A disruption in the conventional food sector is needed. New technology can provide this.

In 2013, the first lab-grown burger was presented in London by the Dutch professor Mark Post [29]. Satellite cells were isolated from a cow and turned into strips of muscle tissue to form a burger through skeletal muscle tissue engineering. This type of engineering aims to replicate the structure and function of muscles in vitro and in vivo, to create models and functional constructs. These techniques are being used in regenerative medicine for the treatment of, for instance, Volumetric Muscle Loss or cardiac repair. In addition, the techniques are used as a model for 3D drug testing, and the modelling of muscle tissue to replace malfunctioning animal models for the understanding of phenotype and therapeutic screening of muscle related diseases (e.g. Duchenne muscular dystrophy, Type II Diabetes, Pompe disease, and Dysferlinopathy) [65]. The reason that similar techniques are being explored by different food-tech startups is that in vitro cultured meat may offer a more animal friendly and sustainable alternative to the conventional meat industry. Regenerative medicine study groups have presented different techniques of engineering three-dimensional muscle tissue, but many hurdles still remain. For the cultivation of muscle tissue, one needs cells, chemical factors in a medium and the appropriate biomaterials that function as a scaffold [6].

1.2. Native skeletal muscle tissue

The first stage of mammalian cell development starts with the fusion of a sperm and an oocyte, called a zygote. From this moment on, the fused cell will proliferate (multiply) and differentiate (change) in numerous ways to eventually form an organism (e.g. muscle tissue).

The stages that a cell goes through can be divided in terms of potency, meaning the potential for differentiation into different cell types. Since this potential diminishes along the way, it has an impact on the usefulness for cell strategies. The different stages, from zygote to muscle cell, are; totipotent, pluripotent, multipotent, oligopotent, and unipotent.

Totipotent stem cells, zygotes, are stem cells that can differentiate into embryonic and extraembryonic cell types. These cells are the fundamentals and origins of a total organism. The zygote will first divide through mitosis into a morula. Once the morula forms a cavity inside, it is called a blastocyst. Blastocysts are **pluripotent**, they are highly potent and can thus differentiate into nearly all cells, and have almost unlimited proliferation and self-renewal capacity. They have a high level of self-renewal. The blastocysts' inner cell mass consists of a primitive endo-

derm which forms the cavity in which the embryo will grow, and the epiblast will develop into the three germ layers; endoderm, mesoderm and ectoderm, forming the embryo itself.

The three germ layers are **multipotent** stem cells. They can thus differentiate into a number of cell types that are part of the cell family, and have limited self-renewal capacities. For the mesoderm, this can be the progenitors for cardiac muscle cells, kidney cells, red blood cells, smooth muscle cells, and skeletal muscle cells. The mesoderm differentiates for example into multipotent Mesenchymal Stem Cells, and multipotent Myosatellite (or satellite) cells. Multipotent stem cells differentiate into **oligopotent** cells which can only differentiate into a few cell types. And these will eventually differentiate into **unipotent** cells. Unipotent stem cells can only differentiate into one cell type and have limited proliferation capacity. For myocytes, the unipotent stem cell (or progenitor cells) are myoblasts, as can be seen in Figure 1. These myoblasts proliferate and start fusing to form myocytes (primary fusion). These myocytes become, as a result of secondary fusion, myotubes. And eventually, these will fuse into mature muscle fibre bundles. [59, 8]

Cells express sets of muscle-specific proteins at the different stages of muscle development, as can be seen in Figure 1. At the early stage of the muscle cell development, Desmin and MyoD are expressed. Desmin integrates the sarcolemma and nuclear membrane. MyoD, or myoblast determination protein 1, marks myoblast commitment. Whereas myogenin (MYOG) is expressed in later stages, and Myosin Heavy Chain only appears in the end phase when muscle fibres are formed. During early development, muscle cells are single nucleated. When myoblasts start fusing they form multi-nucleated skeletal muscle fibres. [17]

Mature skeletal muscle tissue consists of skeletal muscle fibres, blood vessels, nerve fibres, fat, and connective tissue (i.e. extracellular matrix). Human skeletal muscle fibres have a diameter up to 100 μm and a length up to 30 cm (musculus sartorius), and myoblasts have an average diameter size ranging from 15 μm to 45 μm , mostly from 20 μm to 30 μm [63, 67]. Not all skeletal muscle tissue is prevascularized, but the maximum distance that tissue should be from nutrient sources is 150-200 μm [37]. Nerves provide electrical pulses for muscle fibre contraction, which enhances muscle hypertrophy. When muscle tissue is decellularized, the anisotropic tubular structure of the extracellular matrix becomes visible. This structure is extremely important for muscle functioning, mechanical support, dynamic signalling for muscle development, homeostasis, and regeneration. According to Freed et al. the average pore porosity of the skeletal muscle ECM is 90% [26]. Pore architecture concerns the form and interconnectivity of the pores [25, 26]. The size of ECM pores is between 50 – 200 μm [40].

The native skeletal muscle ECM, deposited by fibroblasts, consists of different macromolecules that play key roles in the structure and function. The three main groups are fibrous ECM proteins (collagen, elastin, fibronectin, and laminin), proteoglycans (PGs), and glycosaminoglycans (GAGs) [27]. Collagen is one of the most abundant (30%) ECM proteins in muscle skeletal tissue. It provides strength and resiliency, it regulates cell adhesion, chemotaxis, and migration, and it guides tissue development. Collagen fibres are often a mix of different types, where type I is often the most abundant. [24, 57]

The maintenance and regeneration process of skeletal muscle tissue mainly involves three types of cells; stem cells, muscular

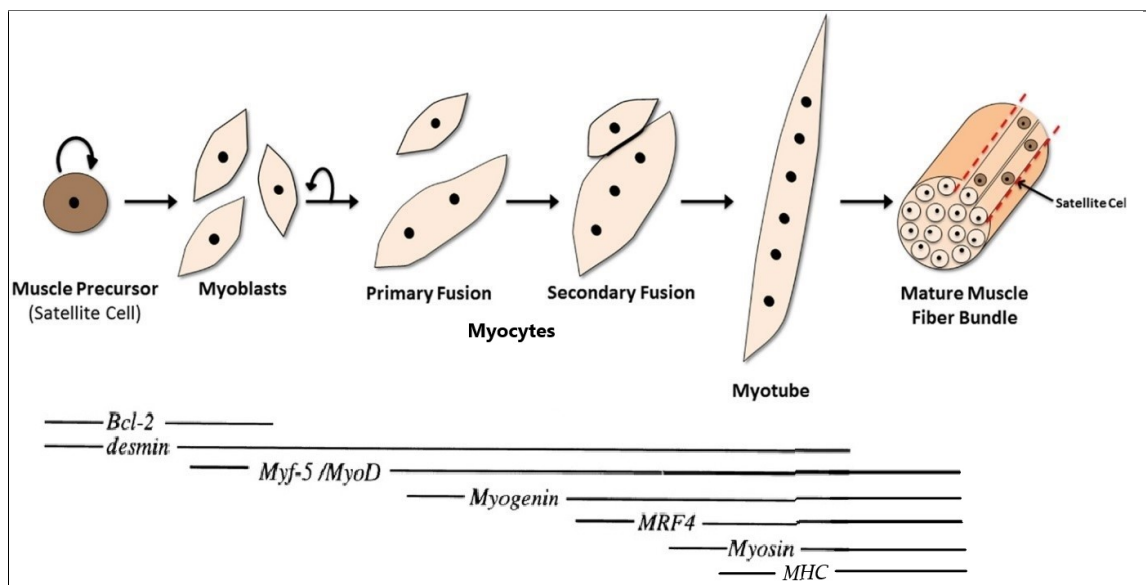


Fig. 1: **Mammalian skeletal Myogenesis** - For the formation of muscle tissue, the population of precursor cells (satellite cells) start proliferating, and differentiate into myoblasts. These myoblasts proliferate and start fusing to form myocytes (primary fusion). These myocytes become, as a result of secondary fusion, myotubes. And eventually, these will fuse into mature muscle fibre bundles. Cells express different defined sets of muscle-specific proteins (e.g. Desmin, MyoD, MyoGenin) at the different stages of muscle development. (Adjusted and compiled from Musaro et al. Figure 6 [44], Dominov et al. Figure 5 [17], and Enwere et al. Figure 1 [20].)

tissue pericytes, and fibro/adipogenic progenitors. The combination of these cells is fundamental for a continuous renewal of daily damaged skeletal muscle tissue. The repair and regeneration of skeletal muscle tissue occurs in a pattern of three main phases, regardless of the severity or kind of injury. Due to the complexity of multiple interactions between different cell types, the entire process is not yet fully understood, but is normally divided into the destruction, repair and remodelling phases [14].

1.3. Cell strategies for cultured meat

Cultured meat strategies harness the use of progenitor cells in combination with ECM like materials. Different strategies exist with regard to the cells used for 3D skeletal muscle tissue engineering. This is due to the different phases of native cell development before forming muscle tissue, as previously described.

For skeletal muscle tissue engineering, the selection of the appropriate cellular source is of high importance for the generation of muscle tissue in vitro. There are, according to a literature data research by Beldjilali et al., four types of cells predominantly used in muscle tissue engineering; myoblasts (C2C12, an immortalised mouse myoblast cell line that easily differentiates and proliferates), primary satellite cells, primary myoblasts, and mesenchymal stem cells [6]. C2C12 myoblasts Satellite cells are easy to isolate and are the direct precursors of myoblasts, but have shown difficulties in proliferation capacity in vitro [37]. They seem to lose their potential for self-renewal and differentiation when transferred to in vitro settings.

In 2006, a milestone in biomedical research was reached due to the discovery of induced pluripotent stem cells (iPSCs). iPSCs are pluripotent cells that can be directly generated from adult cells using the right transcription factors [48]. The enormous benefit of using iPSC is that they can almost unlimitedly self-renew and differentiate into practically all types of cells [38]. In other words, with one correctly induced batch of iPSCs obtained by a biopsy, it is theoretically possible to cultivate skeletal muscle tissue in vitro unlimitedly.

1.4. Biomaterial strategies as scaffold for cultured meat

Cells will only form tissue when they are in the appropriate scaffold [46]. A scaffold is defined as three-dimensional solid biomaterial that mimics the native extracellular matrix, therefore playing a crucial role in tissue regeneration.

There are five important properties one should be aware of when engineering a scaffold; architecture, biocompatibility, biodegradability, bioactivity, and mechanical properties.

Architecture: A porous structure is needed for proper nutrient and waste transport since a majority of the tissue is not pre-vascularized. The main factors that affect these transports are porosity, pore architecture, and tissue thickness. Hence, high permeability facilitates the inflow of nutrients and outflow of waste particles. Porosity is a measure of the construct's total 'empty' volume, that is normally occupied by cells or liquid, and allows the flow and migration of both. Pore architecture concerns the form and interconnectivity of the pores, where the ideal size of pores should be between 50 – 200 μm with a porosity of 90% [25, 26, 40]. When scaffolds are filled with cells, cells have a low viability when distanced more than 150-200 μm from the nutrient source [37].

The architecture of the ECM not only influences the nutrient diffusion and waste removal, but also plays an important role in cell migration [37]. The ECM of functional skeletal muscle tissue is highly orientated. In 1997, Curtis Wilkinson presented the "Cell guidance theory" in which they demonstrated that microgrooved matrices with a parallel micropattern provoke parallel aligned cell growth along the pattern of the scaffold [15]. This parallel alignment of the skeletal muscle tissue is necessary for effective muscle contraction and force-generation along a longitudinal axis. Collagen forms triple helical structures, where elastin is a 1000 times more flexible than collagen and is highly cross-linked to form insoluble complex structures [70, 39]. Cells will adhere to the collagen fibres, and will deform the network, which results in compaction of the hydrogel [9]. If this compaction is controlled by a static constraint in a certain direc-

tion, the gel will deform differently in the constrained and in the unconstrained axis. The result of a certain constraint is an anisotropic tissue with cells and collagen fibres aligned in the constrained axis [9]. Recent studies have shown different strategies to mimic the native muscle myotube alignment structure [71]. Parallel linear microchannels can be constructed, as well as nano and micro-patterning of the scaffold [64].

Biocompatibility: The scaffold has to be non-cytotoxic to the cells, and should not induce an inflammatory response [46]. Biocompatibility has an additional meaning in cultured meat development which is edibility. The engineered scaffold can be replaced by the right cells with native ECM, but residues may remain. [56]

Biodegradability: Ideally, the scaffold should provide physical support for the cells to attach and organize themselves during the first stages of tissue formation. Once this is done, certain cells will extrude a new extracellular matrix. This process can gradually replace the engineered scaffold by a newly formed tissue, but this is dependent on the cells (fibroblasts) and the scaffold that is used. Consequently the material should ideally remain during the first stages, but dissolve when the cells take over. The scaffold by-products should also be biocompatible [56]. If needed, scaffolds can be modified to control these degradation rates, using techniques such as irradiation or oxidation of the material.

Bioactivity: The scaffold needs to facilitate interactions with cellular components and cell adhesion for proper cell proliferation, migration, differentiation, and tissue organization. The surface characteristics of the proteins inside the scaffold play an important role in this interaction. Cell-adhesive ligands, for instance, enhance attachment of cells by giving the right cues. Many different strategies can be used to enhance the bioactivity of a scaffold. [56]

Mechanical properties: The scaffold should be stiff enough to allow cell exposure to relevant mechanical forces and withstand cell contraction. It should also stay elastic enough to accommodate contractile functionality of the cells. The stiffness of scaffolds plays an important role in cell type expression, development, migration and orientation [16, 11]. The average stiffness of relaxed skeletal muscle tissue is around 10 kPa. Mechanosensitivity has been demonstrated by adjusting the stiffness of agarose gel and seeding it with mesenchymal stem cells, resulting in different differentiation tendencies [19]. As previously mentioned, static constraints on the scaffold can influence the alignment and orientation of the cells [66, 9]. For cultured meat, this alignment is of significant importance for the texture and thus taste experience [4].

In order to control the architecture, biocompatibility, biodegradability, bioactivity and mechanical properties, there are many different possibilities for materials to use for skeletal muscle tissue engineering. With different materials come different manufacturing techniques. The three main techniques are hydrogelation, electrospinning, and micropatterning [55]. Of these, hydrogelation is the most common. Hydrogels are networks of hydrophilic polymer chains that form 3D solid materials when crosslinked, see Figure 2. The gels can contain high levels of water, which provides the porosity, and can be made of natural or synthetic polymers [30]. Hydrogels can be cast into many shapes, cells can be seeded homogeneously within the gel, and the gels can obtain high mechanical compliance resembling native tissue. Moreover, the gels can be designed and altered to be, for instance, electroconductive, to have certain swelling rates, different degradation rates, et cetera. Nevertheless, fibre align-

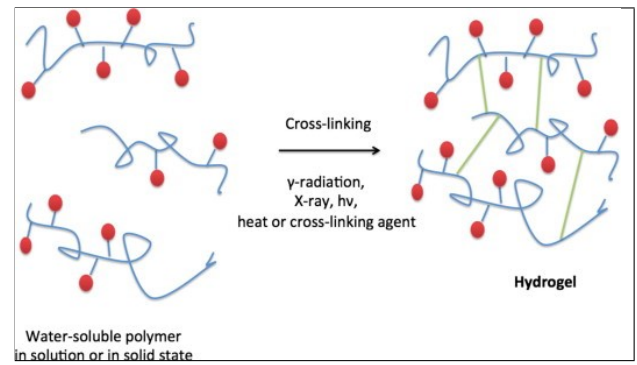


Fig. 2: **Hydrogel formation** - Hydrogels are formed by crosslinking hydrophilic polymers into a scaffold that absorbs water.

ment of myoblasts still remains a challenge in the use of hydrogels for skeletal muscle tissue engineering [60].

Many studies have analysed the different material possibilities for skeletal muscle tissue engineering to eventually imitate the key properties of the extracellular matrix, as described in the work of Fuoco et al. [27]. To date, the types of scaffolds can be divided into biological materials, synthetic materials and hybrid materials (See Appendix A for detailed overview of different scaffolds). Natural materials are popular due to their biocompatibility and close resemblance to the real extracellular matrix. On the other hand, synthetic materials show greater stability, are less expensive and easier to work with [5]. Hybrid materials are combinations of synthetic and natural polymers. Combining the best of both worlds, these composites have many advantages. Synthetic polymers help mimicking the biomechanical properties, whereas the natural polymers enhance cell adhesion and proliferation, but are only recently being studied [6]. In conclusion, the ideal scaffold for cultured meat should be designed according to the right architecture, biocompatibility (and thus edible), biodegradability, bioactivity and mechanical properties.

1.5. Meatable B.V. challenge

Meatable B.V. is a Dutch startup that wants to satisfy the world's appetite for meat without harming people, animals or the planet. They are pioneering the culture of in vitro meat by using a patented iPSC technology in collaboration with the University of Cambridge [50]. Pawlowski et al. have systematically optimized inducible gene expression in human PSCs using a dual genomic safe harbor gene-targeting strategy. This approach provides a powerful platform for the generation of human cell types by forward programming. They reported robust and deterministic reprogramming of human PSCs into neurons and functional skeletal myocytes. The same techniques have been applied to other adult mammalian (e.g. bovine) cells.

The use of iPSCs that have differentiated into myocytes (i.e. muscle cells) in a 3D scaffold for cultured meat has, to the writer's best knowledge, never been done before. These cells are extremely interesting for cultured meat since they have the potential of unlimited proliferation before differentiating into muscle cells. Theoretically, one biopsy from an animal with adult cells that has been reprogrammed into iPSCs could deliver a batch of cells which can subsequently be proliferated for unlimited mass production and be easily differentiated into muscle cells for the production of meat.

In this study, the first experiments of cultivating *in vitro* muscle tissue using iPSCs in a 3D scaffold is presented. The aim of the study was to optimise the extracellular matrix (i.e. scaffold) mimicry of natural biomaterials to serve as a scaffold for 3D skeletal muscle tissue engineering, using iPSCs as cell type. Since iPSCs have never been used for the mass production of muscle tissue for meat, a proof of concept had to be created. The proof of concept was created at Meatable B.V. in collaboration with researchers from the Loughborough University (See Appendix B for the other 3D culture setups that were tried). Capel et al. demonstrated a scalable model for 3D human skeletal muscle tissue engineering [13]. Their strategy was to use a hard plastic mould to confine and provide initial support for the viscoelastic hydrogel (matrigel and rat tail collagen) encapsulated with cells (C2C12 myoblasts). The combination of mould, hydrogel and cells will be referred to as a 'model'. Collagen is, as stated before, one of the biggest representatives in skeletal muscle tissue ECM. Beldjilali et al. already showed that collagen has successfully been used in skeletal muscle tissue engineering [6]. Collagen provides the right mechanical and architectural properties, but has low adherence properties [52]. Therefore, Matrigel, a mixture of reduced growth factor basement membrane products secreted by the ECM proteins from murine Engelbreth-Holm-Swarm tumor cells, is used in the model of Capel et al. [3]. This material enhances cellular functions such as proliferation, adhesion, migration, differentiation, and maintenance by the cell itself. Matrigel can be replaced by Geltrex when working with iPSCs (See Appendix J, Figure 26). The model of Capel et al. (Model A) served as a stepping stone towards a new model with an optimised ECM for iPSCs.

For the optimisation of the ECM for iPSCs for the production of cultured meat, the methods of Capel et al. using 50 μ L moulds have been copied and repeated with different edible scaffold alternatives. The hydrogels tested were alginate, agarose, and Novogel (See Appendix C and D). The requirements for the alternative scaffold were animal free (preferably), cheap, scalable, edible, and it should lead to a piece of muscle tissue competitive to conventional meat. The best alternative biomaterial (Model B) was further optimised in large scale tissue moulds of 500 μ L and compared to the proof of concept model (by Capel et al.). The qualitative and quantitative comparisons were based on various analytical parameters. Tissue construct thickness was analysed through microscopy. Cell development, morphology and arrangement was analysed through immunofluorescence staining and histology. Mechanical properties were obtained through rheometry and unconfined compression tests. Subsequently, the alternative optimised scaffold was, for the first time, seeded with predifferentiated iPSCs in order to culture meat (Model C). To examine the best model for the production of cultured meat, there was examined whether the optimised models (Model B and C) worked as well as, or even better than the existing model from Capel et al. (Model A).

2. Materials and Methods

2.1. The Proof of Concept model (Model A)

The proof of concept model, Model A, was created according to the work of Capel et al. [13]. In their set-up, moulds of different sizes with poles are 3D-printed. These moulds are filled with a mixture of a hydrogel scaffold and cells (C2C12 myoblasts). The scaffolds are statically cultured according to a specific protocol for several days. A description of the selected parts that were used and adapted, is given in this subsection.

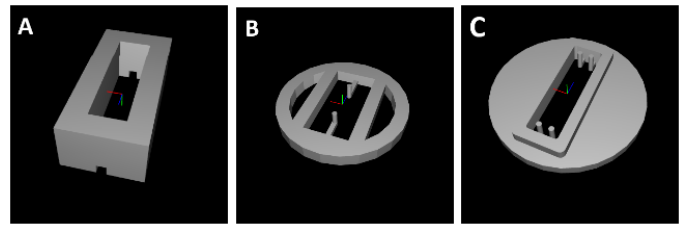


Fig. 3: **3D printed moulds for tissue engineering Model A** - A is clicked in B and forms a 50 μ L mould with one pole on each side of the mould. C is a 500 μ L mould with two poles on each side. [13]

2.1.1. Design and fabrication of 3D printed moulds

3D printing was performed by Fused Deposition Modeling with a commercially available Ultimaker 2+ system (Ultimaker, Netherlands). The designed moulds had a single (50 μ L) or twin (500 μ L) post fixed at the end of a rectangular mould, and were uploaded from the links provided in the article. The 50 μ L sized mould was assembled in 2-parts with a removable barrier (see Figure 3). The FDM parts were printed using polylactic acid and were extruded onto the standard glass build plate, at previously published settings [54]. All samples were sterilized via ultraviolet light for > 1h, prior to being adhered to culture well plates using an in-house bio-adhesive which has been found to be completely compatible [54]. Once adhered, samples were rinsed with 70% IMS and left for the remaining solvent to evaporate prior to use.

2.1.2. C2C12 2D cell culture

C2C12 skeletal muscle myoblast cells (ECACC, all below passage 10) were grown using standard growth medium (GM); composed of Dulbecco's Modified Eagle's Medium (DMEM, Fisher-Scientific, UK), 20% fetal bovine serum (FBS, Pan Biotech, UK), and, 1% Penicillin/Streptomycin (P/S, Fisher-Scientific, UK). Cells were cultured in T80 flasks (NuncTM, Fisher-Scientific, UK) and incubated in a 5% CO₂ humidified atmosphere at 37°C until 80% confluence was attained. GM was changed every 24 h during the culture period for expansion of cells.

2.1.3. Tissue engineered constructs

Collagen/Matrigel constructs were generated using C2C12 myoblasts, with the method based on previous work from Mudera et al. [42]. Hydrogels were formed, as can be read in Table 1, by the addition of 76.5% v/v type I rat tail collagen (First Link, UK; dissolved in 0.1M acetic acid, protein at 2.22mg per mL), with 8.5% v/v of 10X Minimal Essential Medium (MEM) (Gibco, UK). This solution was subsequently neutralized by the addition of 5M and 1M sodium hydroxide (NaOH) dropwise, until a color change to cirrus pink was observed. This was followed by the addition of 10% v/v Matrigel Matrix (Corning, Germany). The cells were added at a seeding density of 4×10^6 cells per mL in a 5% v/v GM solution, before being transferred to the pre-sterilized moulds to set for 10–15min at 37 °C. GM was added for 4 days and changed daily, before being changed to differentiation media (DM, DMEM, 2% Horse Serum (HS), 1% P/S) for a further 10 days in culture, as can be seen in Figure 4.

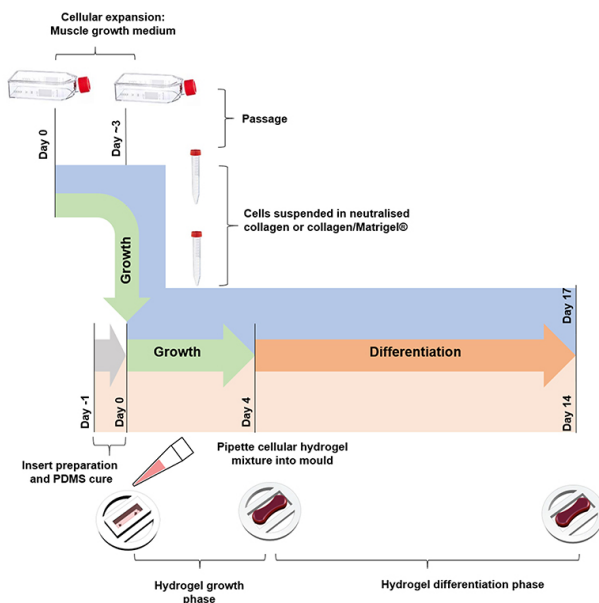


Fig. 4: **3D skeletal tissue culture model by Capel et al.** - An overview of the different steps and time span of 3D tissue culture, where cells are first proliferated in 2D, then placed in a scaffold within a mould, and then further proliferated in 3D and differentiated within the mould. [13]

Table 1: **Model A: hydrogel scaffold** - Overview of different substances that have been used to form a hydrogel scaffold to culture skeletal muscle tissue, based on rat tail collagen.

Model A - Rat tail collagen (1.7mg/mL)	
Rat tail collagen (2.22mg/mL, 0.1M Acetic Acid)	76.5%
Minimum Essential Medium (10x)	8.5%
Matrigel	10%
Cells in medium	5%
Sodium Hydroxide (NaOH)	drops

2.2. The Optimised Meatable B.V. model (Model B & C)

The Proof of Concept model (Model A) was altered and optimised into a more compatible system for meat production at Meatable B.V.. The optimised model was first seeded with C2C12 cells (Model B), and lastly seeded with iPSCs (Model C).

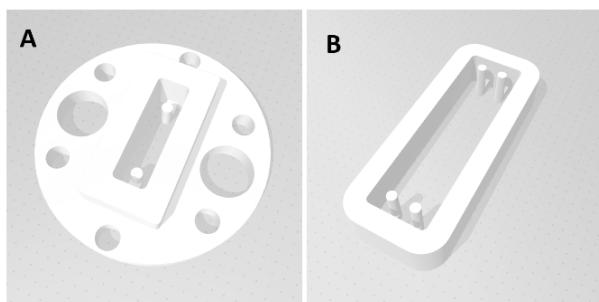


Fig. 5: **3D printed moulds for tissue engineering Model B & C** - (A) single-piece 50µL mould with one pole on each side of the mould. (B) 500µL mould with two poles on each side. [13]

2.2.1. Design and fabrication of 3D printed moulds

3D printing was performed by FDM with a commercially available Ultimaker 2+ system (Ultimaker, Netherlands). The moulds were redesigned to have a single (50 µL) or twin (500µL) post fixed at the end of a rectangular mould. In addition, this design was a single-print mould without assembling parts, where the support platform was redesigned to use less material and to fit in 6 or 12 well plates, as can be seen in Figure 5. The printable file consists of multiply moulds to increase efficiency of printing. The 3D modeling was performed using computer aided design (CAD) SolidWorks software. The moulds were printed using PLA and were extruded onto the standard glass build plate, using the settings provided by the CAD file.

All samples were sterilized via UV for > 1h, prior to being adhered to culture well plates. To adhere the moulds to the culture well plates, a thin layer of PDMS was used under sterile conditions (See Appendix E for detailed information). The PDMS was cured for at least 6 hours at 37°C, where after the plates were sprayed with 70% isopropyl alcohol and set to dry in a flow chamber. Before seeding with the hydrogel, the moulds and plates were treated with UV light for >1hr.

2.2.2. C2C12 2D cell culture

As described under section 2.1.2., with C2C12 myoblasts from ATCC (CRL-1772, ATCC, UK).

2.2.3. iPSC 2D cell culture

Induced pluripotent stem cell vials (Bit Bio, UK) were thawed and diluted in Essential 8 Medium (E8, Thermofisher, USA) supplemented with Rock Inhibitor (10 µM, HelloBio, UK). The iPSC suspension was added to pre-warmed 6-well plates that were coated with Vitronectin (Stem Cell Technologies, Canada) and contained pre-warmed E8 Rock Inhibitor medium. After 24h, when cells had adhered to the bottom of the well, the supernatant was gently aspirated and refreshed with Complete Essential 8 Medium (Essential 8 Medium + E8 Supplement 50x, Thermofisher, USA) without Rock Inhibitor. This refreshing procedure was daily repeated until an 80% confluency was obtained.

Once this confluency was attained, the cells were passaged. The detachment was done by incubating the cells for approximately 5 min at 37°C in Gentle Cell Dissociation Reagent (GCDR, Stem Cell Technologies, Canada). The cells were gently pipetted up and down and dissolved in equal amounts of E8+Rock Inhibitor. Further breaking down of the colonies was performed by gently pipetting the solution up and down using a P1000. The cells were seeded in prewarmed plates with Vitronectine coated wells containing E8+Rock Inhibitor. The supernatant was after 24h daily refreshed with Complete Essential 8 Medium during the culture period for expansion of cells (See Appendix F for detailed information on the maintenance of iPSCs in adherence).

When cells were needed for experiments, the differentiation procedure was started (See Appendix G for detailed information on iPSC differentiation protocol). For this, 80% confluent cells were detached using Stem Pro Accutase (Thermofisher, USA). The cells in solution were centrifuged at 200G for 5 min (Hermle Z446), and the supernatant was refreshed with E8 Complete + Rock Inhibitor. Cell concentration was obtained using Trypan Blue and Countess Automated Cell Counter (Version II, Thermofisher, USA). Cells were plated at a cell density

Table 2: **Model B & C Bovine collagen (3mg/mL)** - Overview of different substances that have been used to form a hydrogel scaffold to culture skeletal muscle tissue, based on bovine type 1 collagen.

Model B & C - Bovine collagen (3mg/mL)	
Bovine type 1 collagen (5mg/mL)	60%
Distilled water	13.5%
Minimum Essential Medium (10x)	10%
Matrigel	10%
Cells in medium	5%
Sodium Hydroxide (1M NaOH)	1.5%

of 5000 cells/cm² in Geltrex (hESC-Qualified Reduced Growth Factor Basement Membrane Matrix, Thermofisher, USA) coated wells containing E8 Complete + Rock Inhibitor Medium. After 24h, the supernatant was refreshed with Differentiation Medium (MyoD Medium; DMEM, Glutamax (100X), Insulin, 2-mercaptoethanol) with a daily fresh addition of Differentiation Supplement (1 µg/mL Doxycycline, 1µM Retinoic Acid, and 40ng/mL FGF2). The medium was for 5 days refreshed with the MyoD + Differentiation Supplement Medium. From day 6 onward, the medium was daily refreshed with MyoD + Maturation Supplement (3µM CHIR99021, 1µM Retinoic Acid, 10% KOSR).

2.2.4. Optimised tissue engineered constructs

Hydrogel constructs were generated using C2C12 myoblasts or 4 days predifferentiated iPSCs. The optimised tissue engineered constructs were formed, as can be read in Table 2, by the addition of 60% v/v GibCo Type 1 Bovine Collagen (Thermofisher, USA; dissolved in dH₂O, protein at 5 mg per mL), with 13.5% dH₂O, 10% 10X Minimum Essential Medium (MEM, Sigmaaldrich, USA), and 1.5% 1M NaOH. The pH was, if needed, adjusted with drops of 5M and 1M NaOH until a colour change to cirrus pink was observed (= pH 7). This was followed by the addition of a mixture of 5% v/v cells in Growth Medium at a seeding density of 4 x 10⁶ cells per mL and 10% Matrigel. The prepared cell-laden hydrogel was transferred to the sterilized moulds to set for 30-40 min at 37°C.

Once solidified, medium was added. For C2C12 myoblasts, the medium was changed daily for 4 days with Growth Medium (DMEM, VWR, USA; 20% FBS, Thermofisher, USA; and 1% PenStep, Fisher-Scientific, UK), and subsequently changed daily for a further 10 days with differentiation media (DMEM, VWR, USA; 2% FBS, Thermofisher, USA; 1% PenStep, Thermofisher, USA).

For the iPSCs, the medium was changed for 4 days with Differentiation Medium (MyoD Medium; DMEM, Glutamax (100X), Insulin, 2-mercaptoethanol) with a daily fresh addition of Differentiation Supplement (1 µg/mL Doxycycline, 1µM Retinoic Acid, and 40ng/mL FGF2). From day 5 onward, the medium was daily refreshed with MyoD + Maturation Supplement (3µM CHIR99021, 1µM Retinoic Acid, 10% KOSR). Tissue constructs were cultivated up until 11 days, depending on the experiment.

2.3. Analyses

Different techniques have been used for analysing the cultivated tissue parts and comparing the different tested models. Tissue samples were tested on thickness, cells in different tissue sam-

ples were tested on development, morphology and arrangement. Scaffolds were tested on stiffness, damping, elastic behaviour and porosity.

2.3.1. Macro-Microscopic analyses

The tissue constructs were daily observed using a brightfield microscope (Euromex, The Netherlands). Pictures were taken for the recording of tissue development, and sizes were measured using the ImageFocusAlpha software. Thereby, were pictures taken of the samples without well plate lid in the fume hood under sterile conditions using an endoscope (MS100 USB Microscope, Teslong, China). Size determination was performed using the ImageJ software with the measure-tool and the given value of pole-diameter (1mm). The thickness of the cultured tissue samples (n=8) was measured at the middle of the tissue, looking at it from top view.

2.3.2. Immunofluorescence staining for Desmin, MyoGenin, and MHC

Tissue constructs in toto were fixed in the mould using 4% PFA (Formaldehyde 4% stabilised, VWR, USA) for 30 min (50µL moulds) or 1hr (500µL moulds), washed with PBS, and permeabilized with 0.1% TRITON X-100 (Sigma-Aldrich, UK) in PBS for 8 min at room temperature (RT) (See Appendix H for detailed information on SOP for immunostaining). Subsequently, the tissue constructs were washed with PBS and blocking solution (1% BSA in 0.05% Tween-PBS) was added for 1 hour at RT. After being washed with PBS, the tissue constructs were incubated in mouse anti-Desmin (M076029-2, Agilent Technologies, USA), mouse anti-MyoGenin (AB2146602, DSHB Biology, USA), or mouse anti-MHC (AB2147781, DSHB Biology, USA) antibody diluted 1:200 in blocking solution for 24 hrs (50µL constructs) in the dark at RT.

After being washed with 0.05% Tween-PBS, the tissue samples were incubated for 3hrs at RT in the dark in the 2nd antibody diluted in blocking solution; 1:500 Donkey anti-mouse AF488 (AB150105, Abcam, UK) and 1:500 Phalloidin-TRiTC (R415, Thermo Fisher, USA). Subsequently, the tissue constructs were washed with 0.05% Tween-PBS and PBS, before being incubated for 1hr at RT in 1:1000 DAPI:Demiwater. The tissues were washed with PBS, mounted on glass slides with EverBrite Hardset Mounting Media (23003, VWR, USA), and viewed and photographed by fluorescence microscopy. Confocal images were made on a Leica inverted confocal microscope (TCS SP5, Leica, Mannheim) operating under the Leica Application Suite Advanced Fluorescence software (Leica, Mannheim). Brightness and contrast adjustments consistent with image manipulation policies were performed either with LAS AF or ImageJ (version 1.8.0_112, <http://imagej.nih.gov/ij>) software.

2.3.3. Histological analyses

Tissue samples (500µL moulds) were in toto fixed using 4% PFA (Formaldehyde 4% stabilised, VWR, USA) for 1h and washed with PBS. The samples were stored in PBS and send to the Veterinary Pathological Diagnostic Centre (University of Utrecht) for further histological analyses. Tissue morphology and structure were assessed using H&E staining. The samples were stained with hematoxylin for blue nuclei, and with eosin for pink extracellular matrices and cytoplasm. Cryosections were

made in the transverse and longitudinal plane. Pictures were taken using a brightfield microscope.

2.3.4. Mechanical analyses

Rheometry for dynamical mechanical analyses

Tissue cultured samples of different scaffold materials (Rat tail collagen 1.7mg/mL; Bovine collagen 3mg/mL; 500 μ L moulds) of different culture days, with C2C12 myoblasts, were in toto fixed using 4% PFA (Formaldehyde 4% stabilised, VWR, USA) for 1h and washed with PBS. Same sized samples, roughly 2.5 x 2.5 x 20 mm, of raw beef (3% fat) and raw minced beef meat (16% fat) were tested as well. Before performing the dynamical tests, the samples were weighted. The density of water, steak and minced meat is around 1 mg/mm³, therefore the scaffold density was assumed to be equal and was used to correct the measurements to true sample volume [49, 1]. A Modular Compact Rheometer (MCR 302, Anton Paar, Austria) with flat disk probe (PP25/P3, SN18674) and profiled plate (P2) was used to study the different cultured tissue samples. The flat disk probe had a diameter of 25mm and the plate had a profile of 0.25mm blocks. The plate was preheated to 25°C, and a tissue placement zone was drawn on it (See Appendix L). The probe was lowered on the sample, and when initial contact was made, the excessive parts of the tissue sample bigger than the probe were cut off. An Amplitude Sweep program was run using RheoCompass program. The sweep increased from 0.01-1% at a frequency of 1Hz, with six measure points on logarithmic scale. Storage and loss moduli, and other rheological parameters, were derived from the data using manufacturer supplied software (RheoCompass, Anton Paar, Austria). The shear storage modulus was obtained using equation 1, where δ is the phase lag between stress and strain. Shear loss moduli were obtained using equation 2. Both moduli were used for obtaining the Complex Shear Modulus, as noted in equation 3.

$$G' = \frac{\sigma_0}{\epsilon_0} \cos(\delta) \quad (1)$$

$$G'' = \frac{\sigma_0}{\epsilon_0} \sin(\delta) \quad (2)$$

$$G^* = G' + iG'' \quad (3)$$

$$\tan(\delta) = \frac{G''}{G'} \quad (4)$$

G' is a measurement of the deformation energy stored during shear process of a sample, and is thus a measurement of stiffness. Whereas G'' represents the energy that has been dissipated during the shear process of a sample, and is thus a measurement of flow (i.e. liquid-like) response of the sample. The complex shear modulus G^* describes the entire viscoelastic behaviour of the material. The Loss Factor ($\tan \delta$) provides a measure of damping in the material, since it is the ratio of energy lost to energy stored during deformation, and can be obtained through equation 4 [43]. If $G'' > G'$ (i.e. $\tan \delta > 1$), the sample behaves more like a viscous liquid [69]. Whilst more elastic-like samples will show $G' > G''$ (i.e. $\tan \delta < 1$).

Unconfined Compression test for static mechanical analyses

Hydrogel samples (3mL) of Rat tail collagen (1.7mg/mL) and

Bovine collagen (3mg/mL) without cells were cast into wells of a 24-well plate, so that cylinders with a diameter of 15mm and an height of approximately 9mm were solidified. Subsequently, the cylinders were fixed using 4% PFA (Formaldehyde 4% stabilised, VWR, USA) for 1h and washed with PBS. Samples of raw beef (3% fat, square, 18x18x8mm) and raw minced beef meat (16% fat, cylinder, diameter 15mm, height 9mm) were tested as well. The unconfined compression tests (stress-relaxation) were performed using a TA.XT compression machine (TA.XT C plus, Stable Micro Systems, UK). A cylindric perspex probe (P/25P, 25mm diameter, Stable Micro Systems, UK) was used. In the software (TA.XT, Stable Micro Systems, UK) supplied by the manufacturer, a testing protocol was installed. To stay within the elastic region (see Appendix I for proof of elastic region), a strain compression of 10% was performed with a loading speed of 2mm/s. The 10% strain was held for 120s, and then released. Measurements started when the probe-sample interaction reached 0.009N to ensure proper seating, and were compressed in longitudinal direction. The output of the measuring device (Force in grams, strain in mm, time in seconds) was converted to Nominal Stress (σ , N/mm²). Stress and strain (ϵ) curves, equilibrium moduli (E_{eq} , an indicator for stiffness), and maximum peak values (σ_{max} , an indicator for porosity and flow) were obtained by exporting the measuring device output data to Microsoft Excel. Graphs were obtained using GraphPad Prism (version 8.3.1.) and smoothed with an interval rate of 15.

2.3.5. Porosity analyses

Hydrogel samples (3mL) of Rat tail collagen (1.7mg/mL) and Bovine collagen (3mg/mL) without cells were cast into wells of a 24-well plate, so that cylinders with a diameter of 15mm and an height of approximately 9mm were solidified. The hydrogels were prepared as described in section 2.1.3 and 2.2.4, except that the volume of cells was replaced by the same volume of PBS. Half of the cylinders were fixed overnight in 4% PFA. All cylinders were immersed in PBS for 24hrs. The sample (n=3) porosity measurement and calculations were based on work of Ho et al. [34]. The scaffold samples were weighted and measured after 24hrs submersion in PBS and placed on absorption paper for 30 min in open air to dry. The initial weight of the sample (γ_1) was measured, the weight of the sample after 30 min drying on absorption paper in open air was measured as well (γ_2). The porosity, P, defined as the ratio of volume of open pores in the scaffold to the entire volume, is stated in equation 5.

$$P = 1 - \frac{\gamma_2}{\gamma_1} * 100\% \quad (5)$$

After weighing the dried samples, the scaffolds were submerged in PBS for 24hrs to re-swell. The weight of the re-swelled samples was measured (γ_3). With this value, the percentage of recovery, R, of the scaffold was calculated according to equation 6.

$$R = \frac{\gamma_3}{\gamma_1} * 100\% \quad (6)$$

Averages and standard deviations were obtained using Microsoft Excel. Graphs were obtained using GraphPad Prism (version 8.3.1.).

2.3.6. Statistical analysis

The standard deviation of different results was obtained through Microsoft Excell standard programmed formula; =STDEV.S.

3. Results

The standard model (Model A) was utilized to establish these protocols in-house. Further optimization was conducted in order to transition to bovine collagen tested with C2C12 myoblasts. With the optimal bovine concentration (Model B), iPSCs were then used instead of C2C12 myoblasts (Model C).

3.1. Macro-Microscopic analyses

In all models, a certain degree of cell-mediated gel compaction was observed. The tissue thickness at the middle of the 11 days cultured tissues with rat tail collagen or bovine collagen (at different concentrations) scaffolds was measured. Figure 6 shows the different cultured tissues at top view, where the red line depicts the measure point. The averages ($n=8$) of the different tissues is showed in table 3. The average center thickness of the rat tail collagen scaffold (1.7mg/mL, Model A) and the bovine collagen scaffold (3mg/mL, Model B) did not differ. Whereas the thickness of the bovine collagen scaffold at a concentration of 1.7mg/mL was significantly lower than that of Model A. Thereby, the tissue samples at a concentration of 1.7mg/mL detached sometimes from the poles due to rupture of the scaffold around the poles. The average center thickness of the Bovine collagen at 4 mg/mL was significantly higher than that of Model A. But when seeding Model B with iPSCs instead of C2C12 (Model C), the average thickness did not change much compared to the initial thickness when casting the hydrogel. Figure 7 depicts Model C, the hydrogel scaffold seeded with iPSCs, in a 50/*mu*L mould after 7 days of culture. No compaction of the gel was observed at this moment.

3.2. Immunofluorescence staining

Eleven days cultured tissue samples of Model A (Rat tail collagen, 1.7mg/mL, C2C12), Model B (Bovine collagen, 3mg/mL, C2C12) and Model C (Bovine collagen, 3mg/mL, iPSC) were stained with different antibodies and assessed with confocal microscopy to evaluate cell morphology and maturation (see Figure 8). As can be seen in Appendix J (Figure 24), the cells at day 6 are more randomly oriented than at culture day 11. Thereby, is the expression of Desmin, MyoG, and MHC (green) lower than at day 11. When comparing different concentrations of bovine collagen at day 6, the cells are more aligned and stretched in 3mg/mL collagen than in 1.7mg/mL. The expression of Desmin (which comes earlier in cell development) is higher than the expression of MyoG and MHC for both Models A & B at day 11.

There is no big difference in cell alignment and presence of maturation markers observed between Model A and Model B. However, Model C has a significant lower presence of maturation markers, way less actin (red), and randomly oriented iPSCs. There are a few green nuclei, which indicate MyoG expression. The cell density seems to be lower than is the case in Model A & B. Nevertheless, there are still quite some nuclei (blue) observed in model C.

3.3. Histology

As revealed by H&E staining in Figure 9, the tissue samples of Model A & B do not differ much in cell alignment. In Model B, more nuclei are displayed in the longitudinal and transverse cross section. Both model A and B have several multi-nucleated C2C12s, as pointed by arrows in sub-figure C and F. Cell density

seems to be highest at the border of the tissue in both Models A & B.

When assessing Model C, the iPSCs in the bovine collagen show differences in cell orientation, cell density, and cell stretching compared to the C2C12s. The iPSCs in Model C seem to be less evenly distributed, stretch less, and do not migrate to the tissue borders. As can be seen in Figure 7, stretching myoblasts are observed in the scaffold in a 50/*mu*L mould. Nevertheless, the differentiated myocytes are not stretching in aligned orientation.

3.4. Mechanical analyses

3.4.1. Rheometry

Quantitative data on the rheological and viscoelastic properties of the different materials (scaffolds with C2C12 cells and positive controls: beef steak, minced beef) were provided by dynamic mechanical analysis. The mechanical response of the samples was measured as they were deformed under periodic strain. The shear storage (i.e. real or elastic) modulus G' , shear loss (i.e. imaginary or viscous) modulus G'' , the Complex Shear Modulus G^* , and Loss Factor $\tan \delta$ are presented in Table 4 and were obtained by manufacturer supplied software and equations stated in subsection 2.3.4. Plots of the different moduli can be found in Figure 10 and were obtained using GraphPad Prism (version 8.3.1.). All storage moduli were higher than the loss moduli, which is an indication for materials that behave more like elastic materials instead of viscous materials. The stiffness (G') and flow-like behaviour (G'') of both rat tail and bovine tissue samples decreased when comparing samples at day 7 and day 11. The tissue engineered muscle tissue (Rat tail and bovine) had a significant lower stiffness than minced meat and steak, but the Model B came closer to the stiffness of steak (factor 5). Scaffolds (Day 11) made of rat tail collagen showed a lower (factor 2) Complex Shear Modulus than scaffolds made of bovine collagen; 0.82 ± 0.05 Pa versus 1.80 ± 0.05 Pa. The damping factor ($\tan \delta$) did not differ when comparing rat tail collagen to bovine collagen, but when comparing these to minced meat and steak, a twofold difference is evident.

3.4.2. Unconfined compression test

Results of the average Maximum stress values and average equilibrium moduli of the different samples ($n=3$) can be found in Table 5, where the scaffolds were without cells. The plots of the different samples are displayed in Figure 11. The peak observed in the stress over time graph due to the loading of the probe on the sample, was distilled from the output data and noted as 'Maximum stress value'. This value is an indicator for the permeability of the material. There was no significant difference in max. stress value observed when comparing rat tail collagen scaffold, bovine collagen scaffold, and steak. A difference in max. stress value was observed when comparing these three to minced meat; $\Delta 1.5$ kPa lower (-50%).

The equilibrium modulus, the value of stagnation of the stress over time graph, of the rat tail (Model A) and bovine (Model B) collagen scaffolds differed with $\Delta 0.027$ kPa, where bovine collagen showed a factor 2 higher equilibrium modulus (Rat: 0.034 ± 0.01 kPa; Bovine: 0.061 ± 0.01 kPa). When comparing the collagen scaffolds to minced meat and steak (resp. 0.303 ± 0.07 kPa and 0.623 ± 0.04 kPa), the differences in equilibrium moduli were much higher (factor 10-20).

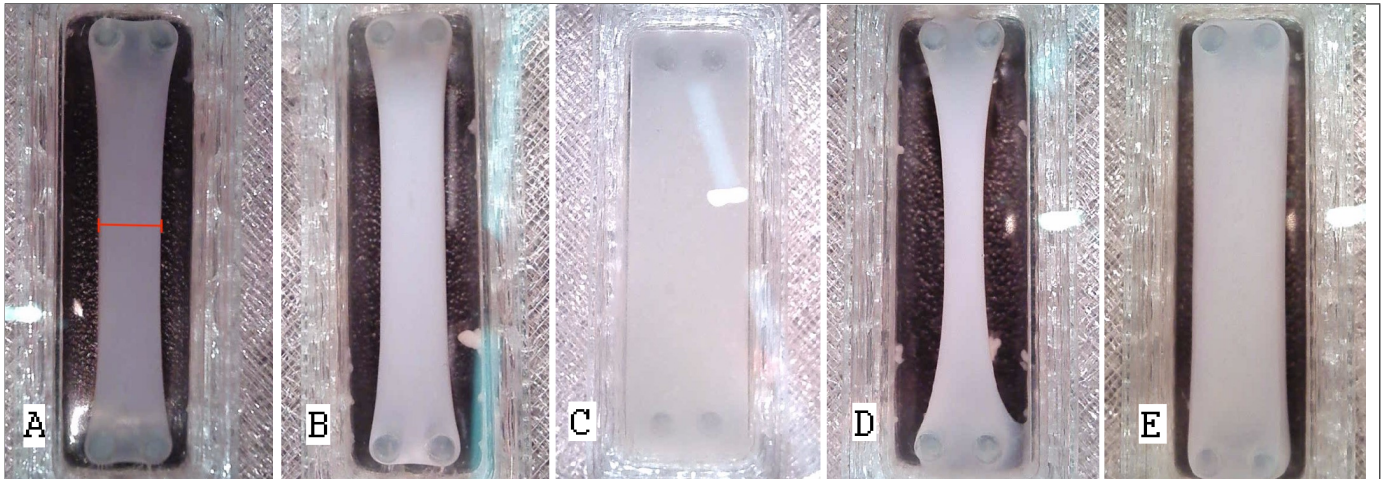


Fig. 6: Different tissue cultured skeletal muscle samples - Different 11 days tissue cultured samples in a 500µL mould, looking from top view. (A) Rat tail collagen [1.7mg/mL] scaffold with C2C12s, Model A. (B) Bovine collagen [3mg/mL] scaffold with C2C12s, Model B. (C) Bovine collagen [3mg/mL] scaffold with iPSCs, Model C. (D) Bovine collagen [1.7mg/mL] scaffold with C2C12s. (E) Bovine collagen [4mg/mL] scaffold with C2C12s. The red line in sub-picture A depicts the measuring area that was used to obtain the Average Center Thickness.

Table 3: Size measurements - Results of the size measurements performed at top view of the cultured tissues at the middle of the tissue sample. Scaffolds of different bovine collagen concentrations were cultured with C2C12 myoblasts, as a comparison to the 'Model A' Rat tail collagen with C2C12 myoblasts as well. Bovine collagen (3mg/mL) scaffold was also seeded with iPSCs. All tissues were cultured for 11 days in the 500µL moulds.

Type of scaffold	Average center thickness (mm) ± SD	
Model A - Rat tail coll. (1.7mg/mL, C2C12 myoblasts)	2.37	0.11
Model B - Bovine coll. (3mg/mL, C2C12 myoblasts)	2.44	0.13
Model C - Bovine coll. (3mg/mL, iPSCs)	4.90	0.10
Bovine coll. (1.7mg/mL, C2C12 myoblasts)	1.55	0.08
Bovine coll. (4mg/mL, C2C12 myoblasts)	3.47	0.19

Table 4: Rheology measurements - Results of the rheology measurements on different cultured tissue samples in either rat tail collagen (Model A) or bovine collagen (Model B) based scaffold hydrogels with C2C12 myoblasts at day 7 and day 11 culture. Collagen samples were cultured in a 500µL mould and fixed in 4% PFA for one hour. Same sized samples of minced bovine meat and bovine steak were tested as comparison. All results were corrected according to the true sample volume. An Amplitude Sweep program was run using RheoCompass program. The sweep increased from 0.01-1% at a frequency of 1Hz, with six measure points on logarithmic scale. Storage and loss moduli, and other rheological parameters, were derived from the data using manufacturer supplied software (RheoCompass, Anton Paar, Austria) and equations stated in subsection 2.3.4. For graphs, see Figure 10.

Type sample	Storage Modulus (G', Pa)	Loss Modulus (G'', Pa)	Complex Shear Modulus (G*, Pa)	Loss Factor (tan δ)
- Rat tail collagen D7 (1.7mg/mL, fixed, Model A)	1.43 ± 0.19	0.20 ± 0.03	1.44 ± 0.19	0.14 ± 0.005
Rat tail collagen D11 (1.7mg/mL, fixed, Model A)	0.80 ± 0.05	0.13 ± 0.02	0.82 ± 0.05	0.15 ± 0.02
- Bovine collagen D7 (3mg/mL, fixed, Model B)	2.78 ± 0.22	0.30 ± 0.01	2.81 ± 0.22	0.11 ± 0.005
Bovine collagen D11 (3mg/mL, fixed, Model B)	1.59 ± 0.06	0.24 ± 0.06	1.80 ± 0.05	0.14 ± 0.03
- Minced meat (bovine, 16% fat)	4.86 ± 0.75	1.34 ± 0.12	5.35 ± 0.76	0.27 ± 0.02
- Steak (bovine, 3% fat)	8.12 ± 2.10	1.89 ± 0.48	8.33 ± 2.15	0.23 ± 0.003

Table 5: **Unconfined compression test results** - As described at Figure 11, have different samples been tested with an unconfined compression test. The average peak values and the average equilibrium moduli of the graphs in Figure 11 are stated.

Type sample	Max. stress value (kPa)	± SD	Equilibrium modulus (kPa)	± SD
Rat tail collagen (1.7mg/mL, fixed, Model A)	3.225	0.22	0.034	0.01
Bovine collagen (3mg/mL, fixed, Model B)	3.616	0.42	0.061	0.01
Minced meat (bovine, 16% fat)	1.500	0.21	0.303	0.07
Steak (bovine, 3% fat)	3.128	0.26	0.623	0.04



Fig. 7: **Model C cultured skeletal muscle tissue** - Microscopical pictures of Model C (Bovine collagen 3mg/mL) scaffold seeded with iPSCs in a 50µL sized mould after 7 days of culture. Above assembled picture depicts the top-view of the 50µL mould with scaffold and cells. Below a detailed (20x) microscopical view of the multi-nucleated stretching myotubes in the scaffold.

3.5. Scaffold porosity and recovery

Results of the porosity test and recovery test are displayed in Table 6, the detailed test values can be found in Appendix K. Appendix K Figure 28 shows that the scaffolds lost a significant amount of liquid content. The average porosity with standard deviation was plotted in figure 12. Measurements show that the porosity of the fixed rat tail collagen (Model A) and the Bovine collagen (Model B) were almost equal ($\Delta 1.42\%$); respectively $97.3\% \pm 0.22\%$, and $95.9\% \pm 0.14\%$. There was no significant difference in porosity observed between fixed and non-fixed hydrogel scaffolds of Bovine collagen. There was a difference of 6.75% observed between fixed and non-fixed rat tail collagen hydrogel scaffolds. The difference in porosity of non-fixed rat tail collagen and bovine collagen scaffolds was 5.27%, which was a bigger difference ($\Delta 3.85\%$) than the fixed collagen scaffolds.

The average recovery modulus for fixed rat tail collagen scaffold and bovine collagen scaffold differed significantly ($\Delta 77.28\%$) and were respectively $16.51\% \pm 1.08\%$ and $93.79\% \pm 0.83\%$. A reversed recovery difference was observed between non-fixed rat tail collagen and bovine collagen scaffolds ($\Delta 39.27\%$). Interesting was that the recovery percentage of rat tail collagen scaffolds decreased ($-\Delta 40.87\%$) when being fixed, whereas the recovery percentage of bovine collagen scaffolds increased ($+\Delta 75.68\%$) when being fixed.

4. Discussion

Planet earth is warming up, natural resources are becoming more scarce, and global inequality is increasing. To continue producing food, especially meat, the way it is now done does not seem to be sustainable. For people to be able to enjoy their delicious piece of steak in the future, the way meat is grown needs to be re-designed. One such disruptive initiative is in vitro cultured meat. Meatable B.V. is a food-technology startup that is a pioneer in this field, using iPSCs. For the production of in vitro cultured meat using iPSCs, a published model using C2C12 myoblasts (Model A, Capel et al.) was reproduced. Hereafter, a for cultured meat optimised Model B was tested and compared to Model A. This optimised model was for the first time seeded with iPSCs (Model C) and compared to Model B and conventional meat.

4.1. Are Model B and C as good as Model A?

To answer the question whether Model B and C were as good as, or even better than Model A, different parameters and aspects were compared. Scaffold mechanics, scaffold porosity, tissue thickness, cell development, cell morphology, and cell arrangement were analysed.

Characterization of the scaffold without cells was performed to understand material characteristics such as porosity, stiffness, et cetera. These parameters are the physical environment that encapsulate the cells. The scaffold permeability of Model A and B were the same, according to the Maximum Stress Values of

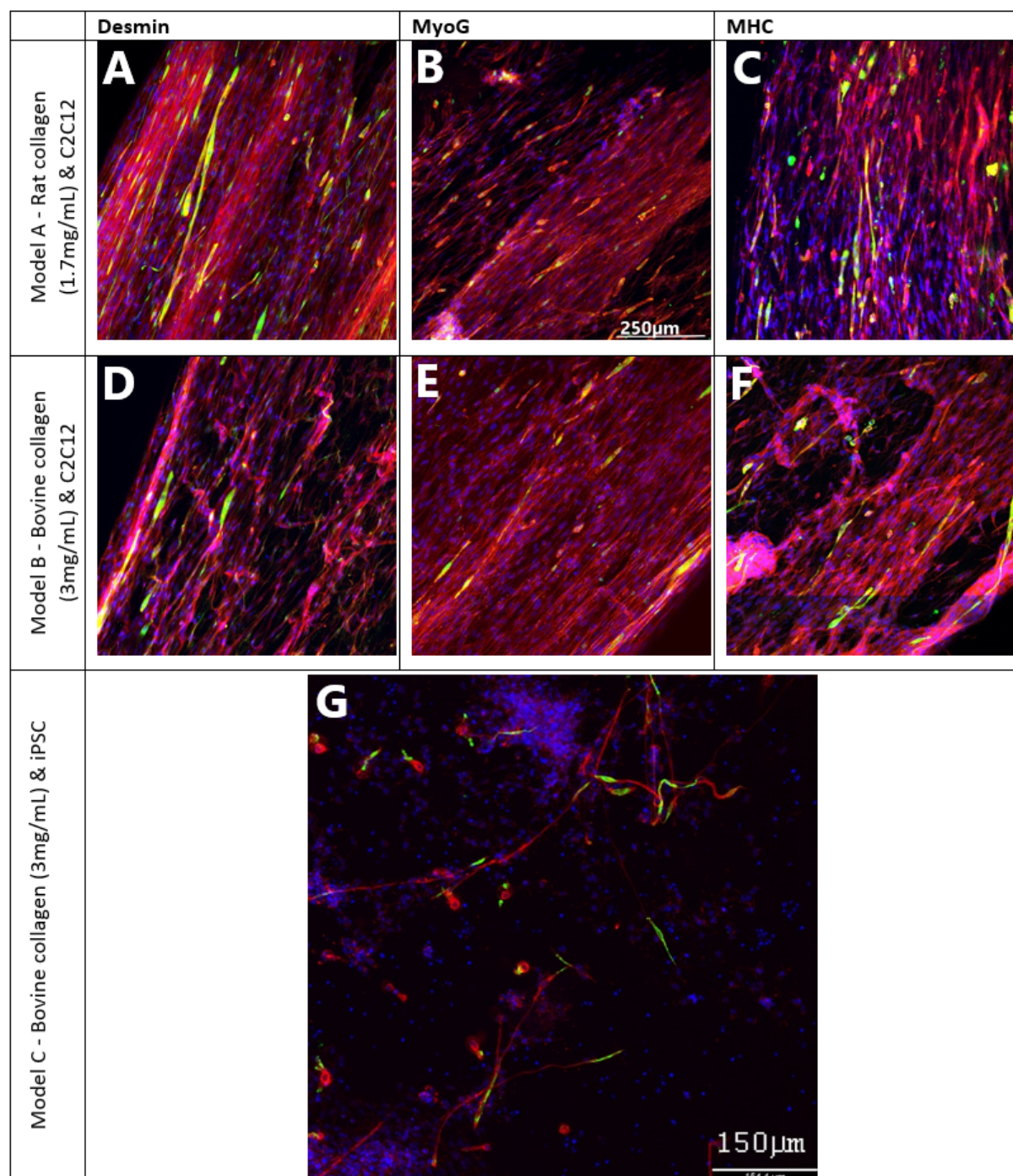


Fig. 8: **Immunofluorescence staining** - Structure of 11 Days bioengineered skeletal muscle bundles and gene expression, visualized through immunofluorescence staining. Where nuclei are blue, actin filaments are red, and the targeted protein (Desmin/ MyoG/ MHC) is green. Scale of sub-images A - F are the same. Confocal images of Day 11 cultured samples in 50 μ L moulds, in different hydrogel scaffolds with different cells. Sub-images A - C represent the samples of Model A. Sub-images D - F represent the samples of Model B, and sub-image G represents Model C. Sub-images A - F are longitudinal, non-stacked shots. G is a longitudinal stacked image of a MyoG staining. Samples were stained for Desmin, MyoG, or MHC.

the unconfined compression test, and the porosity test. The measured porosities were in line with the average pore porosity of skeletal muscle ECM [26]. Model B was twice as stiff as Model A, according to the Equilibrium Modulus of the unconfined compression test. This could be explained by the almost double concentration of collagen. The reason that a double concentration was needed for the same cellular effects could be due to the obtaining process of the different types of collagen and the different

solvents that were used by two different manufacturers. Thereby, Angele et al. state that collagen from different animal species show different physico-chemical properties [2].

When focusing on the scaffolds with cells, there can be seen that Model A and B were the same in terms of tissue thickness, and thus tissue compaction, after several days of culture. The C2C12s seemed to remodel the scaffolds in the same rates. Compaction of the scaffold is a sign for proper cell adherence and cell

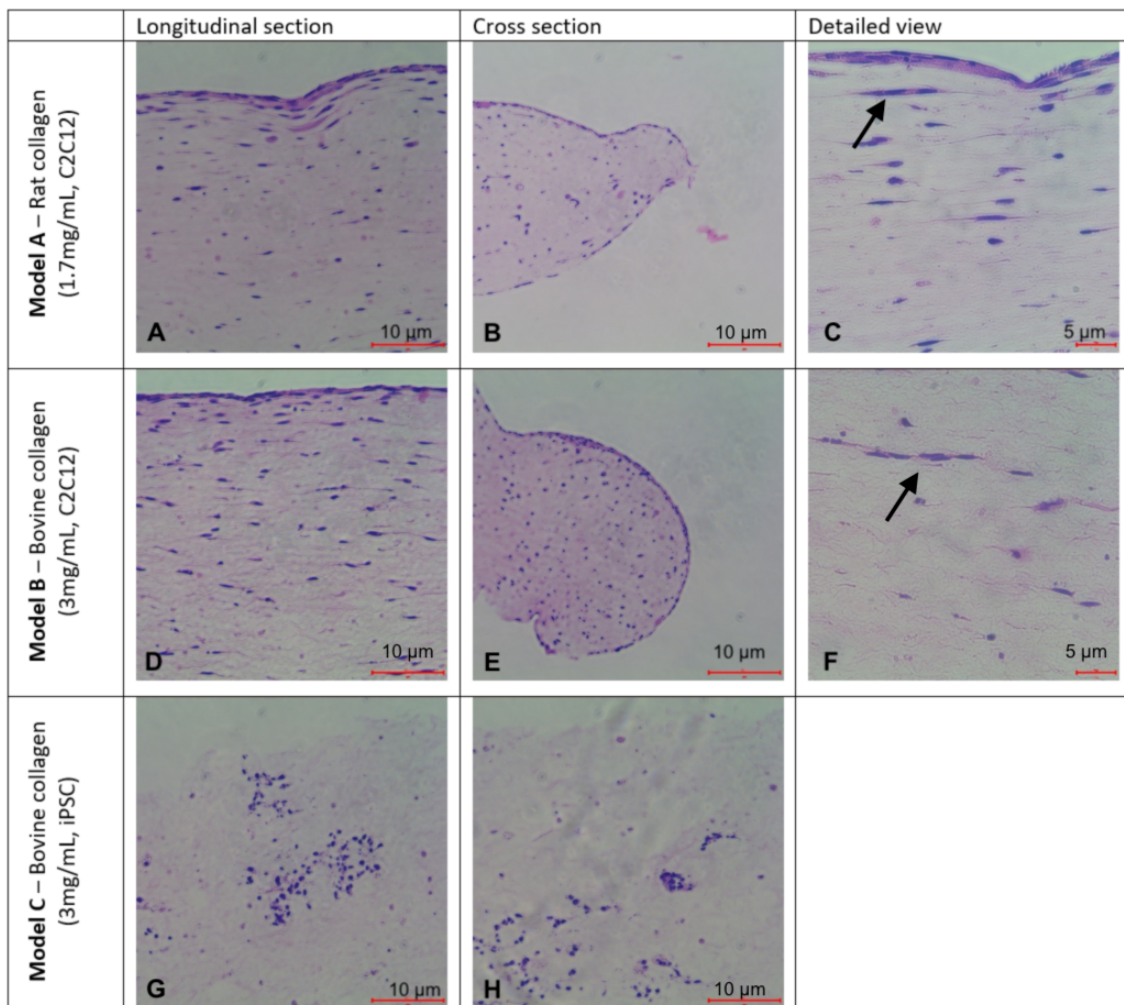


Fig. 9: **Histological H&E staining** - Representative H&E stainings of 11 days cultured samples of the three different models; Model A with Rat tail collagen as a hydrogel seeded with C2C12s; Model B with Bovine type 1 as a hydrogel seeded with C2C12s; Model C with Bovine type 1 as a hydrogel seeded with iPSCs. A, D and G are pictures of longitudinal cut slices. Whereas B, E and H are pictures of transversal cut slices. C and F are detailed pictures of the longitudinal cut slices where multinucleated cells are pointed by the black arrows. All samples were stained with hematoxylin for blue nuclei, and with eosin for pink extracellular matrices and cytoplasm.

Table 6: **Porosity and recovery test results** - Porosity and recovery capacity of different fixed (4% PFA) and non-fixed hydrogel scaffolds without cells prepared according to subsection 2.1.3 and 2.2.4. The Porosity was measured as the percentage of weight change when samples (n=3) were dried for 30 minutes in open air after being submerged in PBS for 24hrs. The Recovery was measured as the percentage of weight change from samples that were re-submerged in PBS after drying for 24hrs and initial weight before drying.

Type hydrogel	Porosity (%)	± SD	Recovery (%)	± SD
Rat tail collagen (1.7mg/mL, fixed, Model A)	97.30	0.14	16.51	1.08
Rat tail collagen (1.7mg/mL, non-fixed, Model A)	90.55	0.65	57.38	5.77
Bovine collagen (3mg/mL, fixed, Model B)	95.88	0.14	93.79	0.83
Bovine collagen (3mg/mL, non-fixed, Model B)	95.82	0.23	18.11	0.58

stretching [9]. The iPSCs in model C did not seem to remodel or compact the scaffold as C2C12s did. This could be explained by the low maturation and low adherence of iPSCs to the scaffold. Cells need to adhere and pull to cause compaction.

There was no remarkable difference observed in cell development and cell alignment between Model A and Model B. The cells form myotubes and show longitudinal alignment in the scaffold as is expected according to the static constraint by the poles on the collagen scaffold [9]. This cell alignment is of importance for the texture and taste experience of the future piece of meat [4]. Although, the histological research showed

that more nuclei were observed in Model B compared to A. This could be explained by the difference in scaffold stiffness, which influences the cell development and migration [16, 11].

The iPSCs in Model C showed some maturation into multinucleated myotubes on the immunofluorescence stainings and microscopy images. Nevertheless, the expression of MyoG, myotubes and actin filaments was significantly lower than in Model A and B, which indicates a less mature cell stage. The orientation of elongated iPSCs seemed randomly organised. When observing the histological research, iPSCs in Model C did not migrate to the edges of the scaffold and were less evenly distributed, un-

Rheology measurements

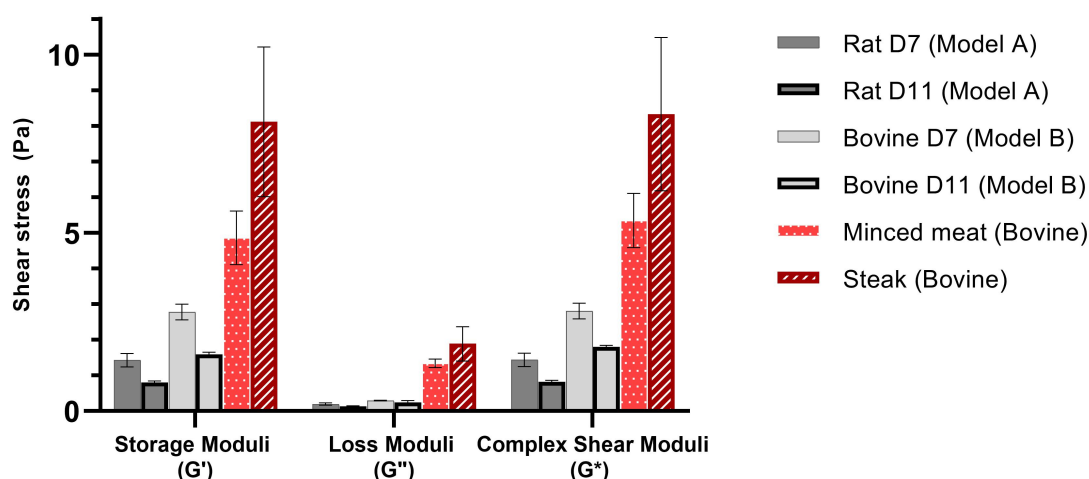


Fig. 10: **Different moduli from rheology measurements** - Rheology measurements on different cultured tissue samples in either rat tail collagen (Model A, 1.7 mg/mL) or bovine collagen (Model B, 3 mg/mL) based scaffold hydrogels with C2C12 myoblasts at day 7 and day 11 culture. Collagen samples were cultured in a 500 μ L mould and fixed in 4% PFA for one hour. Same sized samples of minced bovine meat and bovine steak were tested as comparison. An Amplitude Sweep (0.01-1%, 1Hz) program was run using RheoCompass program.

Stress-relaxation curves of different hydrogel scaffolds and meat

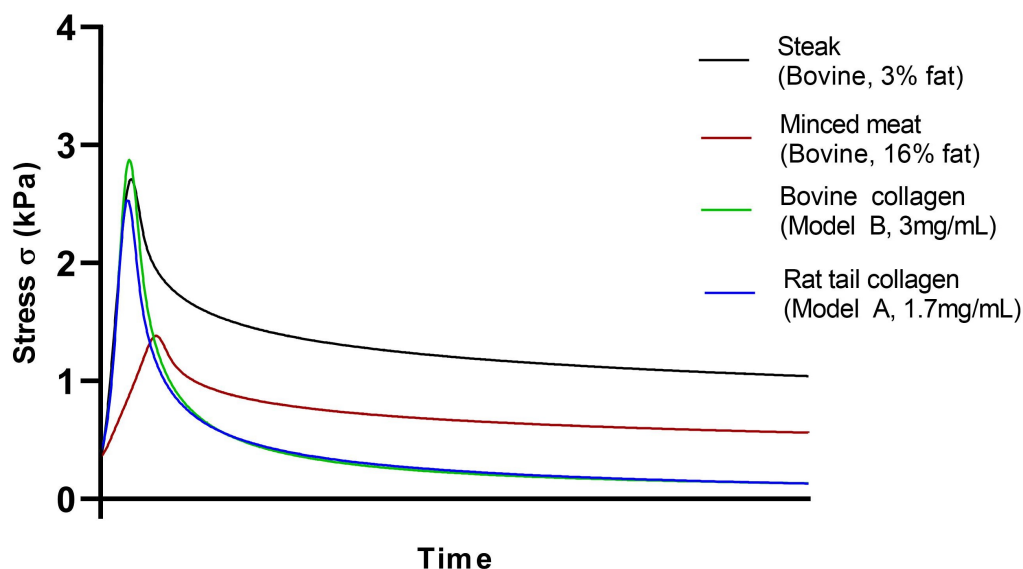


Fig. 11: **Unconfined compression test graphs** - Graphs of different hydrogel scaffolds (Model A Rat tail 1.7mg/mL and Model B bovine 3mg/mL type 1 collagen) without cells and fixed, minced meat, and steak samples that have been tested with an unconfined compression test. The same sized samples were compressed with a strain compression of 10% under a speed of 2mm/s and was held for 120s, before being released again. Quantitative data is stated in Table 5.

like the C2C12s in Model A and B. It seems that differentiated iPSCs find it more difficult to adhere to and migrate through the scaffold in 3D, which is also observed in the low amount of scaffold compaction. IPSCs and C2C12s however show the same rate of adherence to scaffold coatings when cultured in 2D, as can be seen in Appendix D (Figure 18 day 5 and Figure 20 day

5). An explanation could be that iPSCs are less well differentiated inside the scaffold than in a 2D setup. Future work should indicate the level of MyoD expression of both C2C12s and iPSCs at day 0 just before incorporating these in scaffolds. The expression of MyoD indicates the early differentiation of pro-

Porosity of different hydrogel scaffolds (without cells)

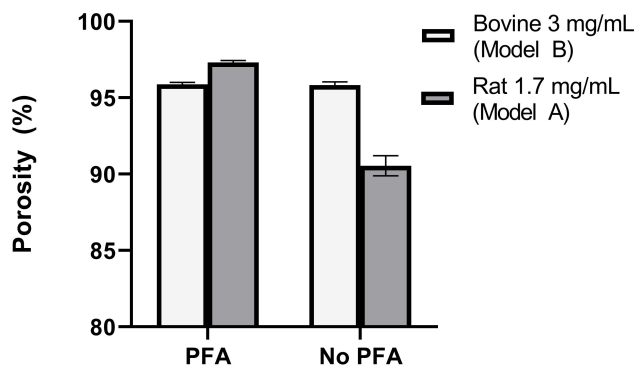


Fig. 12: **Porosity of different hydrogel scaffolds** - The average ($n=3$) porosity of two different hydrogel scaffolds (Model B Bovine 3mg/mL and Model A Rat tail 1.7mg/mL type 1 collagen), fixed in 4%PFA and non-fixed, all without cells are stated.

genitors into myoblasts and should be tried to be the same for C2C12s and iPSCs [19, 20].

The stiffness of Model A with C2C12s was, again, half of the stiffness of Model B with C2C12s which could indicate that the cells have an equal impact on the scaffolds in both models. The Loss Modulus, which is an indicator for flow inside the scaffold, of Model B was higher than that of Model A, which is surprising since the C2C12s in Model B seemed more packed on the histological images and the collagen concentration was higher. Thereby, the bare scaffolds had the same porosity. This small difference could be explained by the difference of both tests, or a difference in cross-linking capacity of the network of collagen between bovine and rat. Both models behave more as an elastic-like material ($\tan \delta < 1$).

The stiffness (storage modulus) and the flow-like behaviour (loss modulus) of the tissue samples seemed to decrease after several days of tissue culture (day 7 versus day 11). When observing the immunofluorescence pictures of the samples at day 6 (Appendix J) and day 11, it can be seen that cells are less aligned and have less densely packed actin filaments at day 6. This is in line with the decreasing flow-parameter, since there is less empty space left in the scaffold for liquid to flow at day 11. At day 11, the cells are more densely packed, better aligned, and have compacted the scaffold even more. The change in stiffness could be caused by the change of scaffold, liquid and cell ratio, or the influence of cell death on the tissue. Future work should show what the differences in stiffness are of the cells and the scaffold without cells through rheology, and give more insight in the percentage of cell death.

According to the above, Model B seems to be very comparable to Model A and perhaps slightly better in terms of cell development and cell density. The setups show the start of cultured skeletal muscle tissue.

Nevertheless, conclusions on immunofluorescence images and histological images were drawn on the basis of visual observations. Due to limited sample size of image analysis for both immunofluorescence microscopy and histology, it was not possible to underpin these findings with exact quantification of, for instance, nuclei or the percentage of cell alignment, using ImageJ software. Further, more precise porosity measurements should be performed through SEM micrographs, as done by Giusti et al.,

to obtain information about pore size and scaffold microstructure in order to further understand nutrient and waste transport, and cell migration. [30]. Lastly, due to time constraints, it was not possible to perform rheology measurements and compression tests on scaffolds with and without cells.

Unfortunately, the scaffold parameters optimized with C2C12s are not translatable to iPSCs (Model C). The limitations of Model C are probably caused by less mature iPSCs when being incorporated in the hydrogel, the lower ability of iPSCs to differentiate within 3D scaffolds and the cell seeding density. Future work should confirm that this could be improved by allowing the iPSCs to pre-differentiate for a longer period of time (>4 days) in 2D setting and checking the level of MyoD expression, before incorporating them in a 3D scaffold. Further, when observing the immunofluorescence images of Model B and C, more or less the same number of nuclei is observed, whilst the image of Model C is a stacked image and Model B is not. This indicates that the cell density of iPSCs was too low. Future research should also focus on different amounts of iPSC seeding densities which could have an influence on tissue development.

Altogether, Model A and B are very comparable models, and Model B even seems to be slightly better for cell development and density than Model A. Therefore, Model B should be set as the basis model to optimise for the culture of iPSCs. The limitations of Model C are evident when considering the results. These limitations are mainly caused by the maturation of iPSCs, which could be improved in different ways.

4.2. Are Model B and C feasible starting models for cultured meat?

To answer the question whether Model B and C were feasible starting models for the production of cultured meat, and thus competitive with conventional meat, the models were assessed on different aspects. The scaffold of Model B (and thus C) had to be compared to several requirements. Subsequently were model B and C compared to conventional meat.

The future requirements of the alternative scaffold are; animal free, cheap, scalable, and edible. The current models do not meet all these requirements. All used materials are theoretically edible, but might not be very appetizing. Bovine collagen and Matrigel are both retrieved from animal sources. The average world wide price of beef meat is 4.34 USD/kg, whereas the price of Bovine Collagen used in this paper is more than 14 USD/mL [51]. According to Bach et al., Matrigel is a successful product to use for in vitro cell culture in combination with structural scaffolds, but the product contains various ECM proteins in undefined varying concentrations which might limit it to experimental setups only [3].

The proof of concept is however still in development, which makes the above requirements less critical. Research groups are already focusing on making recombinant (bovine) collagen. Olsen et al. mention the promising possibility of producing human collagen through yeasts and tobacco plants [47]. In addition, bovine collagen is already a more preferable option in terms of edibility than rat tail collagen. Furthermore, laminin is the main component of Matrigel [3], which is commercially available in recombinant animal free form (e.g. MAPTRixTM). Finally, due to the economy of scale, prices of research models should not yet be taken as a direct price indicator for the end

product.

When comparing Model B and C to steak and minced meat, the cultured tissue pieces were not quite the same. Comparison between steak and the most adult cultured sample (Day 11) should be taken as the most significant measures, since the intention was to culture skeletal muscle. Model C was not included in the mechanical testing since the histological and immunofluorescence images showed that this model was not yet successful, and there was a time constraint for using measuring devices. For minced meat, both the measure of flow and the stiffness were lower than that of steak, which is explainable by the loose structure and less interconnected ECM to transfer liquid flow of minced meat. The measure of flow (Max. stress value) of steak and Model B without cells was almost the same, according to the unconfined compression test. When cells were cultured in Model B, the measure of flow (loss modulus) measured through a different technique was 8 times lower than that of steak. The stiffness of Model B with cells was a factor 5 lower, and without cells a factor 10 lower than that of steak. According to the loss factors, the cultured piece of Model B should be more viscous than elastic, when compared to steak. Therefore the cultured piece of tissue with C2C12s seems to be less porous, less viscous, and less stiff than beef steak.

Nevertheless, these differences between Model B and steak are explainable. Model B was only cultured for 11 days and was far from being mature skeletal muscle tissue. This was confirmed by the low expression of MHC (i.e. the absence of many multi-nucleated myotubes), the amount of nuclei in multi-nucleated cells (which was <5), and the thickness of multi-nucleated myocytes seen on the histological images (which should be 15 - 45 μm in adult tissue, but does not appear thicker than 1 μm in Model B [67]). Further, the cultured tissue samples were fixed in 4% PFA, but the pieces of natural meat were not fixed. This might also influence the accuracy of the comparisons since it influences tissue behaviour as was observed in the porosity and recovery test. Future work could focus on the rheological measurements of fixed and non-fixed cultured tissue and natural tissue, as well as scaffolds without cells.

In summary, the scaffold of the current Model B and C did not meet all the set requirements, and did not result in a competitive piece of tissue with beef steak. Nevertheless, it can still be considered as an improved model compared to Model A, with realistically solvable challenges and drawbacks.

4.3. Future prospects

The results delivered by this research project were positive in many aspects. Successfully reproducing Model A was a valuable step in the developments of the tissue engineering department at Meatable B.V., since no piece of cultured skeletal had been produced previously. The various tests performed on candidate and final scaffolds (Agarose, Alginate, Novigel, and Bovine collagen) give insight in not only the scaffold itself, but also the different analysis parameters that can be used for comparison between scaffolds. This work is a stepping stone for up-scaled models currently used in the tissue engineering laboratory. Finally, the seeding of Model B with iPSCs (thus Model C) for the first time is a valuable contribution to future developments in the cell section of the laboratory.

Nevertheless, there are elements that should be further investigated and improved. The current testing methods could be improved by using more quantitative data for the comparison of images. Visualizing the scaffold through SEM would also contribute to the understanding of the architecture. It would also be interesting to visualize the rate of newly built scaffold by the cells during the remodelling. There should be more research on the development and adherence of iPSCs in 3D scaffolds. This can be done by varying the days of 2D pre-differentiation, and varying the cell seeding concentrations in scaffolds. It would also be recommended to perform mechanical analyses on fixed and non-fixed culture samples, native tissue, and bare scaffolds for a better comparison, since texture is an important factor in taste experience. Also, there should be experimented with Model B made from recombinant collagen and Matrigel, or recombinant collagen and laminin to meet certain requirements. Wang et al. mention the successful usage of fibrin as a scaffold, from which the recombinant animal free version could be tested as well [65]. Other directions that could be explored include using fibroblasts in the scaffold to quickly (re)build an ECM [10, 68]. Lastly, the tissues should be cultured over a longer period of time, in order to hopefully see more adult skeletal muscle tissue. This will also give insight in the change of stiffness, measure of flow, and change in viscous behaviour of the samples. All the above could contribute to a more successful Model C that is comparable to steak.

There are other stimulating factors besides the biochemical ones that play an important role in the desired cell behaviour once the cells are embedded in the scaffold. Many studies underline the advantages of also using physical factors for an increased growth and development of skeletal muscle tissue in vitro setups [7]. Beldjilali et al. found that mechanical and electrical stimulations have the best results for skeletal muscle tissue engineering.

Electrical stimulation plays an important role in native tissue, since the central nervous system provides electrical cues in the development, function, and repair of skeletal muscle tissue [12]. Hashimoto et al. optimized the parameters by suggesting pulses of <8V for three days for better adherence and proliferation, and pulses of 0.1V for better differentiation results [32]. Electrical stimulation stimulates the assembly of sarcomeres which promotes cell proliferation, differentiation, and alignment [7]. Electrical stimulation has several beneficial effects, but also requires biomaterials that transduce the electrical currents.

Mechanical stimulation (i.e. exercise) enhances cell alignment, proliferation, differentiation, and fusion, as well as functioning, myogenesis and muscle remodelling, such as the growth and thickening of muscle fibres [7]. There are many stretch regimes tested, which vary in cycles, stretching elongation, and duration. Zhang et al. found that stretching cells induced activation of FAK via integrin, which led to increased gene expression [72]. It may also influence the inflow of calcium in the cell through the ion channels and activate P13K and p38 signalling pathways, all positively influencing the cultivation of muscle tissue by up-regulating the expression of certain genes responsible for skeletal muscle progenitor development [7]. Mechanical stimulation has a wide range of positive effects on myogenesis and is therefore interesting for skeletal muscle tissue engineering.

When observing the native situation, a contraction of a muscle tissue starts with an electrical stimulation by the nerves, not by an external load that stimulates muscle hypertrophy. For this reason it is possible that electrical stimulation has a priority in in-vitro tissue development, though no article has been found

that clearly states that electrical stimulation should have priority compared to mechanical stimulation. This is probably due to the novelty of the engineering techniques and developments.

When thicker and more mature muscle tissue is cultured, other problems may arise. According to literature, cells should not be further than 150–200 μm from nutrition sources. In this research, the scaffolds with cells are still very porous, due to the less packed density of cells in the early stage of tissue development, and that diffusion is sufficient. Research should focus on creating channels within the scaffold once the tissue shows necrotic cores, by for instance creating micro-channels using soluble sugar scaffolds [45].

Once thicker pieces of tissue are being produced with channels, the focus could be on the flavour. The flavour of meat is influenced by its texture, juiciness, taste and aroma [18]. The flavour forms mainly during the preparation as a result of the Maillard reaction and lipid oxidation. These volatile compounds could be identified using olfactometry and mass spectrometry methodologies as is done by Flores et al. [62]. Cultured meat will probably not have the same colour as beef meat since it does not contain blood. According to Pat Brown, the protein hemoglobin could play a key role in colour and taste experience, since it catalyses the Maillard reaction and lipid oxidation [22, 36]. Recombinant hemoglobin from soybeans, which is very similar to hemoglobin found in blood, is already being produced by yeasts [31]. Future research could focus on the effects of adding recombinant hemoglobin on the colour and flavour of cultured meat.

Certain articles doubt the effectiveness of cultured meat in terms of sustainability, which evokes interesting debates due to the many estimations of the unknown production process [41, 61]. Cultured meat is undoubtedly a better option with regard to animal welfare. Progress in the research of cultured meat will also contribute to the understanding of native skeletal tissue, certain diseases, etc., and the development of treating volumetric muscle loss or cardiac muscle damage.

5. Conclusion

In conclusion, this research describes the successful improvements made to an existing 3D in-vitro skeletal tissue engineering method, seeded for the first time with iPSCs, as prototype model for cultured meat. Model B should be set as the basis model to optimise for the culture of iPSCs. The hydrogel scaffolds of both models were very comparable in terms of permeability, scaffold compaction by cell activity, and cell alignment. The replacement of rat tail with bovine collagen even seems to be better for cell development and cell density, probably due to the increased stiffness. The bovine collagen model with C2C12s was not comparable to steak, but a longer culture period could result in more similar tissue. When the improved model was seeded with pre-differentiated iPSCs instead of C2C12 myoblasts, the results demonstrated different cellular responses within the same scaffolding material. Notwithstanding the limitations of the last model, it can still be concluded that iPSCs will be a significant element in the future of cultured meat, given their endless capacities of self-renewal and broad variety of cell types, and this research has been a baby step towards the end goal of animal-free meat.

Acknowledgements. I wish to thank all the people whose assistance was a milestone in the completion of this project. Part of this work was supported by the bright team of Meatable B.V. with a special thanks to Ruud Out and Duong Nguyen. Thereby, I would like to thank prof. dr. ir. H. H. Weinans for his guidance, and Rowan Rimington for the help in setting the proof of concept model.

References

- [1] Abdallah Belal Adam. "Densities of Muzekah and Dead Chicken". In: *IJIRMPIS-International Journal of Innovative Research in Engineering & Multidisciplinary Physical Sciences* 3.1 (2015).
- [2] Peter Angele et al. "Influence of different collagen species on physico-chemical properties of crosslinked collagen matrices". In: *Biomaterials* 25.14 (2004), pp. 2831–2841.
- [3] AD Bach et al. "Skeletal muscle tissue engineering". In: *Journal of cellular and molecular medicine* 8.4 (2004), pp. 413–422.
- [4] Allen J Bailey. "The basis of meat texture". In: *Journal of the Science of Food and Agriculture* 23.8 (1972), pp. 995–1007.
- [5] JP Beier, RE Horsch, and AD Bach. "Tissue engineering of skeletal muscle". In: *Minerva Biotechnologica* 18.2 (2006), p. 89.
- [6] Megane Beldjilali-Labro et al. "Biomaterials in tendon and skeletal muscle tissue engineering: current trends and challenges". In: *Materials* 11.7 (2018), p. 1116.
- [7] Megane Beldjilali-Labro et al. "Biomaterials in tendon and skeletal muscle tissue engineering: current trends and challenges". In: *Materials* 11.7 (2018), p. 1116.
- [8] Paolo Bianco and Pamela Gehron Robey. "Stem cells in tissue engineering". In: *Nature* 414.6859 (2001), p. 118.
- [9] Jean-Michel Bourget et al. "Alignment of cells and extracellular matrix within tissue-engineered substitutes". In: *Advances in biomaterials science and biomedical applications* (2013), pp. 365–390.
- [10] Jean-Michel Bourget et al. "Human fibroblast-derived ECM as a scaffold for vascular tissue engineering". In: *Biomaterials* 33.36 (2012), pp. 9205–9213.
- [11] Roel GM Breuls, Timothy U Jiya, and Theo H Smit. "Scaffold stiffness influences cell behavior: opportunities for skeletal tissue engineering". In: *The open orthopaedics journal* 2 (2008), p. 103.
- [12] DR Campion et al. "Regulation of skeletal muscle development by the central nervous system in the fetal pig." In: *Growth* 42.2 (1978), pp. 189–204.
- [13] Andrew J Capel et al. "Scalable 3D printed moulds for human tissue engineered skeletal muscle". In: *Frontiers in bioengineering and biotechnology* 7 (2019), p. 20.
- [14] Giorgio Cittadella Vigodarzere and Sara Mantero. "Skeletal muscle tissue engineering: strategies for volumetric constructs". In: *Frontiers in physiology* 5 (2014), p. 362.
- [15] Adam Curtis and Chris Wilkinson. "Topographical control of cells". In: *Biomaterials* 18.24 (1997), pp. 1573–1583.
- [16] Dennis E Discher, Paul Janmey, and Yu-li Wang. "Tissue cells feel and respond to the stiffness of their substrate". In: *Science* 310.5751 (2005), pp. 1139–1143.
- [17] Janice A Dominov, Jonathan J Dunn, and Jeffrey Boone Miller. "Bcl-2 expression identifies an early stage of myogenesis and promotes clonal expansion of muscle cells". In: *The Journal of cell biology* 142.2 (1998), pp. 537–544.
- [18] JS Elmore, DS Mottram, et al. "Flavour development in meat". In: *Improving the sensory and nutritional quality of fresh meat* (2009), pp. 111–146.
- [19] Adam J Engler et al. "Matrix elasticity directs stem cell lineage specification". In: *Cell* 126.4 (2006), pp. 677–689.
- [20] Emeka K Enwere et al. "Role of the TWEAK-Fn14-cIAP1-NF- κ B signaling axis in the regulation of myogenesis and muscle homeostasis". In: *Frontiers in immunology* 5 (2014), p. 34.
- [21] FAO. "Covers Production-level data in terms of kilograms of meat seafood by type; livestock numbers and yields; and per capita food supply of animal products". In: *UN Food and Agriculture Organization (FAO) database since 1961* ().
- [22] Melissa Fellet. *A fresh take on fake meat*. 2015.
- [23] Dan Ferber. *WHO advises kicking the livestock antibiotic habit*. 2003.
- [24] Christian Frantz, Kathleen M Stewart, and Valerie M Weaver. "The extracellular matrix at a glance". In: *J Cell Sci* 123.24 (2010), pp. 4195–4200.
- [25] LE Freed et al. "Kinetics of chondrocyte growth in cell-polymer implants". In: *Biotechnology and Bioengineering* 43.7 (1994), pp. 597–604.
- [26] Lisa E Freed et al. "Biodegradable polymer scaffolds for tissue engineering". In: *Bio/technology* 12.7 (1994), p. 689.
- [27] Claudia Fuoco et al. "Matrix scaffolding for stem cell guidance toward skeletal muscle tissue engineering". In: *Journal of orthopaedic surgery and research* 11.1 (2016), p. 86.
- [28] Pierre J Gerber et al. "Environmental impacts of beef production: Review of challenges and perspectives for durability". In: *Meat science* 109 (2015), pp. 2–12.
- [29] Pallab Ghosh. *World's first lab-grown burger is eaten in London*. <https://www.bbc.com/news/science-environment-23576143>. 2013.

- [30] P Giusti et al. "Hydrogels of poly (vinyl alcohol) and collagen as new bioartificial materials". In: *Journal of Materials Science: Materials in Medicine* 4.6 (1993), pp. 538–542.
- [31] Mark S Hargrove et al. "Characterization of recombinant soybean leghemoglobin a and apolar distal histidine mutants". In: *Journal of molecular biology* 266.5 (1997), pp. 1032–1042.
- [32] Shigehiro Hashimoto et al. "Effect of pulsatile electric field on cultured muscle cells in vitro". In: *Journal of Systemics Cybernetics and Informatics* 10.1 (2012), pp. 1–6.
- [33] Mario Herrero et al. "Biomass use, production, feed efficiencies, and greenhouse gas emissions from global livestock systems". In: *Proceedings of the National Academy of Sciences* 110.52 (2013), pp. 20888–20893.
- [34] Saey Tuan Ho and Dietmar W Hutmacher. "A comparison of micro CT with other techniques used in the characterization of scaffolds". In: *Biomaterials* 27.8 (2006), pp. 1362–1376.
- [35] Ramona Cristina Ilea. "Intensive livestock farming: Global trends, increased environmental concerns, and ethical solutions". In: *Journal of agricultural and environmental ethics* 22.2 (2009), pp. 153–167.
- [36] Martijn Katan. "Plantenvloed voor vegaburgers". In: *NRC Handelsblad* (2020), p. 18.
- [37] Dorothee Klumpp et al. "Engineering skeletal muscle tissue—new perspectives in vitro and in vivo". In: *Journal of cellular and molecular medicine* 14.11 (2010), pp. 2622–2629.
- [38] Yusaku Kodaka, Gemachu Rabu, and Atsushi Asakura. "Skeletal muscle cell induction from pluripotent stem cells". In: *Stem cells international* 2017 (2017).
- [39] JH Kristensen and MA Karsdal. "Elastin". In: *Biochemistry of Collagens, Laminins and Elastin*. Elsevier, 2016, pp. 197–201.
- [40] Min Lee, Benjamin M Wu, and James CY Dunn. "Effect of scaffold architecture and pore size on smooth muscle cell growth". In: *Journal of Biomedical Materials Research Part A: An Official Journal of The Society for Biomaterials, The Japanese Society for Biomaterials, and The Australian Society for Biomaterials and the Korean Society for Biomaterials* 87.4 (2008), pp. 1010–1016.
- [41] John Lynch and Raymond Pierrehumbert. "Climate impacts of cultured meat and beef cattle". In: *Frontiers in Sustainable Food Systems* 3 (2019), p. 5.
- [42] V Mudera et al. "The effect of cell density on the maturation and contractile ability of muscle derived cells in a 3D tissue-engineered skeletal muscle model and determination of the cellular and mechanical stimuli required for the synthesis of a postural phenotype". In: *Journal of cellular physiology* 225.3 (2010), pp. 646–653.
- [43] Hiroshi Murata. "Rheology-Theory and application to biomaterials". In: *Janeza Trdine* 9.51000 (2012), pp. 403–426.
- [44] Antonio Musarò et al. "Stem cell-mediated muscle regeneration is enhanced by local isoform of insulin-like growth factor 1". In: *Proceedings of the National Academy of Sciences* 101.5 (2004), pp. 1206–1210.
- [45] Showan N Nazhat et al. "Controlled microchannelling in dense collagen scaffolds by soluble phosphate glass fibers". In: *Biomacromolecules* 8.2 (2007), pp. 543–551.
- [46] Fergal J O'Brien. "Biomaterials & scaffolds for tissue engineering". In: *Materials today* 14.3 (2011), pp. 88–95.
- [47] David Olsen et al. "Recombinant collagen and gelatin for drug delivery". In: *Advanced drug delivery reviews* 55.12 (2003), pp. 1547–1567.
- [48] Maria del Carmen Ortuño-Costela et al. "iPSC s: A powerful tool for skeletal muscle tissue engineering". In: *Journal of cellular and molecular medicine* (2019).
- [49] Z Pan and R Paul Singh. "Physical and thermal properties of ground beef during cooking". In: *LWT-Food Science and Technology* 34.7 (2001), pp. 437–444.
- [50] Matthias Pawlowski et al. "Inducible and deterministic forward programming of human pluripotent stem cells into neurons, skeletal myocytes, and oligodendrocytes". In: *Stem Cell Reports* 8.4 (2017), pp. 803–812.
- [51] H. Plecher. "Average prices for meat (beef) worldwide 1995 - 2025". In: <https://www.statista.com/statistics/675826/average-prices-meat-beef-worldwide/> (2019), p. 1.
- [52] Beth E Pollot et al. "Natural polymeric hydrogel evaluation for skeletal muscle tissue engineering". In: *Journal of Biomedical Materials Research Part B: Applied Biomaterials* 106.2 (2018), pp. 672–679.
- [53] RJ Prasad et al. "Global warming: genesis, facts and impacts on livestock farming and mitigation strategies". In: *Int. J. Agric. Innov. Res* 3 (2015), pp. 2319–1473.
- [54] Rowan P Rimington et al. "Biocompatible 3D printed polymers via fused deposition modelling direct C 2 C 12 cellular phenotype in vitro". In: *Lab on a Chip* 17.17 (2017), pp. 2982–2993.
- [55] Brittany L Rodriguez and Lisa M Larkin. "Functional three-dimensional scaffolds for skeletal muscle tissue engineering". In: *Functional 3D Tissue Engineering Scaffolds*. Elsevier, 2018, pp. 279–304.
- [56] Carlo Alberto Rossi, Michela Pozzobon, and Paolo De Coppi. "Advances in musculoskeletal tissue engineering: moving towards therapy". In: *Organogenesis* 6.3 (2010), pp. 167–172.
- [57] Tania Rozario and Douglas W DeSimone. "The extracellular matrix in development and morphogenesis: a dynamic view". In: *Developmental biology* 341.1 (2010), pp. 126–140.
- [58] Pierre Sans and Pierre Combris. "World meat consumption patterns: An overview of the last fifty years (1961–2011)". In: *Meat Science* 109 (2015), pp. 106–111.
- [59] Patrick Seale, Atsushi Asakura, and Michael A Rudnicki. "The potential of muscle stem cells". In: *Developmental cell* 1.3 (2001), pp. 333–342.
- [60] Janet Shansky et al. "A simplified method for tissue engineering skeletal muscle organoids in vitro". In: (1996).
- [61] Lieven Thorrez and Herman Vandenburgh. "Challenges in the quest for 'clean meat'". In: *Nature biotechnology* 37.3 (2019), p. 215.
- [62] Fidel Toldrá. *Lawrie's meat science*. Woodhead Publishing, 2017.
- [63] Michael J Toth et al. "Skeletal muscle fiber size and fiber type distribution in human cancer: Effects of weight loss and relationship to physical function". In: *Clinical nutrition* 35.6 (2016), pp. 1359–1365.
- [64] Jonathan H Tsui et al. "Harnessing sphingosine-1-phosphate signaling and nanotopographical cues to regulate skeletal muscle maturation and vascularization". In: *ACS nano* 11.12 (2017), pp. 11954–11968.
- [65] Jason Wang et al. "Engineered skeletal muscles for disease modeling and drug discovery". In: *Biomaterials* (2019), p. 119416.
- [66] Ling Wang et al. "Nanofiber yarn/hydrogel core-shell scaffolds mimicking native skeletal muscle tissue for guiding 3D myoblast alignment, elongation, and differentiation". In: *ACS nano* 9.9 (2015), pp. 9167–9179.
- [67] Wei Wang et al. "Compatibility of hyaluronic acid hydrogel and skeletal muscle myoblasts". In: *Biomedical materials* 4.2 (2009), p. 025011.
- [68] T Wong, JA McGrath, and H Navsaria. "The role of fibroblasts in tissue engineering and regeneration". In: *British Journal of Dermatology* 156.6 (2007), pp. 1149–1155.
- [69] Congqi Yan and Darrin J Pochan. "Rheological properties of peptide-based hydrogels for biomedical and other applications". In: *Chemical Society Reviews* 39.9 (2010), pp. 3528–3540.
- [70] Beatrice Yue. "Biology of the extracellular matrix: an overview". In: *Journal of glaucoma* (2014), S20.
- [71] Susi Zatti et al. "Micropatterning topology on soft substrates affects myoblast proliferation and differentiation". In: *Langmuir* 28.5 (2012), pp. 2718–2726.
- [72] Sarah Jingying Zhang, George A Truskey, and William E Kraus. "Effect of cyclic stretch on β 1D-integrin expression and activation of FAK and RhoA". In: *American Journal of Physiology-Cell Physiology* 292.6 (2007), pp. C2057–C2069.

Appendices index

Appendix A:

Overview of different possible scaffolds for tissue engineering based on a literature review

Appendix B:

Different tested ways of casting and cultivating 3D hydrogel scaffolds

Appendix C:

Different tested hydrogel scaffolds in 3D

Appendix D:

Different tested hydrogel scaffolds in 2D

Appendix E:

SOP for assembling and preparing 3D printed moulds

Appendix F:

SOP for maintenance of iPSCs in adherence (2D)

Appendix G:

SOP for the differentiation of iPSCs

Appendix H:

SOP for immunofluorescence staining of tissue in toto

Appendix I:

Unconfined compression test of scaffold samples

Appendix J:

Immunofluorescence staining

Appendix K:

Porosity and recovery test results

Appendix L:

Rheometry setup and background information

Appendix A.

Overview of different possible scaffolds for tissue engineering based on a literature review

Natural materials

Natural Material	Advantages for Skeletal Muscle Tissue Engineering	Disadvantages for Skeletal Muscle Tissue Engineering	Remarkable	Ref.
Collagen	<ul style="list-style-type: none"> - Native ECM - Biocompatible/ Biodegradable - Used as hydrogel or electrospun - Promotes cell differentiation 	<ul style="list-style-type: none"> - Limited cell migration 	Most research seems to be done with collagen	63,79
Fibrin	<ul style="list-style-type: none"> - RGD present; enhances cell adhesion - Biocompatible/ Biodegradable - Composition adaptable (thrombin) - Enhances cell migration, proliferation - Stores growth factors - Degrades symmetrically with formation of new cell-produced ECM 	<ul style="list-style-type: none"> - Not optimal mechanical properties; 	Highest potential long-term use in skeletal muscle tissue engineering ⁶³	63,64,80
Alginate	<ul style="list-style-type: none"> - Biocompatible/ Biodegradable - Cheap - Biodegradable - Adjustable stiffness 	<ul style="list-style-type: none"> - Quick degradation - No optimal connected pores - Hard to gelate in specific form - Poor cell attachment 	Made of seaweed; useful when combined with adhesion molecules	22,63,65–69,71
Gelatin	<ul style="list-style-type: none"> - Biocompatible/ Biodegradable - Cheap 	<ul style="list-style-type: none"> - Only been used successfully in electrospun form 	Hydrolysed collagen	12,65
Hyaluronic acid	<ul style="list-style-type: none"> - Present in native ECM - Promotes cell proliferation & migration - Mediates repair process - Biocompatible/ Biodegradable 			12,65
Chitosan	<ul style="list-style-type: none"> - Antibacterial properties - Biocompatible/ Biodegradable - High mechanical strength - Cheap 		Produced using fungi or exoskeleton of arthropods; resembles cellulose	73,81,82
Agarose	<ul style="list-style-type: none"> - Enhances molecular transport - Biocompatible/ Biodegradable - Enhances cell metabolism & migration - Porous - Stable degradability - Cheap 	<ul style="list-style-type: none"> - Inhibits cell adhesion - Cannot be used with cold preparation conditions - Brittle material 	Made of seaweed	63,74,83
Matrigel & Geltrex	<ul style="list-style-type: none"> - Enhances cell proliferation, adhesion, migration, differentiation 	<ul style="list-style-type: none"> - Must be used in combination with other materials for 3D scaffolding structure 	Secreted by murine Engelbreth-Hold-Swarm tumor cells	1,68
Soy protein	<ul style="list-style-type: none"> - Biodegradable/ Biocompatible - Adjustable bioactive properties - Cheap 	<ul style="list-style-type: none"> - Little studied yet 	Used as gels and films	75
Decellularized scaffolds	<ul style="list-style-type: none"> - Is the native ECM 	<ul style="list-style-type: none"> - Contrasting results in literature - Donor needed - Manufacturing procedure requires toxic chemicals that can remain in end product 		32,84–86
Fibroblasts	<ul style="list-style-type: none"> - Synthesise and deposit the native ECM 	<ul style="list-style-type: none"> - Only used in 2D - Substratum required for myotube alignment - Hard to control - More success in in-vivo setup 	Non-scaffold approach	8,87–90

Synthetic Materials

Synthetic materials	Advantages for Skeletal Muscle Tissue Engineering	Disadvantages for Skeletal Muscle Tissue Engineering	Remarkable	Ref.
<i>PGA</i>	<ul style="list-style-type: none"> - Biodegradable (non-enzymatic hydrolysis) - Biocompatible - Myoblasts survive, organise and regenerate - Adjustable mechanical and structural properties 	<ul style="list-style-type: none"> - Binding site required 	A lot studied	93,94
<i>PLA</i>	<ul style="list-style-type: none"> - Biodegradable / biocompatible - Cells adhere in 2D - Adjustable mechanical and structural properties 	<ul style="list-style-type: none"> - More research required on more precise and detailed printing nozzle for enhanced scaffold designs 	Made of corn starch or sugarcane	95,96
<i>PLGA</i>	<ul style="list-style-type: none"> - Biocompatible / biodegradable - Adjustable degradability - Adjustable mechanical and structural properties 	<ul style="list-style-type: none"> - Low hydrophobicity - Poor cell affinity - Needs to be altered with different biological factors 	Often used to prepare fibrous scaffolds for tissue engineering	97
<i>PEG</i>	<ul style="list-style-type: none"> - Hydrophilic - Minimal inflammatory response - Promotes myotube development and alignment - Adjustable mechanical and structural properties 	<ul style="list-style-type: none"> - Still no ideal mechanical properties - No physical biological cues 	Used as a hydrogel with C2C12	98
<i>PDMS</i>	<ul style="list-style-type: none"> - Biocompatible - Oxygen highly soluble in PDMS - Adjustable mechanical and structural properties 	<ul style="list-style-type: none"> - Hydrophobic - No cell adherence (coating needed) 	Used by solvent casting and particulate leaching techniques, in combination with human mesenchymal stem cells	99,100
<i>PCL</i>	<ul style="list-style-type: none"> - Flexible - Cheap - Cells adhere, but not optimal - Adjustable mechanical and structural properties 	<ul style="list-style-type: none"> - Slow biodegradable - Hydrophobic 	Used by electrospinning. Using in combination with PLGA improved myoblast proliferation.	101
<i>PANi</i>	<ul style="list-style-type: none"> - Semi-flexible - Biocompatible - Conducting - Adjustable mechanical and structural properties 	<ul style="list-style-type: none"> - Only recently being used in science 	Used by electrospinning; positive effects of conductivity, mechanical strength and surface requirements showed	102

Hybrid materials

Hybrid materials	Advantages for Skeletal Muscle Tissue Engineering	Disadvantages for Skeletal Muscle Tissue Engineering	Remarkable	Ref.
<i>PEG-fibrinogen</i>	<ul style="list-style-type: none"> - Accurate control of material properties - Inherent bioactive cues - Well controllable liquid-solid transition - Adjustable mechanical and structural properties 	<ul style="list-style-type: none"> - Only recently studied 	Used in-vivo for a functional artificial muscle tissue in mice	22,105,106
<i>PDMS-Fibrin</i>	<ul style="list-style-type: none"> - Successfully used with myoblasts - Adjustable mechanical and structural properties 	<ul style="list-style-type: none"> - Only recently studied 	Used as micropatterned scaffold with myoblasts, formed myotubes	103
<i>PLGA-Collagen</i>	<ul style="list-style-type: none"> - Enhances attachment myoblasts - Enhances proliferation myoblasts - Increaseable hydrophilicity - Adjustable mechanical and structural properties 	<ul style="list-style-type: none"> - Only recently studied 	Several times successfully used (electrospinning) with myoblasts, but adding Graphene Oxide even made it better	51,107
<i>PCL-Collagen</i>	<ul style="list-style-type: none"> - Stimulates myoblast alignment - Stimulates myotube formation - Adjustable mechanical and structural properties - Biocompatible - Biodegradable - Easily fabricated 	<ul style="list-style-type: none"> - Only recently studied 	Used by electrospinning	104
<i>PCL-Silk fibroin</i>	<ul style="list-style-type: none"> - Biocompatible - Enhances cellular alignment & elongation - Enhances myotube formation - Easily fabricated - Adjustable mechanical and structural properties 	<ul style="list-style-type: none"> - Only recently studied 	Used by electrospinning, seeded with C2C12 in PEGS-M polymer as a hydrogel	16

1. Bach, A. D., Beier, J. P., Stern-staeter, J. & Horch, R. E. Skeletal muscle tissue engineering. **8**, 413–422 (2004).
8. Rodriguez, B. L. & Larkin, L. M. Functional three-dimensional scaffolds for skeletal muscle tissue engineering. *Univ. Michigan* (2018). doi:10.1016/B978-0-08-100979-6.00012-4
12. Wang, W., Fan, M., Zhang, L., Liu, S. & Sun, L. Compatibility of hyaluronic acid hydrogel and skeletal muscle myoblasts. **025011**,
16. Al, W. E. T. Nano fi ber Yarn / Hydrogel Core À Shell Sca ff olds Mimicking Native Skeletal Muscle Tissue for Guiding 3D Myoblast. 9167–9179 (2015). doi:10.1021/acsnano.5b03644
22. Fuoco, C., Petrilli, L. L., Cannata, S. & Gargioli, C. Matrix scaffolding for stem cell guidance toward skeletal muscle tissue engineering. *J. Orthop. Surg. Res.* 1–8 (2016). doi:10.1186/s13018-016-0421-y
32. Qazi, T. H., Mooney, D. J., Pumberger, M., Geißler, S. & Duda, G. N. Biomaterials Biomaterials based strategies for skeletal muscle tissue engineering : Existing technologies and future trends. *Biomaterials* **53**, 502–521 (2015).
51. Shin, Y. C. *et al.* Stimulated myoblast differentiation on graphene oxide-impregnated PLGA-collagen hybrid fibre matrices. 1–11 (2015). doi:10.1186/s12951-015-0081-9
63. Pollot, B. E., Rathbone, C. R., Wenke, J. C. & Guda, T. Natural polymeric hydrogel evaluation for skeletal muscle tissue engineering. **0075**, 672–679 (2017).
64. Weijers, E. M. Review : Fibrin matrices for tissue engineering.
65. Chachques, J. C. & Pradas, M. M. Biomaterials for Cardiac Tissue Engineering. (2008).
66. Ali, A. & Ahmed, S. Recent Advances in Edible Polymer Based Hydrogels as a Sustainable Alternative to Conventional Polymers. *J. Agric. Food Chem.* **66**, 6940–6967 (2018).
67. Venugopal, J. R. *et al.* Biomaterial strategies for alleviation of myocardial infarction. *J. R. Soc. Interface* **9**, 1–19 (2012).
68. Nelson, D. M., Ma, Z., Fujimoto, K. L., Hashizume, R. & Wagner, W. R. Intra-myocardial biomaterial injection therapy in the treatment of heart failure: Materials, outcomes and challenges. *Acta Biomater.* **7**, 1–15 (2011).
69. Rowley, J. A., Madlambayan, G. & Mooney, D. J. Alginate hydrogels as synthetic extracellular matrix materials. **20**, 45–53 (1999).
71. Ansari, S. *et al.* Muscle tissue engineering using gingival mesenchymal stem cells encapsulated in alginate hydrogels containing multiple growth factors. **44**, 1908–1920 (2017).
73. Shit, S. C. & Shah, P. M. Edible Polymers : Challenges and Opportunities. **2014**, (2014).
74. J Jeppson, C Laurell, B. F. Agarose Gel Electrophoresis. **25**, 629–638 (2001).
75. Chien, K. B. & Shah, R. N. Acta Biomaterialia Novel soy protein scaffolds for tissue regeneration : Material characterization and interaction with human mesenchymal stem cells. *Acta Biomater.* **8**, 694–703 (2012).
79. Beldjilali-Labro, M. *et al.* Biomaterials in tendon and skeletal muscle tissue engineering: Current trends and challenges. *Materials (Basel)*. **11**, (2018).
80. Borschel, G. H., Dow, D. E., Dennis, R. G. & Brown, D. L. Tissue-engineered axially vascularized contractile skeletal muscle. *Plast. Reconstr. Surg.* **117**, 2235–2242 (2006).
81. Mucha, M., Wańkiewicz, K. & Balcerzak, J. Analysis of water adsorption on Chitosan and its blends with hydroxypropylcellulose. *E-Polymers* 1–10 (2007). doi:10.1515/epoly.2007.7.1.181
82. Kim, S. J., Shin, S. R., Lee, S. M., Kim, I. Y. & Kim, S. I. Electromechanical properties of hydrogels based on chitosan and poly(hydroxyethyl methacrylate) in NaCl solution. *Smart Mater. Struct.* **13**, 1036–1039 (2004).
83. Yixue, S. *et al.* Modification of agarose with carboxylation and grafting dopamine for promotion of its cell-adhesiveness. *Carbohydr. Polym.* **92**, 2245–2251 (2013).
84. Borschel, G. H., Dennis, R. G. & Kuzon, W. M. Contractile skeletal muscle tissue-engineered on an acellular scaffold. *Plast. Reconstr. Surg.* **113**, 595–602 (2004).
85. Conconi, M. T. *et al.* Homologous muscle acellular matrix seeded with autologous myoblasts as a tissue-engineering approach to abdominal wall-defect repair. *Biomaterials* **26**, 2567–2574 (2005).
86. Urciuolo, A. & De Coppi, P. Decellularized tissue for muscle regeneration. *Int. J. Mol. Sci.* **19**, 1–11 (2018).
87. Michael Williams, Tatiana Kostrominova, Ellen Arruda, L. L. Effect of implantation on engineered skeletal muscle contstructs. *J. Tissue Eng. Regen. Med.* 434–442 (2011). doi:10.1002/term
88. Vandusen, K. W., Syverud, B. C., Williams, M. L., Lee, J. D. & Larkin, L. M. Engineered skeletal muscle units for repair of volumetric muscle loss in the tibialis anterior muscle of a rat. *Tissue Eng. - Part A* **20**, 2920–2930 (2014).
89. Syverud, B. C., Vandusen, K. W. & Larkin, L. M. Effects of Dexamethasone on Satellite Cells and Tissue Engineered Skeletal Muscle

- Units. *Tissue Eng. - Part A* **22**, 480–489 (2016).
90. Huang, Y. C., Dennis, R. G., Larkin, L. & Baar, K. Rapid formation of functional muscle in vitro using fibrin gels. *J. Appl. Physiol.* **98**, 706–713 (2005).
 93. Saxena, A. K., Willital, G. H. & Vacanti, J. P. Vascularized three-dimensional skeletal muscle tissue-engineering. **11**, 275–281 (2001).
 94. Zambon, J. P. *et al.* Histological changes induced by Polyglycolic-Acid (PGA) scaffolds seeded with autologous adipose or muscle-derived stem cells when implanted on rabbit bladder. **10**, 278–288 (2014).
 95. Ricotti, L. *et al.* Adhesion and proliferation of skeletal muscle cells on single layer poly (lactic acid) ultra-thin films. 809–819 (2010). doi:10.1007/s10544-010-9435-0
 96. Rimington, R. P., Christie, S. D. R., Capel, A. J. & Lewis, M. P. Lab on a Chip Biocompatible 3D printed polymers via fused phenotype in vitro †. 2982–2993 (2017). doi:10.1039/c7lc00577f
 97. Zhao, W. *et al.* Fabrication of functional PLGA-based electrospun scaffolds and their applications in biomedical engineering. *Mater. Sci. Eng. C* **59**, 1181–1194 (2016).
 98. Salimath, A. S. & García, A. J. Biofunctional hydrogels for skeletal muscle constructs. 967–976 (2016). doi:10.1002/term
 99. Eileen Pedraza, Ann Brady, Christopher Fraker, C. S. Synthesis of Macroporous Poly(dimethylsiloxane) Scaffolds for Tissue Engineering Applications. *Biomater Sci Polym Ed.* **24**, 1041–1056 (2013).
 100. Lam, M. T., Sim, S., Zhu, X. & Takayama, S. The effect of continuous wavy micropatterns on silicone substrates on the alignment of skeletal muscle myoblasts and myotubes. **27**, 4340–4347 (2006).
 101. Padilla, C. *et al.* Improving myoblast differentiation on electrospun poly (e -caprolactone) scaffolds. 2241–2251 (2017). doi:10.1002/jbm.a.36091
 102. Hosseinzadeh, S., Mahmoudifard, M. & Mohamadyar-toupanlou, F. The nanofibrous PAN-PANi scaffold as an efficient substrate for skeletal muscle differentiation using satellite cells. *Bioprocess Biosyst. Eng.* **39**, 1163–1172 (2016).
 103. Lam, M. T., Huang, Y., Birla, R. K. & Takayama, S. Biomaterials Microfeature guided skeletal muscle tissue engineering for highly organized 3-dimensional free-standing constructs. *Biomaterials* **30**, 1150–1155 (2009).
 104. Choi, J. S., Lee, S. J., Christ, G. J., Atala, A. & Yoo, J. J. Biomaterials The influence of electrospun aligned poly (3 -caprolactone)/ collagen nanofiber meshes on the formation of self-aligned skeletal muscle myotubes. **29**, 2899–2906 (2008).
 105. Almany, L. & Seliktar, D. Biosynthetic hydrogel scaffolds made from fibrinogen and polyethylene glycol for 3D cell cultures. *Biomaterials* **26**, 2467–2477 (2005).
 106. Peyton, S. R., Kim, P. D., Ghajar, C. M., Seliktar, D. & Putnam, A. J. The effects of matrix stiffness and RhoA on the phenotypic plasticity of smooth muscle cells in a 3-D biosynthetic hydrogel system. *Biomaterials* **29**, 2597–2607 (2008).
 107. Chen, D. W. *et al.* Sustainable release of vancomycin, gentamicin and lidocaine from novel electrospun sandwich-structured PLGA/collagen nanofibrous membranes. *Int. J. Pharm.* **430**, 335–341 (2012).

Appendix B.

Different tested ways of casting and cultivating 3D hydrogel scaffolds

Before implementing the 3D printed moulds with poles for 3D skeletal muscle tissue engineering, designed by Capel et al. at the Loughborough University, different other ways of cultivating cells in hydrogels were tried. This appendix gives an overview in chronological order of the different ideas that were used by the author. The iPSCs were cultured according to the proliferation and differentiation protocols. The hydrogels were prepared according to appendix D.

1. Drops in 24-well plates

At the beginning of the research project, different hydrogels were selected as a possible scaffold for the cultivation of skeletal muscle tissue from iPSCs. There was no existing set-up for 3D cultivation of muscle tissue. Therefore, the initial experiments of testing the gelation of different hydrogels, and testing the survival and proliferation of cells were done in a simple set-up.

1.1. Materials and Methods

The hydrogels were prepared according to the hydrogel-related protocol. At the start of the research project, there were no C2C12 myoblasts at the laboratory. This is why the experiments were performed with pre-differentiated iPSCs. iPSCs were seeded at a density of 200.000 cells per 50uL hydrogel. Drops of 50uL hydrogel scaffold plus cells were placed at the bottom of a 24 well plate. The drop was solidified in the incubator, where after warm growth medium was added.



Figure 1. 24 well plate with hydrogel drops in each well

1.2. Results & Conclusion

The microscopical pictures of the edge and center of the hydrogel scaffold drops are pictured in Figure 2. Cell survival was assessed with Tripian Blue staining. As can be seen in figure 2, do the cells proliferate, but not stretch or align.

There was concluded that the cells might need better adherence molecules, and a kind of mechanical stimulus. Many articles that culture in-vitro skeletal tissue, use something like poles for static mechanical tension. The Noviolgel should be altered with binding peptides.

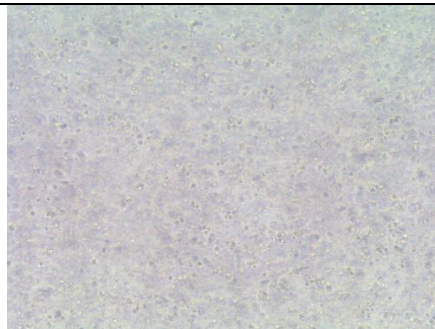
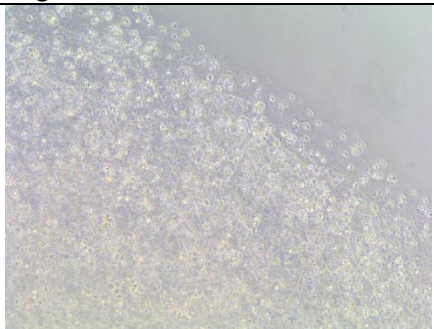
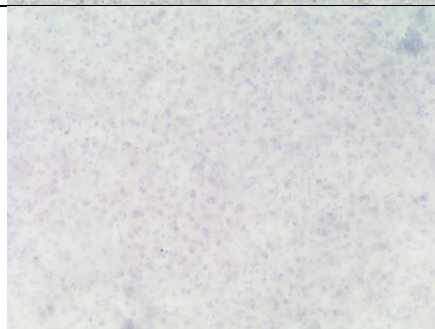
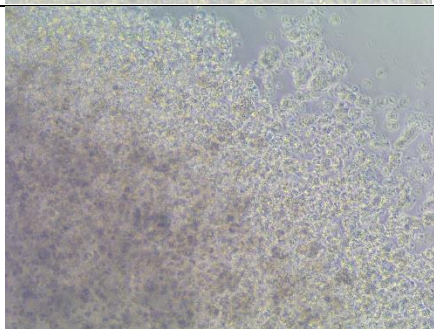
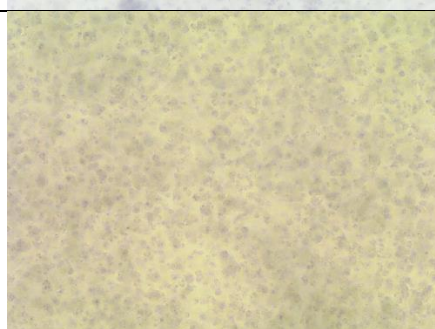
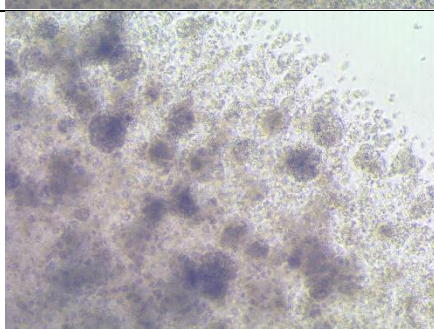
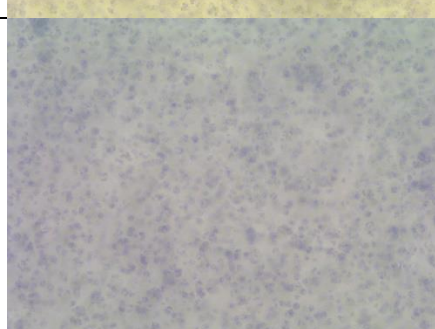
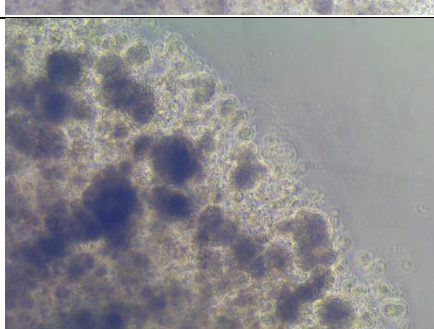
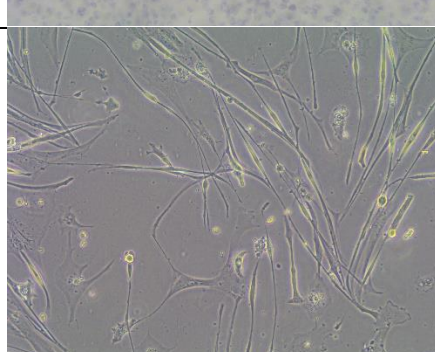
Type hydrogel	Center	Edge
Rat tail collagen (1.7mg/mL)		
Noviogel P1K		
Noviogel P5K1		
Noviogel P5K2.5		
Control (iPSCs in Geltrex coated well, no hydrogel scaffold)		

Figure 2. Overview of microscopical pictures from center and edge of a hydrogel drop seeded with iPSCs after 12 days of culture. The drops were 50uL and placed in wells of a 24 well plate.

2. Carbon poles

To initiate a static mechanical stimulus within the hydrogel for the cells to align and stretch, inserts for in the wells of a 24 well plate were made. The gel was cast between and around the poles within the 24 well plate well. The poles were first made of carbon steel, but these started to rust after several days in medium. Therefore, the poles were changed by poles made from stainless steel. The hydrogels were seeded with iPSCs, but experiments were stopped after 5 days since there was no change in cell stretching or alignment observed, even though the cells survived well.

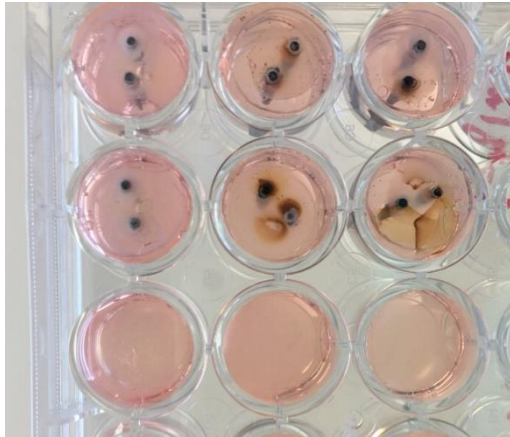


Figure 3. Bottom view of carbon steel pole inserts in the wells with medium and hydrogel. Several wells show stains of rust.

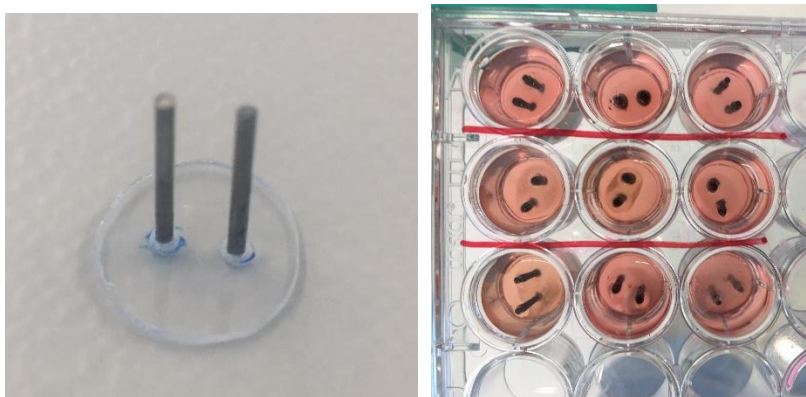


Figure 4. Left: Designed insert for in a well of a 24 well plate, poles made of stainless steel. Right: Bottom view of stainless steel inserts with cast hydrogel around the poles in medium

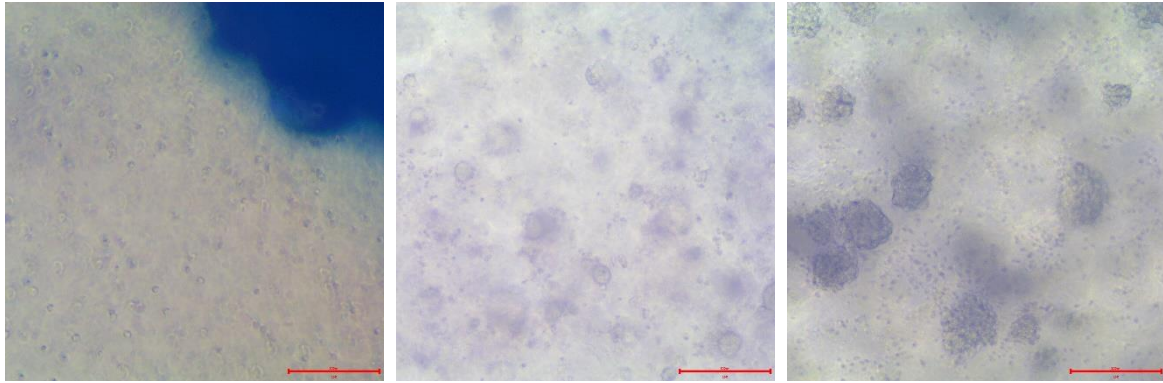


Figure 5. Left: microscopical picture of ipsc seeded rat tail collagen hydrogel with in the right top corner a part of the stainless steel pole. Middle and right: detailed view of the iPSCs in the hydrogel that form agglomerates instead of stretch.

3. Chamber #1 and Ospin Bioreactor

To optimise the culture set-up, there was a need of controlled pH, temperature and oxygen of the medium. Therefore, an Ospin Bioreactor was installed. The bioreactor monitors the flow, temperature, pH and Oxygen of the medium that is added to the tissue culture chamber. A closed chamber for the hydrogel was designed, including poles, and Euler locks to connect it to the Ospin Bioreactor circuit.

3.1. Materials & Methods

Hydrogels were made according to the different protocols, and seeded with 2.000.000 cells (iPSC) per 500uL hydrogel. The chamber was under sterile conditions filled with 500uL hydrogel+cells, and the lid was added. After solidification, the medium was added and the chamber was attached to the Ospin bioreactor circuit (figure 7).

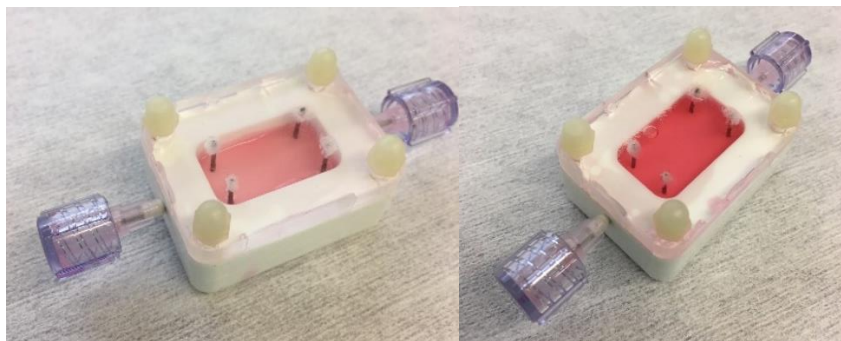


Figure 6. Designed closed chamber for skeletal muscle tissue cultivation, with removable transparent lid. On the left, the chamber is filled with 500uL hydrogel (rat tail collagen) and cells without medium. On the right, the hydrogel was set and medium was added to it.

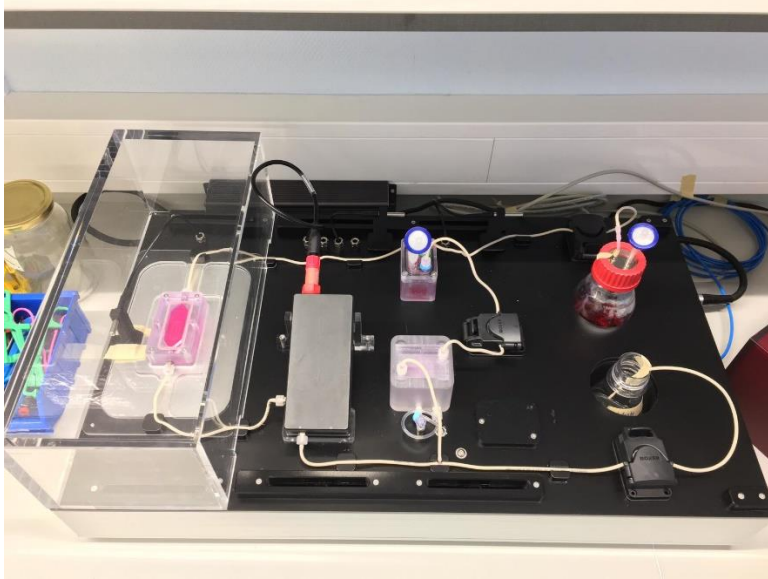


Figure 7. Picture of the Ospin Bioreactor, with on the left a perplex hood where under the tissue culture chamber is settled (pink). The inflow and outflow tubes can be seen as well.

3.2. Results & Conclusion

Rat tail collagen was used as scaffold for the hydrogel in the closed chamber. Microscopical analyses showed that the cells survived, but the survival rate was not very high. There was no stretching or alignment of the cells observed.

The set-up was still not ideal. Maybe, the distance between the poles was too big for a proper static mechanical tension.

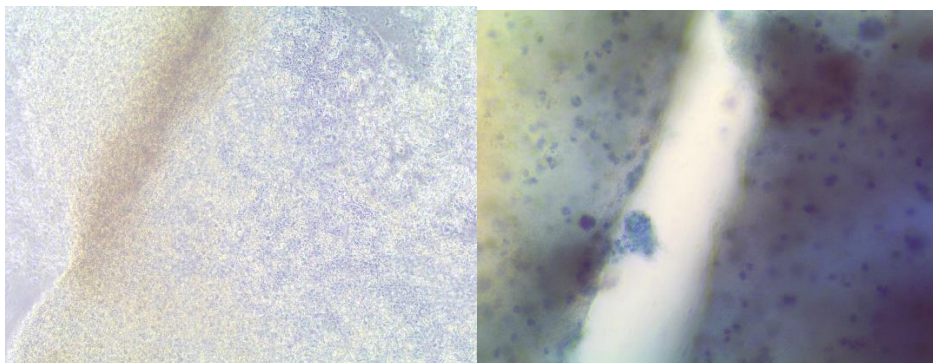


Figure 8. Left; microscopical analysis of iPSC laden hydrogel made of rat tail collagen. Right; Tripan Blue staining to visualize cell death within scaffold.

4. Chamber #2 and Ospin Bioreactor

The height between inflow point in the chamber for medium and the bottom of the chamber are the limiting factor of the thickness of the hydrogel. For more pole contact, and thus a thicker hydrogel scaffold, the chamber was redesigned and made deeper. This allowed the casting of a thicker layer of hydrogel. For the first experiments with this chamber, the gels (250uL, P5K2.5 Novigel and Rat tail collagen 1.7mg/mL) were only cast between two poles on one side of the chamber (see figure 9).

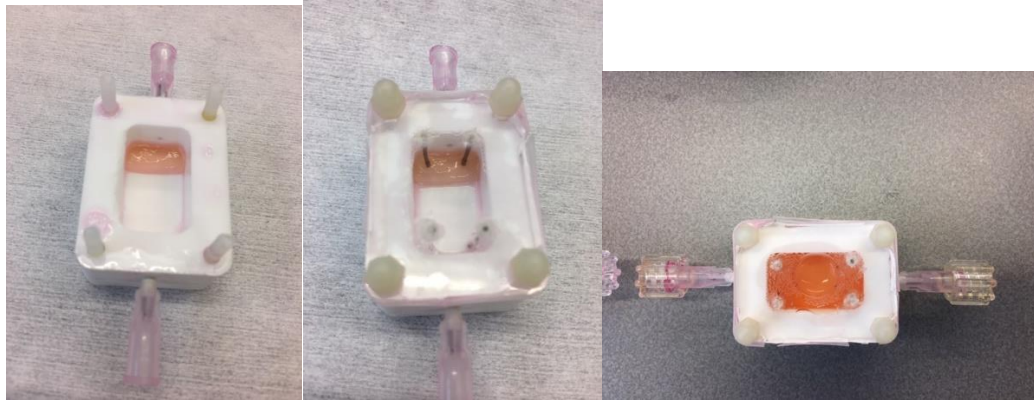


Figure 9. Redesigned chamber with hydrogel cast between two poles on one side of the chamber. Left; chamber without lid and with hydrogel. Middle; chamber filled with hydrogel and lid with poles added. Right; chamber filled with medium.

4.1. Results & Conclusion

After 10 days of culture, the samples of Rat tail collagen (1.7mg/mL), as can be seen in Figure 10, showed a certain stripes. Future research should provide more information on what these stripes were. They could be stretching cells, which could be proved by immunofluorescence staining, or could be folds in the scaffold material. Thereby, did the staining with Tripian Blue show that there was not a lot of cell death. Cells seemed to proliferate, but did not stretch.

The hydrogel samples made from Noviolgel P5K2.5 did not show any stripes, but showed that the cells started to form agglomerates, which is an indicator for cell proliferation. Staining the gel with Tripian Blue showed that there was not a lot of cell death.

The set-up was still not optimal, but the thickness, distance to the poles, and flow of medium seemed to have some improving effect on the cells.

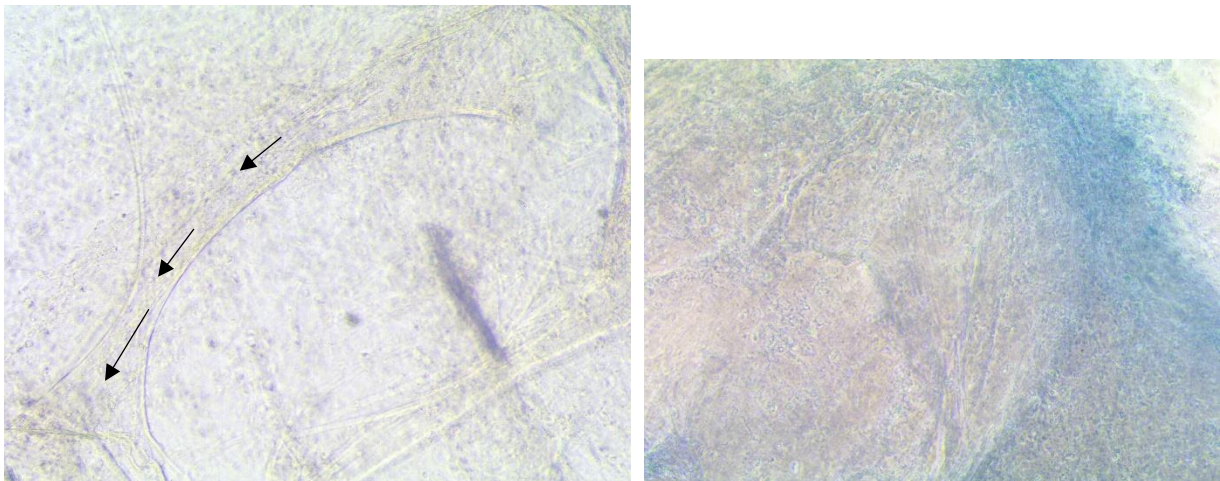


Figure 10. Left: Microscopical analysis of Rat tail collagen in Chamber #2, where stripes were observed. Right; Tripian Blue staining of rat tail hydrogel with iPSCs after 10 days of culture.

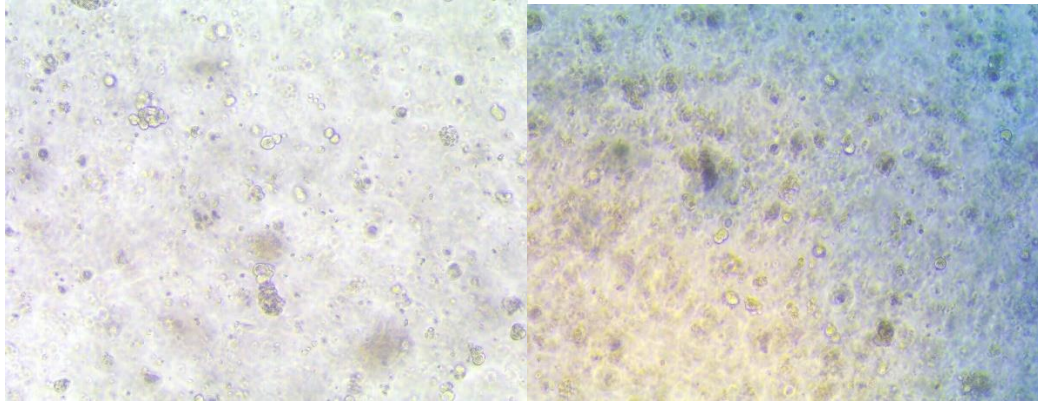


Figure 11. Left: microscopical analysis of Noviolgel P5K2.5 hydrogel with iPSCs after 10 days of culture. Right; Tripian Blue staining of Noviolgel P5K2.5 hydrogel with iPSCs after 10 days of culture.

Appendix C.

Different tested hydrogel scaffolds 3D

This appendix describes the different experiments that were performed to test different possible alternatives for the rat tail collagen in the Model A set-up. Through literature review, the most attractive scaffolds for 3D tissue engineering were selected. The requirements for the alternative scaffold were (preferably) animal free, cheap, scalable, and edible. Therefore, bovine collagen (animal-based), agarose (plant-based), alginate (plant-based), and Noviolgel (synthetical-based) were tested. The experiments in 3D performed on agarose, alginate, and Noviolgel will be reported in the following part. These were a follow up after the 2D tests which can be found in '*Appendix D; Different tested hydrogel scaffolds 2D*'.

1. Agarose

Agarose is extracted from certain types of red seaweeds. The material can be fractionated into two types; agaropectin (which has a high content of sulfate and carboxyl groups), and agarose (nearly neutral fraction). It is often used to separate large molecules, such as DNA, during electrophoresis. The powder dissolves in hot water and gels when cooling down. Agarose hydrogels have been proven to positively influence molecular transport and cell metabolism.¹ The gel is interconnective porous and stable, which improves cell migration, and has shown to be promising for muscle tissue engineering.¹ Nevertheless, agarose hydrogels have not been proven to enhance cell proliferation due to the inhibition of cell attachment.¹

Pollot et al. demonstrated that agarose has a high elastic modulus and big interconnected pores compared to collagen, alginate, and fibrin.⁶³ Even though the material has a higher stiffness and is more resistant to deformation, the material was the most brittle. The material seems promising for 3D skeletal tissue engineering.¹

1.1. SOP for preparation of agarose hydrogel scaffold

Based on work of Varoni et al.²

- Pre-warm plates to 37°C for a couple of hours or from the previous day onwards
- Pre-warm medium to 37°C
- Prepare cell solution:
 - o Detach the cells from the well plate and suspend in solution
 - o Count the cells with cell viability marker and adjust to desired concentration
- Prepare agarose hydrogel stock solution:
 - o Dissolve low-gelling agarose in PBS (without Ca & Mg) to a final concentration of 1.3% wt
 - o Heat the mixture in a microwave at 800W for around 2 min; stir every 15 seconds until everything is dissolved.
 - o Let mixture cool to 42 °C.
- Prepare mixture:
 - o Mix the cells, MEM and Matrigel
 - o Mix the above mixture with Agarose working solution

¹ Pollot, B. E., Rathbone, C. R., Wenke, J. C. & Guda, T. Natural polymeric hydrogel evaluation for skeletal muscle tissue engineering. 0075, 672–679 (2017).

² Varoni et al. Agarose gel as biomaterial or scaffold for implantation surgery: characterization, histological and histomorphometric study on soft tissue response, 2012.

- Transfer hydrogel mixture to desired mould or well
- Gelate the gel at at least 26-30 °C
- Gently add warm medium to each well via the side of the well
- Incubate samples for the duration of the experiment at 37 °C. When required; refresh medium using a micropipette to gently remove the old medium and gently add fresh warm medium

Agarose hydrogel scaffold (1% w/v)	
Agarose working solution (1.3% w/v, in PBS)	76.5%
Minimum Essential Medium (10x)	8.5%
Matrigel	10%
Cells	5%

1.2. Agarose tests and results

1.2.1. Finding the ideal Agarose concentration

Based on literature by Varoni et al. the used concentration of Agarose hydrogel as biomaterial for scaffolding was 1.5%wt. When comparing this gel to Model A (Rat tail collagen 1.7mg/mL, without cells), the agarose was much stiffer (manual testing). Therefore, different concentrations (0.25%wt, 0.5%wt, 1%wt, 1.5%wt) of agarose hydrogel without cells were tested without cells to find a resembling stiffness to rat tail collagen.

An agarose hydrogel with a concentration of 1%wt mostly resembled Model A in terms of stiffness (Rat tail collagen 1.7%mg/mL).

1.2.2. Agarose 2D coating with cells

See appendix *"Different tested hydrogel scaffolds 2D"*.

Agarose hydrogel was prepared without Matrigel. A thin layer of hydrogel without cells was applied in a well of a 24wp. The layer was set to dry in an incubator, where after a layer of medium with iPSCs was added. Compared to the control (Geltrex coating), the cells adhered less well to the agarose coating. Thereby, did cells form agglomerates instead of stretched cells.

1.2.3. Agarose 3D hydrogel with cells

Agarose hydrogel scaffolds were prepared according to above instructions, and were seeded with C2C12 myoblasts. This mixture was cast into 50µL moulds and cultivated in an incubator.

The cells proliferated in the hydrogel, but did not stretch. There was no shrinkage of the hydrogel observed in the mould, which is the case with Model A Rat tail collagen. Cells died after several days and experiment was stopped.

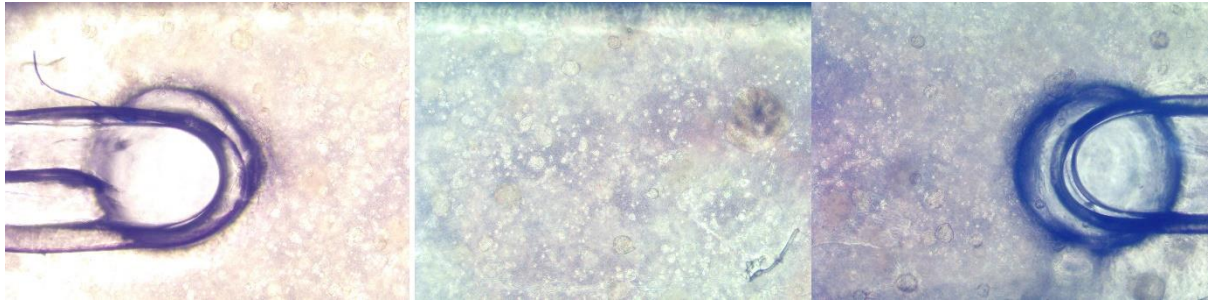


Figure 12. 50µL mould with Agarose 1%wt hydrogel and C2C12 myoblasts – Top view with assembled pictures from microscope, where the two poles are visible with hydrogel plus cells between and around poles. Experiment was at day 5 culture.

1.3. Conclusion Agarose hydrogel

A hydrogel based on agarose does not seem to be a feasible alternative to the rat tail collagen in Model A. The material is cheap, plant-based, and edible, which makes it very attractive for clean meat purposes. But the material is not easy to work with, since the gel cannot be prepared on ice, and does not seem to provide the needed properties for cell culture ECM. Further research could be done on a combination of agarose with different other materials, to increase mechanical properties.

2. Alginate

Alginate, or alginic acid, is a hydrophilic polysaccharide that is made of the cell walls of sea weed. The material is biocompatible, cheap, edible, and biodegradable.³ When dissolved in aqueous solution, it can be turned into a gel when put in contact with metal ions, such as calcium, due to the negatively charged polysaccharides. The gel is tough, rigid and well-ordered, and properties can be adjusted by adapting the alginate or calcium-solution concentration.³ The binding strength is mainly caused by the nature of the metal that is used. Alkaline earth cations form ionic bonds, while the transition metal ions form strong coordination-covalent bonds; $\text{Cu} > \text{Co}^{2+} > \text{Zn}^{2+} > \text{Mn}^{2+} \gg \text{Mg}^{2+} > \text{Ca}^{2+} > \text{Sr}^{2+}$.³ Where higher concentrations will induce an increased mechanical strength, viscosity, and degradation time. However, the quick degradation time of the gel still remains hard to control. And the pores of alginate are not optimal connected.⁴

Alginate, on its own, has low protein adsorption properties and does not enhance cell attachment. But different studies report successful experiments where an alginate hydrogel is used for muscle tissue engineering.^{5 6 7} Key in these experiments, was the combination of adhesion molecules to improve the scaffold. Rowley et al. found that skeletal myoblast proliferation and differentiation are dependent on the type of alginate and the density of the adhesion ligands presented at the surface. The adhesion ligand they used was Arginylglycylaspartic acid (RGD); a mammalian peptide sequence that is responsible for cell adhesion on the ECM, and can mimic the

³ Ali, A. & Ahmed, S. Recent Advances in Edible Polymer Based Hydrogels as a Sustainable Alternative to Conventional Polymers. J. Agric. Food Chem. 66, 6940–6967 (2018).

⁴ Pollot, B. E., Rathbone, C. R., Wenke, J. C. & Guda, T. Natural polymeric hydrogel evaluation for skeletal muscle tissue engineering. 0075, 672–679 (2017).

⁵ Rodriguez, B. L. & Larkin, L. M. Functional three-dimensional scaffolds for skeletal muscle tissue engineering. Univ. Michigan (2018). doi:10.1016/B978-0-08-100979-6.00012-4

⁶ Qazi, T. H., Mooney, D. J., Pumberger, M., Geißler, S. & Duda, G. N. Biomaterials Biomaterials based strategies for skeletal muscle tissue engineering : Existing technologies and future trends. Biomaterials 53, 502–521 (2015).

⁷ Fuoco, C., Petrilli, L. L., Cannata, S. & Gargioli, C. Matrix scaffolding for stem cell guidance toward skeletal muscle tissue engineering. J. Orthop. Surg. Res. 1–8 (2016). doi:10.1186/s13018-016-0421-y

cell adhesion functionality of fibronectin.⁸ Ansari et al. also used an RGD-coupled alginate hydrogel to create an environment for the cultivation of gingival mesenchymal stem cells for muscle tissue engineering.⁹ This combination resulted in differentiation of mesenchymal stem cells into muscle like morphological tissue. It has been found that alginate with a stiffness between 13 and 45 kPa is able to improve myoblast proliferation and differentiation, and even promote the release of growth factors.

2.1. SOP for preparation of alginate hydrogel scaffold

Most articles report a concentration of Alginate of 1-2% w/v for scaffolding for skeletal muscle tissue engineering. The follow procedure was based on work of Rowley et al., and Ansari et al.

- Prepare Alginate stock: dissolve 1.5% w/v in 0.9 NaCl (or PBS)
- Let dissolve overnight in incubator
- Dilute the stock to working solution concentration with 0.9 NaCl or PBS.
- Detach the cells from the well plate and suspend in solution
- Count the cells with cell viability marker and adjust to desired concentration
- Mix on ice the cells in solution in 50mL tube
- Mix on ice Matrigel with cells/medium
- Mix on ice Matrigel/Cells and the Alginate working solution/MEM
- Fill the moulds with the mixture and distribute by tapping the well on the table gently
- Check if the poles are well surrounded by the gel; if needed use a small pipet and manually distribute the gel around the pole
- Gently add 2mL 0.05M CaCl₂ to each well and incubate for 1 hour
- Aspirate and wash twice with PBS
- Drip gently growth medium on/in the mould of all the wells

Alginate hydrogel scaffold (1% w/v)	
Alginate working solution (1.3% w/v, in PBS)	76.5%
Minimum Essential Medium (10x)	8.5%
Matrigel	10%
Cells	5%

2.2. Alginate test results

2.2.1. Finding the ideal Alginate concentration

Based on literature by Rowley and Ansari et al., the used concentration of alginate hydrogel as biomaterial for scaffolding was 1-2%wt. When comparing 2% wt gel to Model A (Rat tail collagen 1.7mg/mL), the alginate was way stiffer (manual testing). Different concentrations (0.25%wt, 0.5%wt, 1%wt, 1.5%wt, 2%wt) of alginate hydrogel were tested without cells to find the most resembling stiffness to rat tail collagen.

Alginate hydrogel was difficult to solidify, since the CaCl was added on liquid alginate hydrogel, which disturbs the solidifying form. But Alginate with a concentration of 1%wt mostly resembled Model A (Rat tail collagen 1.7 mg/mL) in terms of stiffness.

⁸ Rowley, J. A., Mooney, D. J., Arbor, A. & Arbor, A. Alginate type and RGD density control myoblast phenotype. (2001). doi:10.1002/jbm.1287

⁹ Ansari, S. et al. Muscle tissue engineering using gingival mesenchymal stem cells encapsulated in alginate hydrogels containing multiple growth factors. 44, 1908–1920 (2017).

2.2.2. Alginate 2D coating with cells

See appendix “Different tested hydrogel scaffolds 2D”.

Alginate hydrogel was prepared without Matrigel. A thin layer of hydrogel without cells was applied in a well of a 24wp. The layer was set to solidify with 0.05M CaCl_2 , where after the supernatant was replaced by a layer of medium with iPSCs. Compared to the control (Geltrex coating), the cells adhered less well to the Alginate coating and formed agglomerates instead of stretched cells.

2.2.3. Alginate 3D hydrogel with cells

Alginate hydrogel scaffolds were prepared according to above instructions, and were seeded with C2C12 myoblasts. This mixture was cast into 50 μL moulds and cultivated in an incubator.

The cells proliferated in the hydrogel, but did not stretch. There was after a few days a quick shrinkage of the hydrogel observed in the mould, which could be related to the degradation capacity of the material. The experiment was stopped when the hydrogel scaffold detached from the poles.

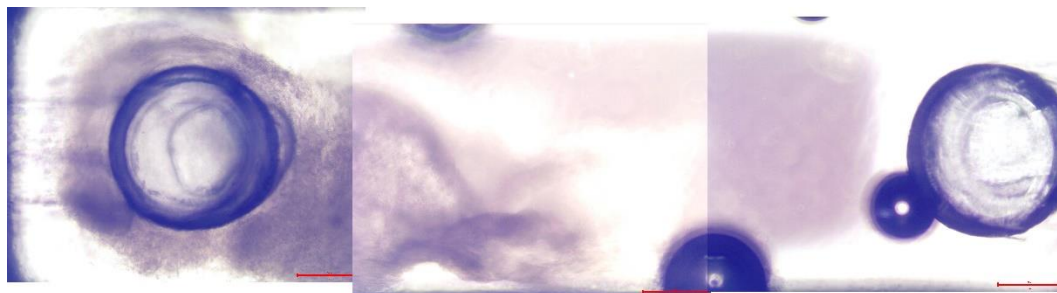


Figure 13. 50 μL mould with Alginate 1%wt hydrogel and C2C12 myoblasts – Top view with assembled pictures from microscope, where the two poles are visible with a detached hydrogel plus cells. Gel is still surrounding the left pole. Experiment was stopped at day 4 culture.

2.3. Conclusion Alginate hydrogel

A hydrogel based on alginate does not seem to be a feasible alternative to the rat tail collagen in Model A. The material is cheap, plant-based, and edible, which makes it very attractive for clean meat purposes. But the material is not easy to work with, since the gel needs to be solidified by the addition of another liquid solvent, and does not seem to provide the needed properties for cell culture ECM. The material degrades too quick. Future work could focus on the usage of different solidification liquids instead of CaCl_2 which can change the material properties. Several studies report the use of alginate as capsulate material for drops of cells.¹⁰ These techniques could be further investigated to be translated to the usage for clean meat. For example, to be used for the growth of iPSCs before seeding these in a final scaffold.

3. Noviogel

Noviogel is a commercially available improved synthetic hydrogel platform for cell studies, produced by the company Noviocell. Noviogel mechanically mimics collagen, while possessing the reproducibility and tunability of synthetic hydrogels. The porous fibrous polymer network has a stiffness that increases under applied force similar to collagen or fibrin. Noviogel is fully reversible thermo-sensitive which allows for ease of cell/tissue recovery and downstream processing after culturing. By adding peptide sequences or growth factors, the hydrogels can be readily functionalized for different cell types. The unique combination of tunable biofunctionality and biomechanics of the Noviogels makes them excellent matrices for 3D stem cell culture or

¹⁰ Ansari, S. et al. Muscle tissue engineering using gingival mesenchymal stem cells encapsulated in alginate hydrogels containing multiple growth factors. 44, 1908–1920 (2017).

regenerative medicine.¹¹

Noviogel is a new class of advanced polymers. The complex chemistry of the polymer allows the organization into a helix-like structure that is similar to the conformation of collagen, abundantly present in the extracellular matrix (structure around cells). Noviogel is an improved platform for cell studies, because it combines the unique benefits of natural and synthetic biomaterials. Noviogels uniquely perform like collagen, while possessing the same characteristics as other commercial hydrogels. Furthermore, it is fully reversible thermo sensitive, cells can be easily recovered and downstream processing after culturing is straightforward. The unique combination of tunable biofunctionality and biomechanics of the Noviogels makes them excellent matrices for 3D stem cell culture or regenerative medicine. In addition, Noviogel has a strain stiffness that increases under applied force, thereby enabling hydrogel strain stiffness modulation according to the needs of each cell type. Hereby, Noviogel creates a cellular microenvironment with the right mechanical cues to control cell expansion and differentiation.

3.1. SOP for preparation of Noviogel hydrogel scaffold

The preparation methods was according to manufacturer's inscriptions.

- Prepare Stock solutions of 5mg/mL
 - o before opening vial, let slowly reach room temperature
 - o add desired volume of COLD SOLVENT (0-4°C), shake manually
 - o incubate 3 hours at 4°C, manual shaking/swirling once every hour
 - o After 3 hours, place vial on ice and pipet gently up and down
 - o (if air bubbles; centrifuge)
 - o Prepare aliquots and store at -20°C (4 months ok).
- Prepare cell solution
 - o Detach the cells from the well plate and suspend in solution
 - o Count the cells with cell viability marker and adjust to desired concentration
- Prewarm plates and cell culture medium at 37°C
- Defreeze the gels
- Put on ice your cells, noviogel polymers and empty epps or tubes
- Mix the cells, noviogel and medium together for each of the four conditions by gently pipetting up and down on ice
- Add the hydrogel mixture to the desired mould
- Start the gelation by placing the plate for 10 minutes at 37°C
- The hydrogels with encapsulated cells have now been formed. Add gently cell culture medium
- Culture the cells at 37°C according to cultivation protocol

Noviogel	P1K	RGD1K	P5K	P5K
<i>concentration (mg/mL)</i>	<i>1</i>	<i>1</i>	<i>1</i>	<i>2.5</i>
MEM (10x)	70%	58%	58%	34%
Noviogel stock (5mg/mL)	20%	17%	17%	42%
Cells in medium	10%	25%	25%	25%

Figure 14. Overview of different Noviocell gels, where RGD1K was the only one with RGD binding peptide.

¹¹ <https://www.noviocell.com/products/noviogel-p/>

3.2. Novigel test results

3.2.1. Finding the ideal Novigel concentration

Different Novigels and novigel concentrations were delivered by the manufacturer. The different gels and concentrations were tested in 2D and in 3D as described below.

3.2.2. Novigel 2D coating with cells

See appendix *“Different tested hydrogel scaffolds 2D”*.

Best results were obtained with RGD5K (5mg/mL, where RGD1K was 1mg/mL). The coating with RGD5K had the best adherence of cells, which could be explained by the addition and increasing concentration of binding peptide. Coatings with P1K and P5K had a visible lower adherence of cells.

3.2.3. Novigel 3D hydrogel with cells

Novigel hydrogel scaffolds were prepared according to above instructions, and were seeded with iPSCs. These mixtures were cast as a drop in a 24 well plate and set to solidify in the incubator. Where after the differentiation protocol was used. Results of the different concentrations and types (P1K, P5K1, P5K2.5, and RGD1K) can be seen in Figure 15. The cells proliferated and differentiated best in the RGD1K scaffold (based on the amount of cells and agglomerates observed), which is a scaffold with RGD binding protein incorporated. But the cells did not stretch or align. The cells formed bigger agglomerates in the RGD1K hydrogel.

Hereafter, the RGD5K hydrogel was used and seeded with C2C12 myoblasts and cast in the 50uL mould inserts for 3D tissue engineering. Results can be seen in Figure 16. The cells proliferated in the hydrogel, but did merely stretch. There was no change in scaffold size after several culture days, which is expected when comparing to Model A (rat tail collagen 1.7mg/mL).

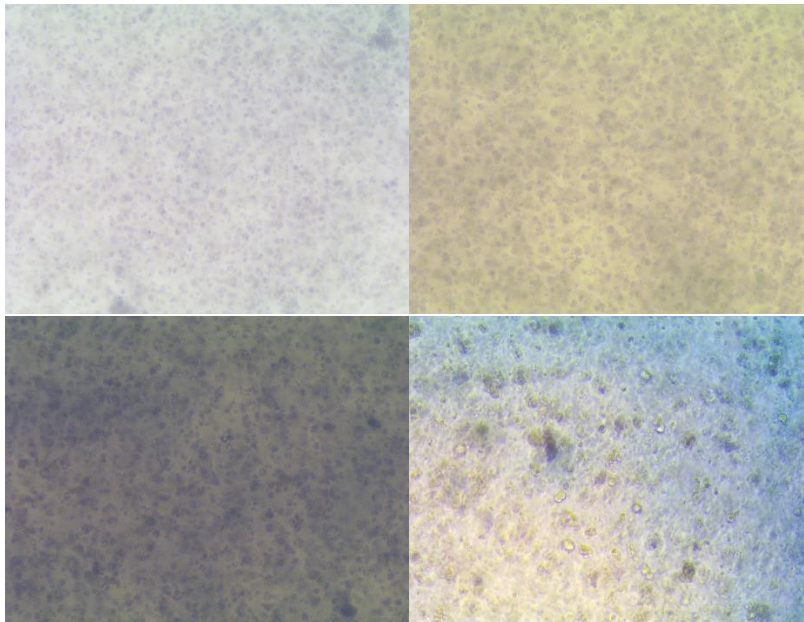


Figure 15. Upper Left: P1K hydrogel with iPSCs after 14 days culture; Upper right: P5K1; down left: P5K2.5 hydrogel with iPSCs after 14 days culture; down right: RGD1K hydrogel with iPSCs after 14 days of culture. All pictures were from 3D tissue samples.

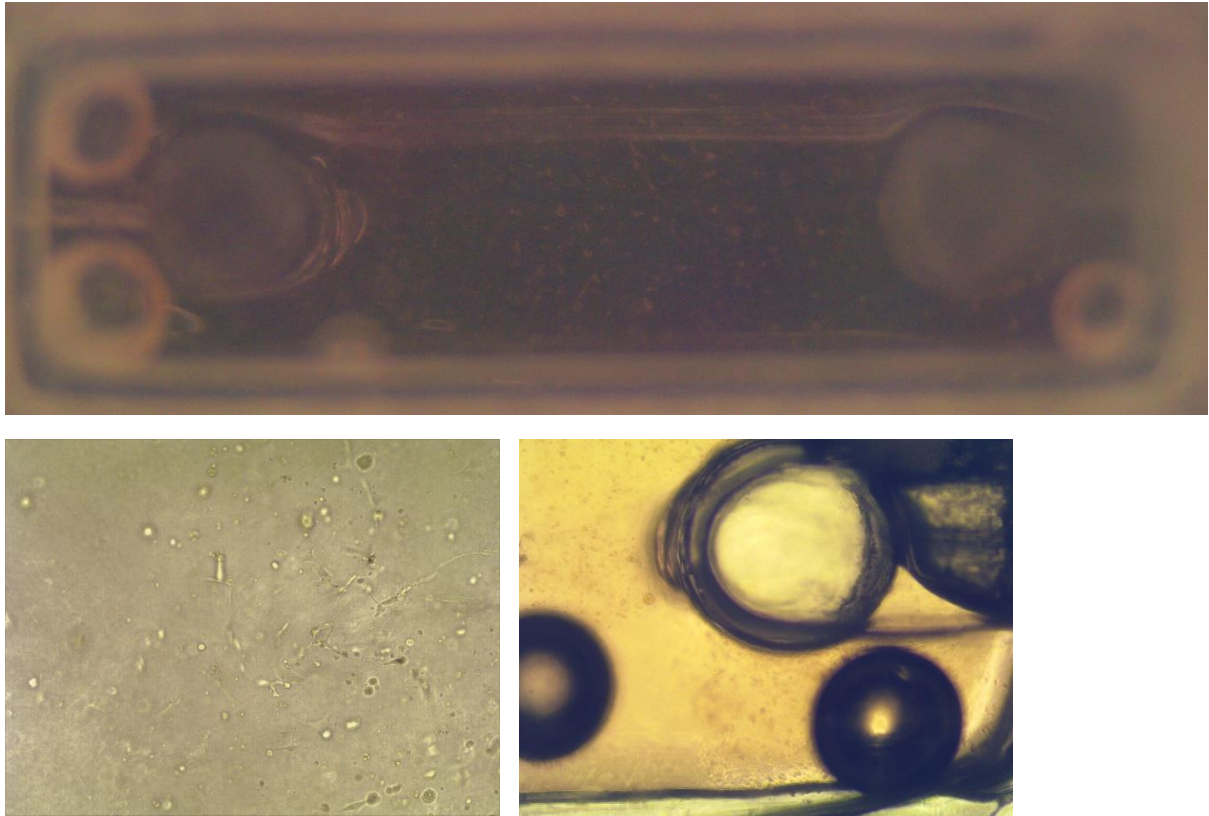


Figure 16. Top: 50uL mould with Noviolgel RGD5K hydrogel and C2C12 myoblasts, top view after 4 days of culture. Below left: detailed microscopical view of cells in hydrogel, where not much cell alignment is observed. Below right: detailed top view of the right pole from the tissue culture mould from the top picture.

3.3. Conclusion Noviolgel hydrogel

Noviolgel could be an interesting alternative for Model A since the gel is mostly synthetically produced, which means that the gel properties can be tweaked to desire. The manufacturer even claims that the gel is edible. But several adjustments should be done for better skeletal muscle tissue development. The cells seem to survive, but do not stretch much in the gel. Adding a natural binding peptide such as RGD enhances the stretching of the cells. Future research could focus on the addition of more RGD binding peptide, and the exact mechanical properties of the gel.

Appendix D.

Different tested hydrogel scaffolds in 2D

This appendix describes the different experiments that were performed to test different possible alternatives for the rat tail collagen in the Model A set-up. Through literature review, the most attractive scaffolds for 3D tissue engineering were selected. The requirements for the alternative scaffold were (preferably) animal free, cheap, scalable, and edible. Therefore, bovine collagen (animal-based), agarose (plant-based), alginate (plant-based), and Noviolgel (natural and synthetical based) were tested. The experiments in 2D performed on agarose, alginate, and Noviolgel will be reported in the following part.

1. Introduction

Initially, the reaction of iPSCs on a thin layer (400µL in a 24well plate well) of different hydrogels was tested. For this, Matrigel, which enhances cell attachment, was not mixed with the gels, so that the cell behaviour and attachment on pure hydrogels could be observed. This was compared to a thin layer of Rat tail collagen (Model A) without Matrigel and a thin layer of Geltrex (which is similar to Matrigel, and served as a positive control of cell adherence). On all thin layers, pre-differentiated iPSCs were seeded (95.000 per well) in medium suspension. The SOP for further differentiation was used. Each day, the supernatant was gently removed and replaced by fresh medium. Cells that did not adhere, were mostly removed with the medium refreshment.

2. Materials and methods

Briefly: a thin layer of 400µL hydrogel (n=3) in a 24 well plate was solidified, where after growth medium with iPSCs (95.000 per well) were added to the thin layer of hydrogel. The differentiation SOP was used and medium was thus daily refreshed.

2.1. Alginate

Make 1600µL of hydrogel:

- Prepare stock: dissolve 1.5% w/v in 0.9 NaCl (or PBS)
- Take 1512 µL alginate-NaCl-solution
- 168µL of E8 Complete Rock (without cells) mixed with 1512µL of alginate solution
- Transfer 400µL of above mixture to 3 wells of 24 well plate
- Form hydrogel by adding 1 mL 20mM BaCl₂ (or 0.1M CaCl₂) for 1 hour in incubator
- Remove the CaCl₂ and wash hydrogel twice with PBS
- Add growth medium with iPSCs

	1400 µL hydrogel
Alginate	1.5% w/v
Alginate solution	1512 µL
E8 Complete Rock	168 µL
0.1 M CaCl ₂	3 mL

2.2. Rat tail collagen

- Prewarm 24w plate at 37°C. And E8 complete Rock
- Make 1600 µL of 1.7mg/mL hydrogel:
- Dilute the rat tail collagen on ice:
 - Dilute on ice the collagen (5.05mg/mL) to 2mg/mL: 1020 µL collagen + 1530 µL AcAc
- Prepare the hydrogel mixture on ice:
 - Mix 1530 µL of type I rat tail collagen (2mg/mL) with 180 µL MEM
 - Neutralize this solution by the addition of 5 M (and when getting close, 1M) NaOH until a pink colour occurs; mix every time gently with 1mL pipette dropwise in 50mL tube
 - Add 90 µL E8 Rock and Mix by stirring the tube
 - Fill 3 wells of 24w warm chambers by pipetting 400 µL of the gel mixture in each well
 - Start the gelation by placing the plates for 10 minutes at 37°C
- Add warm medium with iPSCs and put back in incubator

concentration (mg/mL)	1.7	MEM (µL)	Collagen (µL)	E8 Complete Rock (µL)
	A	180	1530	90

2.3. Noviogel

- Prewarm plates and cell culture medium at 37°C
- Prepare 1600 µL of each hydrogel
- Defreeze the gels stock solutions
- Put on ice your noviogel polymers and empty 2mL cups
- Mix the noviogel and medium together for each of the four conditions by gently pipetting up and down on ice
- Add the hydrogel mixture to the 24 well plates
- Start the gelation by placing the plate for 10 minutes at 37°C
- Add gently cell culture medium with iPSCs
- Culture the cells at 37°C according to cultivation protocol

Noviogel	P1K	RGD1K	P5K1	P5K2.5
<i>concentration (mg/mL)</i>	<i>1</i>	<i>1</i>	<i>1</i>	<i>2.5</i>
MEM (10x)	70%	58%	58%	34%
Noviogel stock (5mg/mL)	20%	17%	17%	42%
E8 Complete Rock medium	10%	25%	25%	25%

2.4. Agarose

- Pre-warm plates to 37°C for a couple of hours or from the previous day onwards
- Pre-warm medium to 37°C
- Prepare 1600 µL of agarose hydrogel:
- agarose hydrogel stock solution:
 - Dissolve low-gelling agarose in PBS (without Ca & Mg) to a final concentration of 1.3% wt

- Heat the mixture in a microwave at 800W for around 2 min; stir every 15 seconds until everything is dissolved.
- Let mixture cool to 42°C.
- Prepare mixture:
 - Mix the MEM and Agarose working solution
- Transfer hydrogel mixture to 24 well plates
- Gelate the gel at at least 26-30°C
- Gently add warm medium with iPSCs to each well via the side of the well
- Incubate samples for the duration of the experiment at 37°C.

Agarose hydrogel thin layer (1% w/v)	
Agarose working solution (1.3% w/v, in PBS)	76.5%
Minimum Essential Medium (10x)	8.5%
E8 Complete Rock	15%

2.5. Geltrex

- Coat 3 wells with GelTrex
- Dilute the Geltrex 1:100 in chilled DMEM/F12 (e.g. 100µL in 10mL)
- Coat the surface area of your culture vessel with the Geltrex:DMEM coating solution. We recommend the follow coating volumes (circa 100µL per cm²):
 - 24w plate = 1.9cm² → 190 µL GelTrex per well (3x)
- After incubating at 37°C for 1 hour, the plate is ready to use.
- Add growth medium with iPSCs and put back in incubator.

3.1. Results and Conclusion iPSC on coatings

The experiment ran for 5 days. Due to the refreshment of supernatant medium each day, the cells that did not adhere were removed from the well. Due to this, the Noviogels P1K, P5K1, and P5K2.5 have no picture, since all cells were removed and nothing adhered.

As can be seen in Figure 17, is there on all the different remaining hydrogels some cell adherence observed and have cells proliferated. But not similar to the positive control Geltrex. Cells mainly form agglomerates that attach to the hydrogel surface. Whereas it would be more desirable to see the cells stretching.

Figure 19 shows that iPSCs have partially differentiated into myocytes (green dots with MHC staining) on the rat tail collagen coating. Especially at the borders of the cell sheets. There is no clear difference observed when comparing GelTrex or Matrigel coatings. But there are less cells adhered and less cells differentiated on the collagen coating compared to Matrigel/GelTrex.

The above indicates that the adherence properties of the different gels is not sufficient for differentiating iPSCs to myocytes. Adding Geltrex or Matrigel to the hydrogel scaffolds could enhance this property. Further research could focus on testing the hydrogels with C2C12 myoblasts, which weren't available in the laboratory at that time. These are easier to culture and have less complicated differentiation pathways.

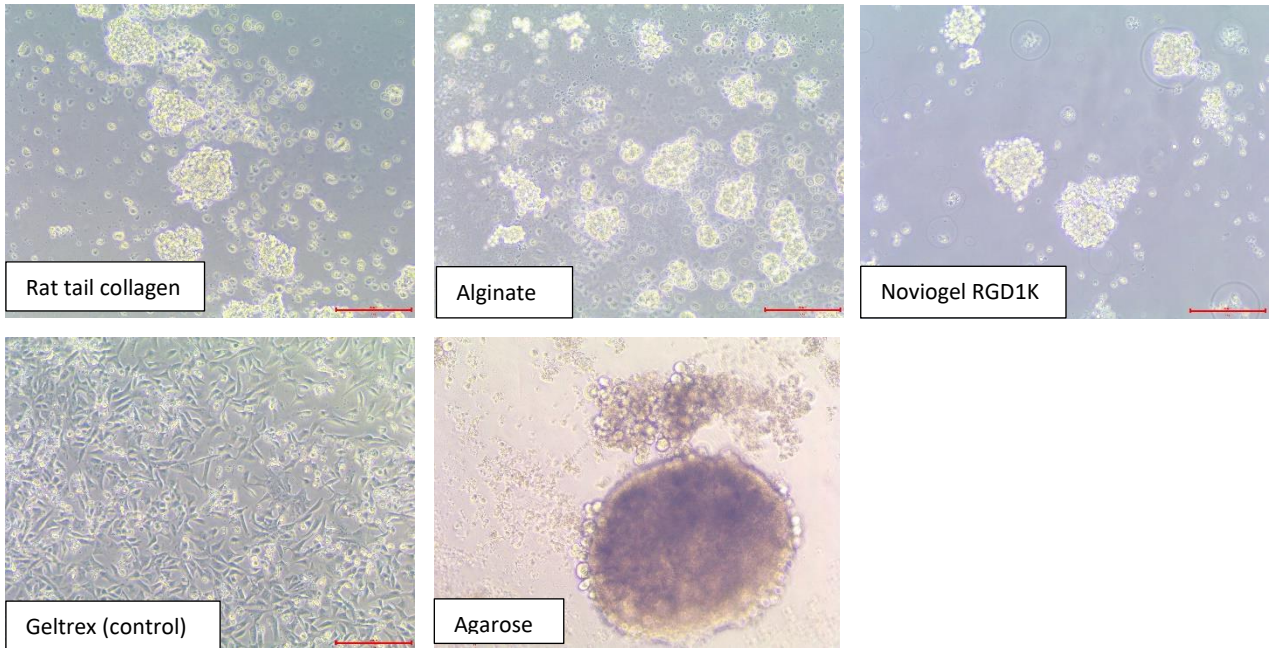


Figure 17. Microscopical pictures of adhered iPSCs to different hydrogel thin layers after 5 days of culture.

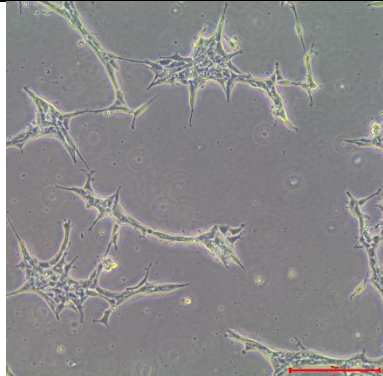

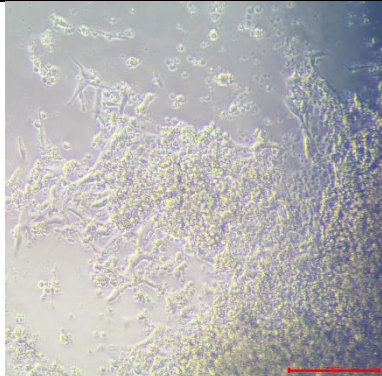
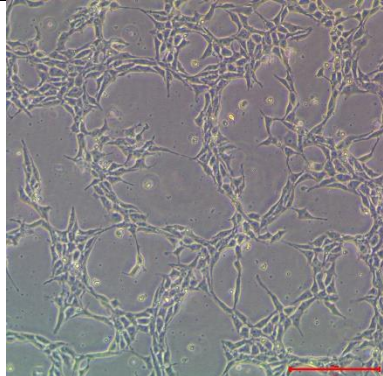

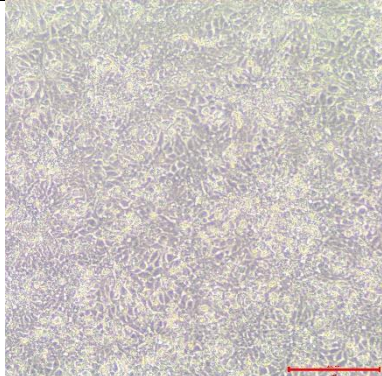
	Day 1	Day 3	Day 5
Rat tail collagen coating			
Geltrex coating (+ control)			

Figure 18. Microscopical pictures of iPSCs on a rat tail collagen and Geltrex (positive control) coating. The cells adhere well on the Geltrex coating, and seem to adhere to collagen after 24hrs of cell culture. After 5 days of culture, less adherence is observed at the collagen coating compared to the geltrex coating.

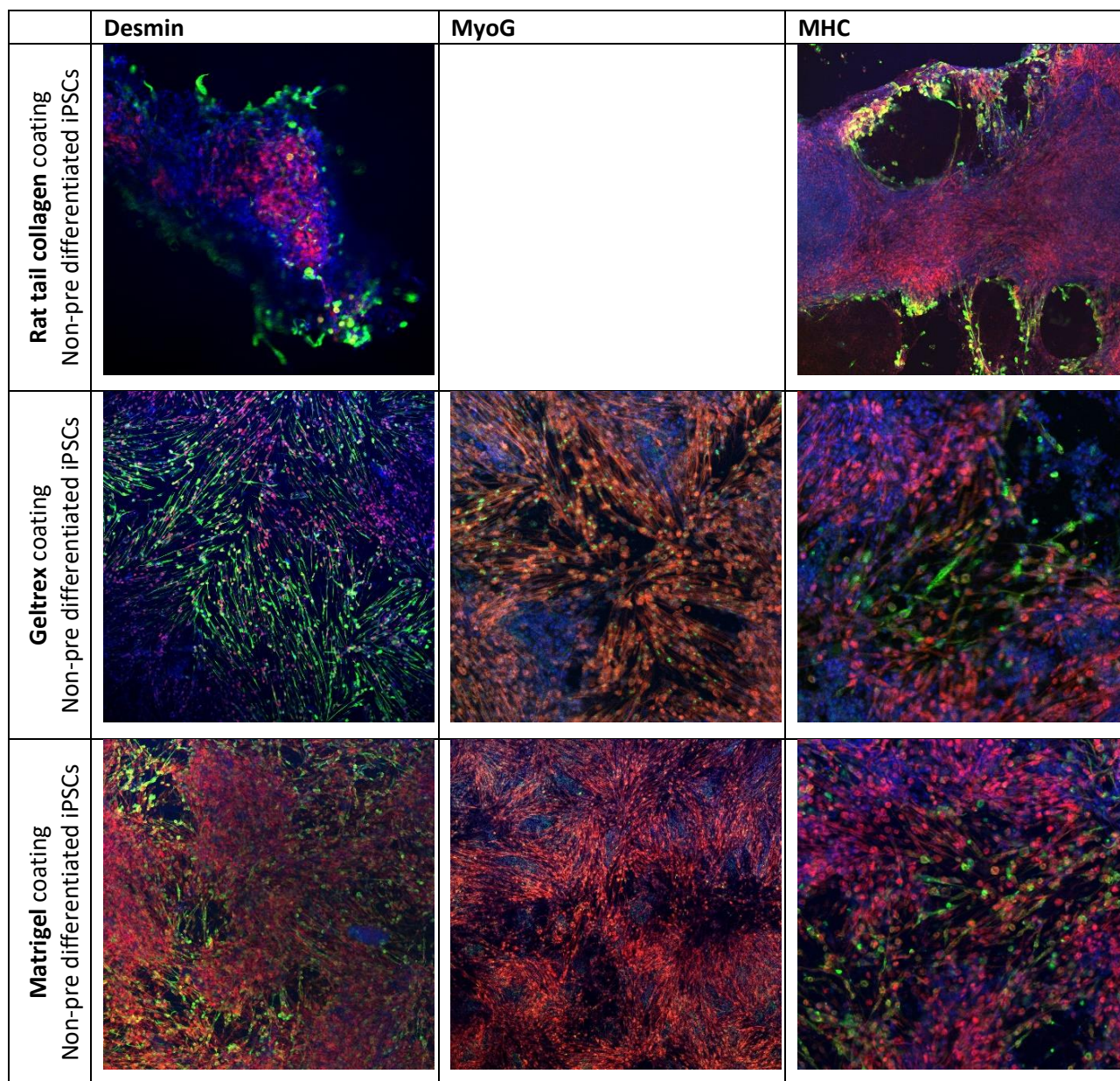


Figure 19. Immunofluorescent microscopical pictures of differentiated iPSCs on different coatings after 10 days of culture.

3.2. Results and conclusion C2C12 myoblasts on coating

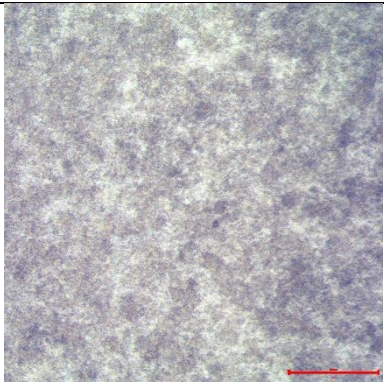
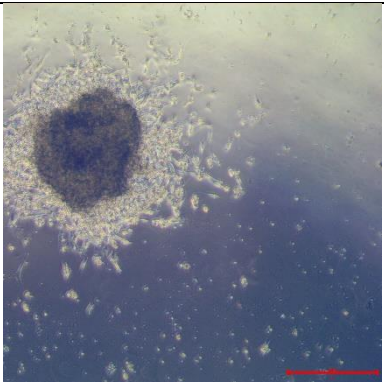
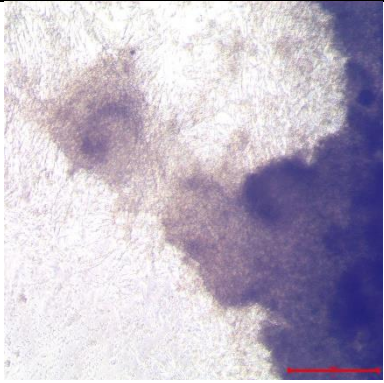
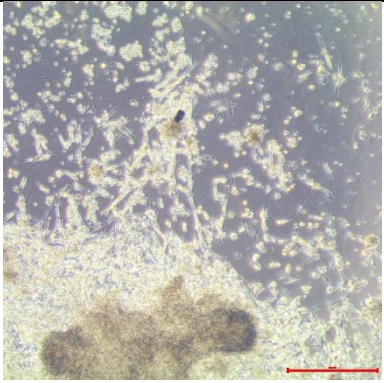
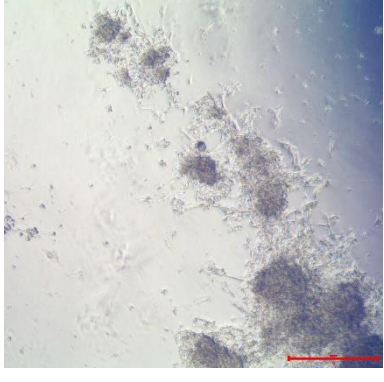
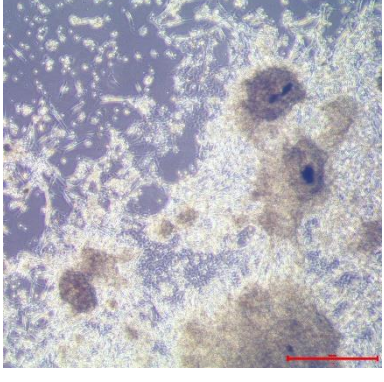
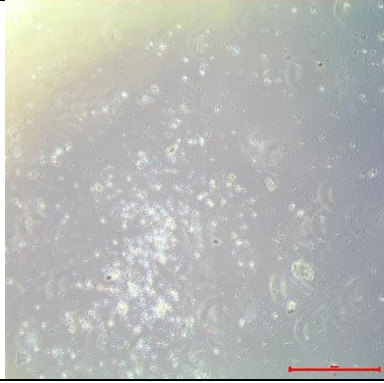
	<i>Day 5</i>		<i>Day 5</i>
<i>Matrigel coating</i>		<i>Noviogel P5K2.5 coating</i>	
<i>Rat tail collagen coating</i>		<i>Noviogel RGD1K coating</i>	
<i>Alginate (1%) coating</i>		<i>Noviogel RGD5K coating</i>	
<i>Noviogel P5K1 coating</i>			

Figure 20. Microscopical pictures of C2C12 myoblasts on different coatings after 7 days of culture.

24 well plates were coated according to above procedures, but this time seeded with C2C12 myoblasts instead of iPSCs. Thereby was the concentration of RGD in the Noviolgel increased (5x). The density of cells was increased to 150.000 cells per well, since these cells undergo less proliferation cycles with the culture protocol. After 7 days of culture according to the standard protocols, cells attached to all different coatings, but in different amounts, as can be seen in Figure 20.

No coating was as densely covered by attached cells as the Matrigel coating. The Noviolgel P5K1 had the least amount of attached cells. Best results were obtained with rat tail collagen coating, and the Noviolgel with increased RGD concentration (Noviolgel RGD5K).

Above results suggest that C2C12s adhere best to a Matrigel coating, but are also well adhering to rat tail collagen and Noviolgel with enhanced RGD peptides. Thereby, when comparing the results of Figure 20 to the results of Figure 17 and Figure 18, there could be concluded that C2C12s adhere more easily to different coatings than iPSCs. Future research should be focussed on incorporating Matrigel in Rat tail collagen, and comparing this to Noviolgel RGD5K. And on the improvement of adherence of iPSCs. Maybe, the iPSCs need to be pre-differentiated for longer time before seeding on the coating/scaffold.

Appendix E.

SOP for assembling and preparing 3D printed moulds

Following SOP is based on work of Capel et al.¹², steps 2 – 6 and 9 – 11 are performed in a fume hood.

Materials

- Ultimaker 3D printer, PLA
- PDMS
- 12 well plates
- IPA

Before starting (preparing the moulds)

1. 3D Print with PLA the desired amount of 50uL or 500uL moulds and inserts, using the CAD files from the paper by Capel et al.
2. Mix the PDMS (1:10, curing:monomer) and pour it in a 50mL tube, prepare the amount of 12w plates needed
3. Transfer a part of the PDMS into a 15mL tube (~1-2 mL PDMS / well of a 12wp), and pour very gently a small drop of PDMS into the wells, without stopping the flowing PDMS (so work quick; 2 plates at a time)
 - a. Too much and the chamber of the mould will be filled by PDMS, too little and the collagen will leak out of the chamber
4. Insert a fingertip and move the PDMS all around the bottom of the plate for an equal coating
5. Insert the moulds (check which side goes up), press on them, and turn 45degrees around (+ and – direction) several times so that the PDMS is well distributed under the moulds
6. Check if the PDMS is properly sealing the moulds by turning the plate around (moulds should stick to bottom)
7. Place the plates+moulds for 1-2 hours in a 50°C oven (or incubator for > 24hrs)
8. When PDMS is cured; plates can be stored

Prepare moulds for experiment:

9. Spray inside wells with IPA and dry in fume hood under UV light
10. When dried well; pipet 50uL DMEM in the mould (the material is hydrophobic; so it needs to get a bit more hydrophile before inserting the gel)
11. Tap plate gently on worktable so that the DMEM is well divided inside the mould between and around poles

¹² Andrew J Capel et al. “Scalable 3D printed moulds for human tissue engineered skeletal muscle”. In: Frontiers in bioengineering and biotechnology 7 (2019), p. 20.

Appendix F.

SOP for maintenance of iPSCs in adherence (2D)

1. MATERIALS AND EQUIPMENT

1.1 Equipment

Product	Catalogue number/Product ID Meatable
Biosafety cabinet	M-027; M-028; M-029
Big centrifuge	M-032
Aspirator	M-045; M-046; M-047
Inverted microscope	M-051
Countess cell counter	M-034

1.2 Reagents, chemicals and solutions

Product	Manufacturer / Supplier	Catalogue number/Product ID Meatable/SOP#
Essential 8™ Medium, E8	Thermofischer	A1517001
Gentle cell dissociation reagent GDCR	Stem cell technologies	07174
Cell adhere buffer CAD	Stem cell technologies	07183
Vitronectin	Stem cell technologies	07180
ROCK inhibitor Y-27632	helloBio	HB2297
DMSO	VWR	A3672.0050
FBS	VWR	S1300-500

1.3 Consumables

Product	Manufacturer / Supplier	Catalogue number/Product ID
6-well plates	VWR	657160
T75 flasks	VWR	658175
15ml Falcon tubes	greiner	188271
50mL falcon tubes	greiner	227261

2. SAFETY AND WORKING PRECAUTIONS

It is essential that universal precautions be taken while working with biological specimens. Appropriate personal protective equipment, including protective eyewear, gloves and a lab coat/gown, should be worn at all times, to ensure safe handling of samples.

Procedures should be conducted under strict sterile techniques, surfaces and consumables wiped with Klercide before putting them in the flow hood; hand gloves should be disinfected frequently with Klercide while working. Flow hood should be wiped with Klercide before and after work.

3. MANUALS AND REFERENCES

https://cdn.stemcell.com/media/files/manual/MADX20809-Maintenance_of_Human_Pluripotent_Stem_Cells_in_TeSR-E8.pdf?_ga=2.106221063.568342.1565002195-883818275.1558337161&_gac=1.170666388.1561445665.EAlaIQobChMI_Ziu7K6C4wIVbb7tCh0_lw1LEAAYASAAEgJsT_D_BwE

4. PROCEDURES

4.1. Extracellular matrix preparation: Vitronectin

Below the volumes necessary to coat a well of a 6-well plate are given. Adjust volumes as appropriate for experimental condition.

Aliquoting of vitronectin

1. Upon receipt, thaw the vial of vitronectin (VN) at room temperature and prepare 80, 160 and 240- μ L aliquots of vitronectin in polypropylene tubes. Freeze the aliquots at -20°C to -80°C or use immediately.

Coating procedure

1. For one well of a 6-well plate: dilute 40 μ L of VN in 960 μ L of Cell Adhere dilution buffer (CAD), add 1mL into the well. Incubate at RT, for 1h. Plates can be stored at 2–8°C wrapped in parafilm for up to 2 weeks.
2. After incubation, aspirate the coating solution, wash 1x with 1mL of CAD and add medium.
Don't let the coating dry.

4.2. Cell culture media preparation: Essential 8 Medium

1. When required, remove the E8 supplement (50x) from the freezer and thaw overnight at 2–8°C prior to use. Do not thaw at 37°C (shortens the life of the growth factors).
2. Aseptically remove 10 mL of E8 basal medium to leave 490 mL.
3. Mix the thawed supplement by gently inverting the vial a couple of times. Add 10 mL of E8 supplement (50x) to the 490 mL of E8 basal cold (2–8°C) medium. Swirl the bottle to mix and obtain 500mL of homogeneous complete medium.
4. Aliquot medium into 40mL volumes.
5. Complete E8 may be stored at 2–8°C for 1 week or at -20°C for 6 months. Frozen complete E8 may be thawed once. *Do not repeatedly freeze thaw medium. Prior to use, warm E8 to room*

temperature (not at 37°C). Do not leave medium at room temperature for longer than 2 hours per day and avoid exposure to light to avoid degradation of medium components.

4.3. Thaw and recover iPSCs (for 1x10⁶ cells)

1. Pre-warm complete Essential 8™ Medium and Vitronectin-coated 6-well plates to room temperature.
2. Add Rock inhibitor to essential 8 medium to a final concentration of 10uM.
3. Remove the vial of iPSCs from liquid nitrogen storage and quick-thaw cryopreserved iPSCs in a 37 °C water bath until only a small ice crystal remains. Remove the vial from the water bath, spray the outside of it with 70% ethanol, and place it in the hood.
4. Add 1ml of complete E8+RI to the vial and gently collect the cells into a 15mL falcon tube containing 6mL of medium.
5. Centrifuge cell suspension at 200 × g for 5 minutes. Aspirate the medium, being careful not to disturb the cell pellet. Gently resuspend the cells in 1mL Essential 8 medium supplemented with Rock inhibitor (10uM final concentration).
6. Slowly add the iPSC suspension into a pre-warmed, Vitronectin-coated 6-well plate containing 1 mL of Essential 8 Medium supplemented with Rock inhibitor (RI) per well.
7. Next day refresh into complete E8 without RI.

4.4. Passaging iPSC using GDCR

Volumes below are for a well of a 6-well plate. Adjust volumes as appropriate for experimental condition.

1. Prior to starting, have your Vitronectin-coated plate equilibrated to room temperature (1h) and pre-warm the required volume of Essential 8 medium at room temperature (1h). Add Rock inhibitor to the Essential 8 medium to a final concentration of 10uM.
2. Aspirate the medium and add 1mL of gentle cell dissociation reagent (GDCR), incubate for 4 to 8 minutes at RT (incubation times are cell line-dependent). When the cells start to separate and round up and small holes appear in the colonies aspirate the GDCR and add 1 mL of medium.
3. Lift the colonies of the plate using a cell scraper.
4. Transfer into a 15mL falcon using a 5mL serological pipette, very carefully to not break down the colonies.

5. With a P1000 pipette up and down until the colonies have the desired size (be careful to not make them too small or into single-cells). Transfer the necessary dilution into a new well (ranging from 1:10 to 1:30)
6. Refresh with 2mL of medium everyday, if for the weekend 6mL.

4.5. Freezing cells

Cells can be routinely frozen in Cryomedium: 80%KSR with 20% DMSO. Keep reagents and freezing container chilled during the cryopreservation procedure. Cells must be cryopreserved when in their log phase of growth to enhance survival upon thaw. The optimal time for harvest is normally when cells are approximately 70-80% confluent

1. Thaw and pre-chill the Cryomedium at 2°C to 8°C. Distribute 500 µl per vial. Keep chill.
2. Harvest iPSCs according to standard cell passaging protocol with GDCR (see above) but keep colonies bigger than usually.
3. If cryopreservation of more wells is desired, pool cells from different wells together.
Centrifuge harvested cells at 200 × g for 2 minutes.
4. Aspirate the medium, being careful not to disturb the cell pellet.
5. Resuspend in cryomedium (chilled to 2°C to 8 °C) adding dropwise to the cells while gently rocking the tube back and forth followed by gentle resuspension of cell pellet.
6. Distribute 500 µl per cryovial, again adding gently dropwise.
7. Cryopreserve cells in an automated or manual controlled rate freezing apparatus following standard procedures (approximately 1°C decrease per minute). Transfer frozen cell vials to liquid nitrogen (vapor phase) after 24h; *Cells can be stored in liquid nitrogen for more than 5 years.*

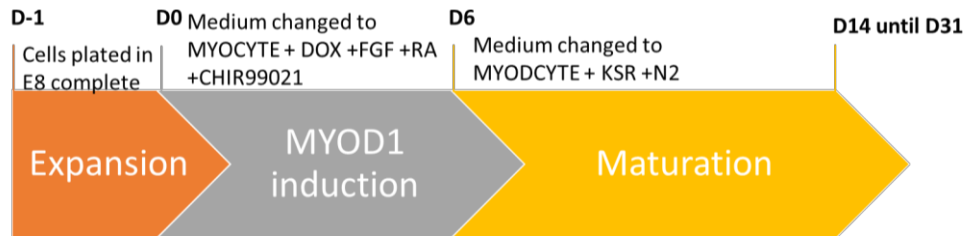
Reconstituting ROCK inhibitor:

- a. Rock inhibitor is light sensitive, avoid/minimize exposure to light
- b. Centrifuge stock vial for a few seconds to bring down powder to the bottom of the vial, spray and wipe the vial with 70% ethanol and place it in the safety cabinet.
- c. Add the appropriate volume of sterile molecular grade water to the lyophilized ROCK inhibitor to get a stock concentration of 10mM.
- d. Mix thoroughly, incubate for 3min at room temperature and aliquot into xµl aliquots.
- e. Store aliquots at -20°C and avoid repeated thawing and freezing. (-80°C stable 1year, Beers et al.)
- f. Once thawed aliquots may be kept at 4°C for a week.
 1. Add ROCK inhibitor to appropriate medium at 10uM final concentration. To obtain the required concentration dilute 10mM of stock 1:1000 in cell culture medium.

Appendix G.

SOP for the differentiation of iPSCs

1. PROCEDURES



1.1 Extracellular matrix preparation: Geltrex or Matrigel

Make sure that every material (tips, tubes, eppendorfs etc...) you use to work with Geltrex and Matrigel are chilled (keep in the fridge for minimum 1h before using).

Work on ice.

Aliquoting of Geltrex or Matrigel

1. Upon receipt, thaw the vial of Geltrex or Matrigel at 4°C and prepare 100µL aliquots in polypropylene tubes. Freeze the aliquots at -20°C to -80°C or use immediately.

Coating procedure

2. Dilute 100 µL of Geltrex or Matrigel in 10mL of chilled DMEM/F12. Incubate 1h at 37°C or 1h at room temperature (RT), for Geltrex or Matrigel, correspondently.

Coating solution	12well	6well	T25 flask	10cm dish
Geltrex:DMEM or Matrigel:DMEM	500µL	1mL	3mL	6mL

1.2 Cell counting and plating (D-1)

1. Wash cells with PBS, incubate with accutase/accumax for 5 min at 37°C. Use 0.5 mL for a well of a 6-well plate.
2. Add 0.5 mL of E8 complete. Loosen all the cells by pipetting, collect into a 15 mL falcon tube.
3. Centrifuge at 200g for 5 minutes.
4. Discard supernatant and resuspend in 1 mL of E8 complete +Ri.
5. Take out 50 µL into a 1.5 mL Eppendorf for cell count. Add 50 µL of Trypan blue. Mix well. Take 10 µL for cell count using the Countess.

- Calculate the number of cells needed to have 50000 cells/cm². Dilute the total amount of cells needed in the correspondent amount of media.
- Aspirate the coating and distribute the media+cells into the well.

1.3 Start differentiation (D0), MYOD1 induction, 24h after plating

Doxycycline and retinoic acid are very light sensitive, keep the aliquots wrapped in foil. Upon defrosting the aliquots can be used maximum for 2 weeks. Supplemented medium should be kept wrapped in foil and always warmed at RT. Medium should be prepared daily

- Prepare Myocyte medium and aliquot into 40mL aliquots. Store at -20°C.

Myocyte media	500mL
DMEM	490 mL
Glutamax (100X)	5mL
ITS	1:100 (5mL)

- Before use, defrost the medium at RT. It can be kept at 4°C for maximum 3 weeks.
- Supplement MYOD media fresh with 1µg/mL doxycycline, 3µM of CHIR99021, 1µM Retinoic acid and 40ng/mL of FGF. Prepare this fresh everyday. Change media every day from day 0 to day 5.

Myocyte media	1mL
Doxycycline	1 µl
retinoic acid	1 µl
CHIR99021	1 µl
FGF (stock 100ng/ml)	0.4µl

1.4 Maturation phase (D6)

- From D6 onward supplement MYOD medium with 10% KOSR (no doxycycline) and 1% N2. Refresh everyday until D14; if desired until D31.

Myocyte media	44,5 mL
KSR	5 mL
N2 supplement	0.5 mL

Appendix H.

SOP for immunofluorescence staining of tissue in toto

1. PROCEDURES

1.1 Fixation

1. Prepare 3.7% formaldehyde by diluting 1:10 a 37% formaldehyde solution. (for 1ml= 100µL 37%formaldehyde + 900µL PBS). *Work in the fume hood.*
2. Remove the media, wash 1x with PBS,
3. Transfer the tissue/sample using tweezers into an Eppendorf or 15ml falcon. Add enough PFA to cover the tissue. Fix for 1h at RT.
4. Collect the formaldehyde into a dedicated vessel.
5. Wash 3x with PBS. Collect into a dedicated vessel.
6. Samples can be stored in PBS at 4°C for maximum 3 months before staining.

1.2 Immunofluorescence staining

Use enough volume to completely cover the samples. Staining and washes can be performed in a 24/12-well plate and the sample moved into different wells containing different solutions or in the Eppendorf/falcon tubes, where the solutions are changed.

1. Permeabilization: incubate with 0.1% Triton in PBS, 10 min at RT
2. Wash 3x with PBS
3. Blocking: incubate with blocking solution (1%BSA in 0.05% tween-PBS), 1h at RT
4. Incubate 1st antibodies diluted in blocking, o/n at RT; for samples bigger than 50 µl, incubate for 24h.
5. Wash 3x with 0.05% tween-PBS (PBST) for 15 min.
6. Incubate 2nd antibodies diluted in blocking, 3h at RT.
7. Wash 3x with 0.05% tween-PBS (PBST) for 15 min.
8. Wash 2x with PBS
9. Incubate DAPI diluted in mQ water (1:1000) for 1h at RT.
10. Wash 1x with PBS
11. Transfer the sample into a glass slide and add enough medium to cover it. Add a rectangular glass coverslip on top and squeeze lightly. Let dry before imaging.
12. Store samples in the dark, at RT, until ready to image.

Appendix I.

Unconfined compression test of scaffold samples

1.1. Results of stress-strain test within elastic region

To ensure that the stress-relaxation tests were performed within the elastic region of the scaffolds, samples were tested under a certain strain, put back in PBS for one hour, and tested again. When the graphs would be the same, there was no plastic deformation within the scaffold which indicates that it was tested within the elastic region.¹³

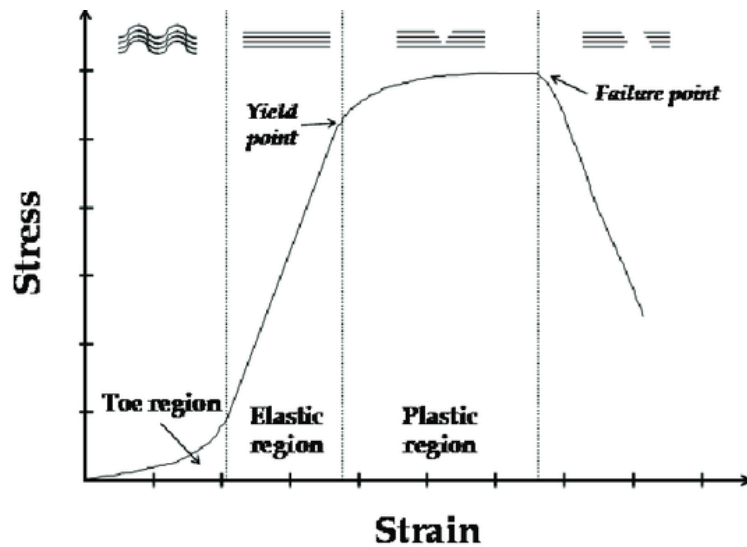


Figure 21. Stress strain curve in elastic and plastic region.

The results of the first and second round of the stress-relaxation tests on bovine and rat tail collagen samples can be found in Figure 22. The maximum stress value and the equilibrium moduli of the first and second run for both Rat tail and Bovine collagen do not differ significantly. From this can be concluded that the test was performed within the elastic region of the materials.

Type sample		Max. Stress Value (kPa)	± SD	Equilibrium modulus (kPa)	± SD
Rat tail collagen (1.7 mg/mL, fixed, Model A)	1 st run	3.225	0.42	0.034	0.01
	2 nd run	3.943	0.85	0.022	0.01
Bovine collagen (3 mg/mL, fixed, Model B)	1 st run	3.616	0.42	0.061	0.01
	2 nd run	3.984	0.78	0.046	0.01

Figure 22. Overview of 1st and 2nd round values of stress-relaxation test (n=3) of two types of scaffolds without cells. The strain was set at 10% and held for 1.5 minute.

¹³ Ochshorn et al. Material properties Stress – Strain, 2010

1.2. Pictures of experimental set-up

The tests were performed with a TA.XT compression machine (TA.XT C plus, Stable Micro Systems, UK) using a cylindric Perspex probe (P/25P, 25mm diameter, Stable Micro Systems, UK).

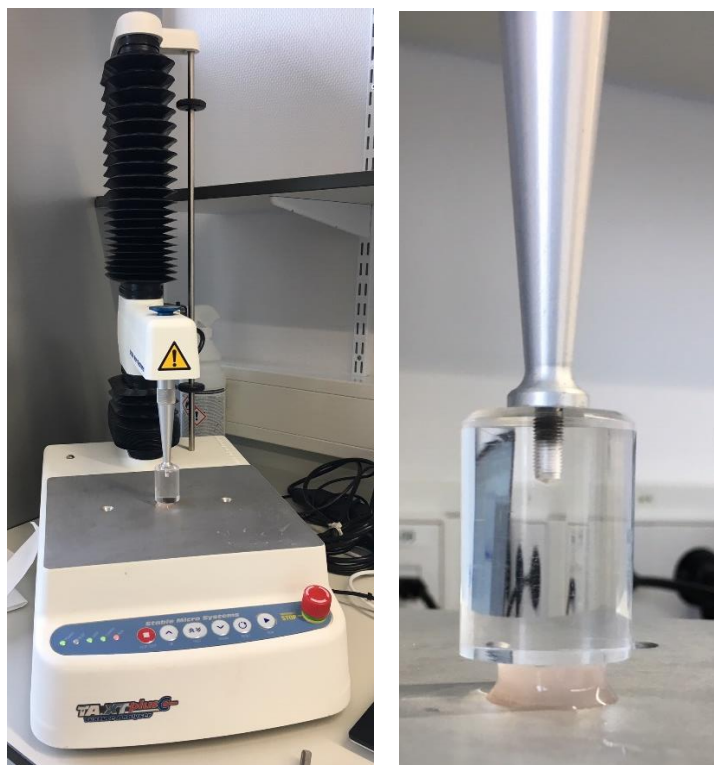


Figure 23. left; experimental set-up. right; detailed picture of hydrogel scaffold under compression.

Appendix J.

Immunofluorescence staining

1.1. Day 6 tissue samples in toto

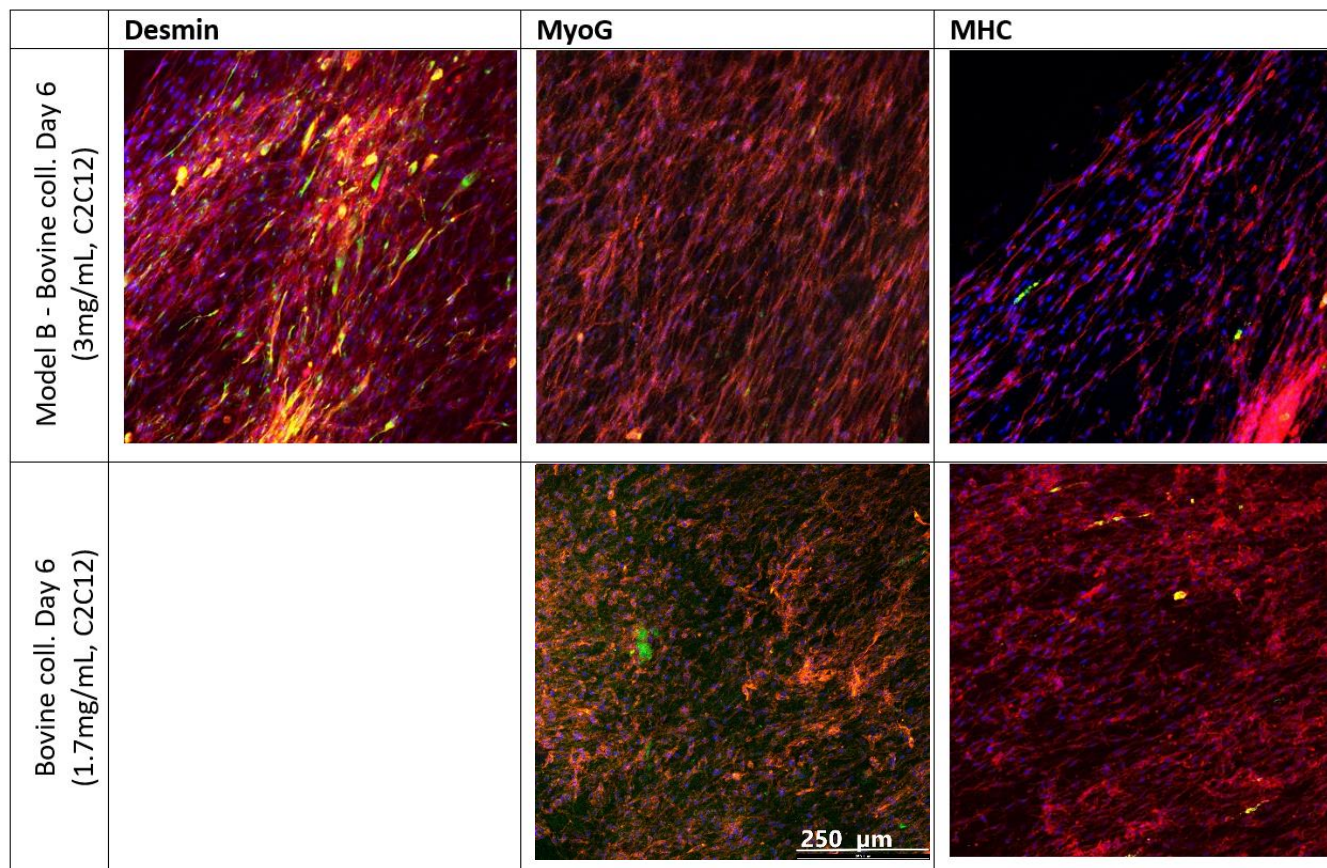


Figure 24. **Immunofluorescence staining** - structure of bioengineered skeletal muscle bundles and gene expression, visualized through immunofluorescence staining. Where nuclei are blue, actin filaments are red, and the targeted protein (Desmin/ MyoG/ MHC) is green. All sub-images are of the same scale. Confocal images of Day 6 cultured samples in 50 μ L moulds, in different hydrogel scaffolds all with C2C12 cells. All pictures are non0stacked longitudinal shots.

Results & Conclusion

The above Figure 24 shows different immunofluorescence staining pictures of two different cultured tissue samples. The upper images are from the Model B samples, where Bovine collagen (3mg/mL) was used and seeded with C2C12s. The lower set of images are from the same model, but with a lower bovine collagen concentration (1.7mg/mL). Both tissue samples were cultured for 6 days. When comparing the tissue samples from 3 mg/mL with the 1.7mg/mL samples, a difference in cell orientation and alignment can be observed. Cells grow more randomly and are less stretched in the 1.7mg/mL bovine collagen. Thereby is the expression of MyoG and MHC lower in the 1.7mg/mL scaffold. This could be explained by the lower stiffness of the scaffold (1.7 mg/mL) which is less able to transport the mechanical stiffness of the poles. The cells let the 1.7 mg/mL scaffold compact even more, which could be explained by the weakness of this scaffold and the same strength of cells.

1.2. 2D iPSC cell culture

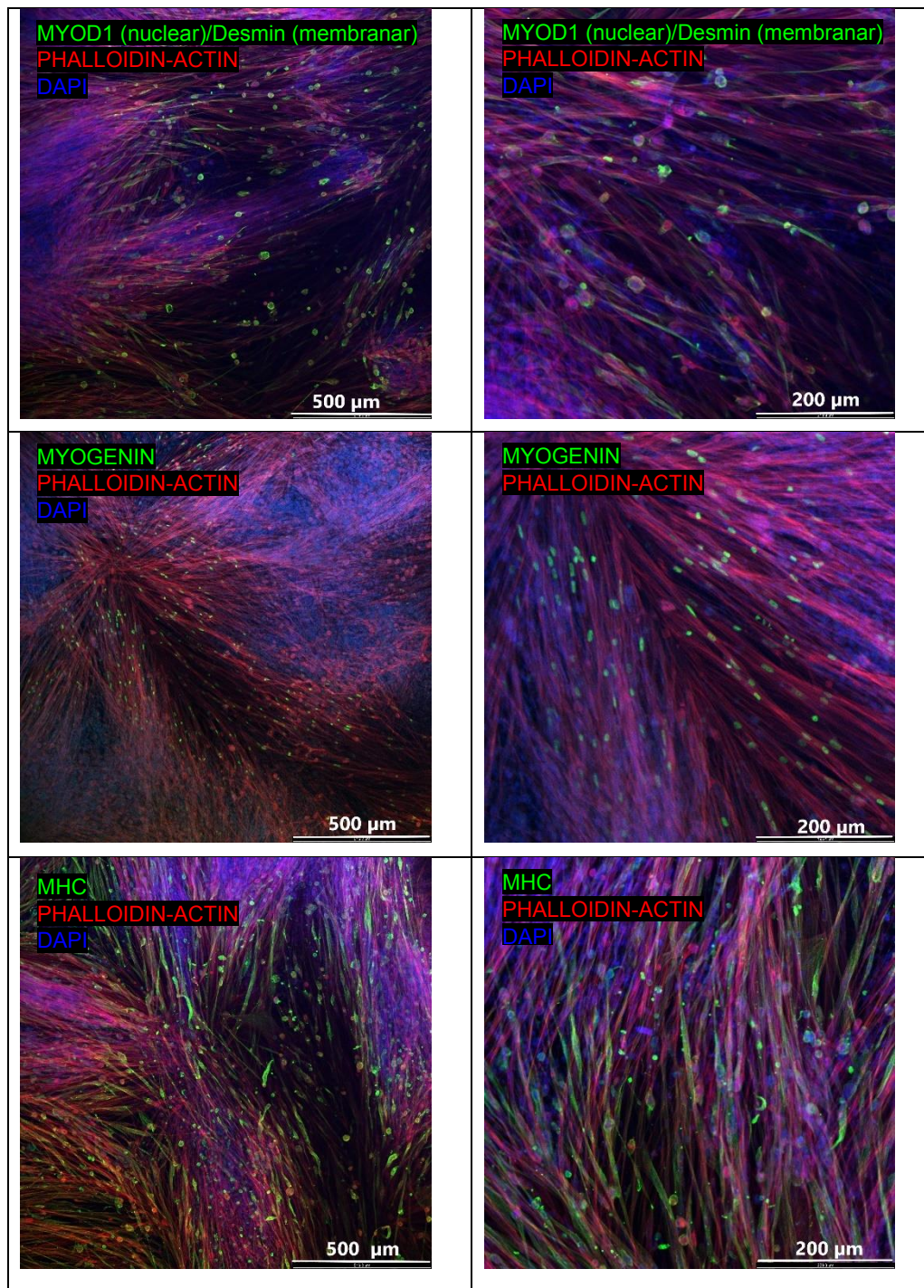


Figure 25. Immunofluorescence staining - iPSCs were differentiated according to the differentiation protocol in 2D on a Geltrex coating for 15 days to see if the techniques could be mastered.

Results & Conclusion

After 15 days of differentiation on Geltrex coating, the iPSCs have differentiated into myoblasts. The cells aligned and stretched, as can be seen from the Phalloidin-Actin (red) staining. The cells express all the three marked proteins (Desmin/ MyoG/ MHC). But the highest expression is observed when staining for MHC, which expresses later in the cell development compared to MyoG. The expression of MHC only comes up when myoblasts start fusing to become myotubes.

The differentiation protocol led to the desired differentiation of iPSCs to myoblasts.

1.3. 2D iPSC on different coatings

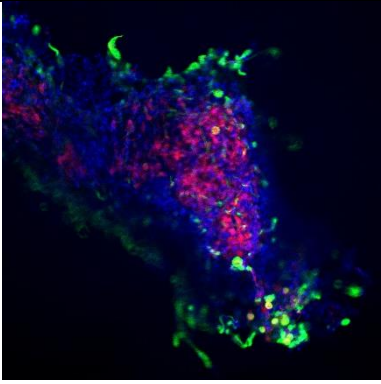

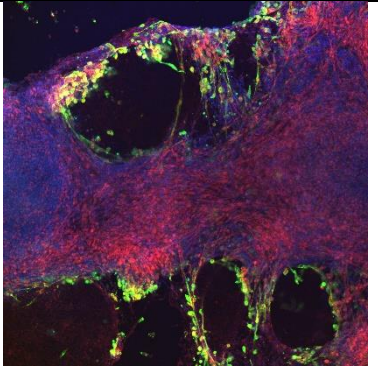
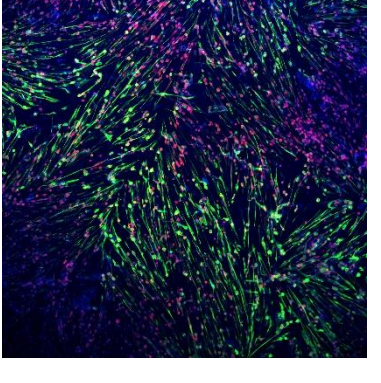
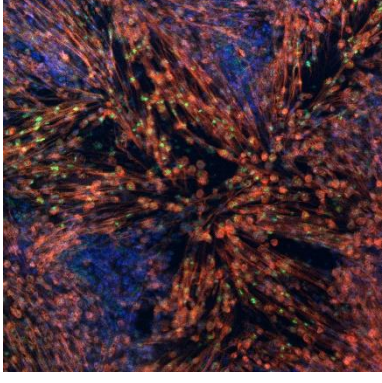
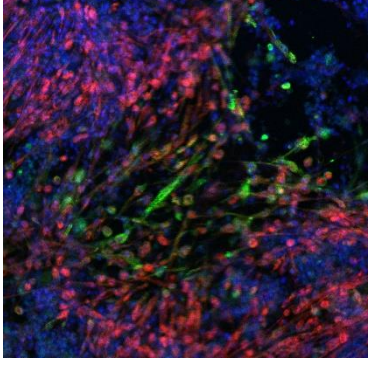
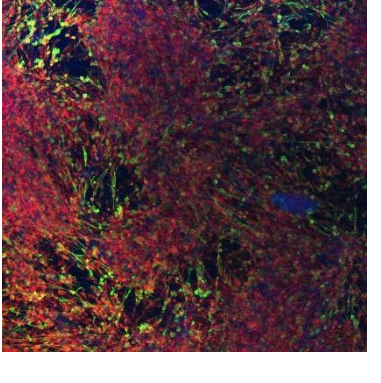
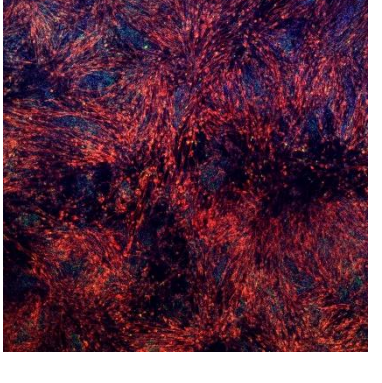
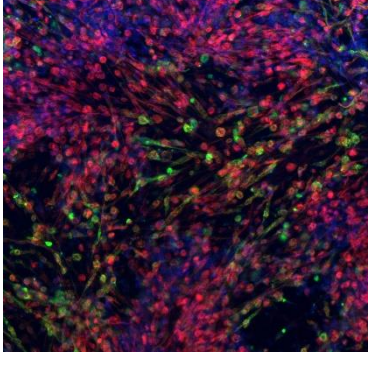
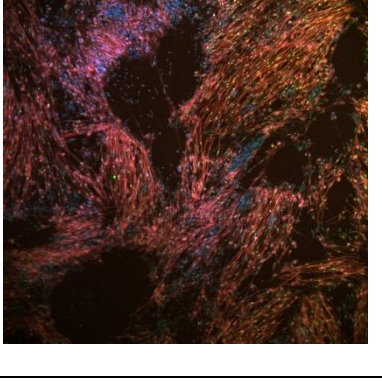
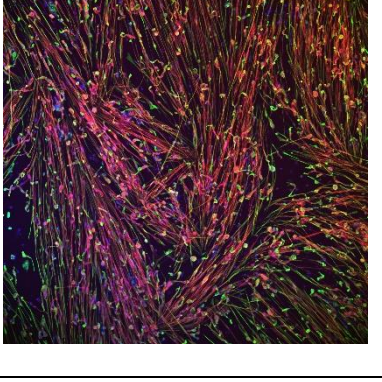
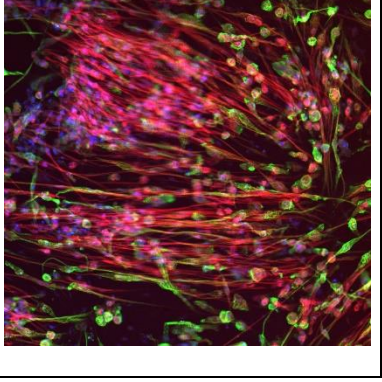
	Desmin	MyoG	MHC
Rat tail collagen coating Non-pre differentiated iPSCs			
Geltrex coating Non-pre differentiated iPSCs			
Matrigel coating Non-pre differentiated iPSCs			
Matrigel coating pre differentiated iPSCs			

Figure 26. . **Immunofluorescence staining** - structure of 2D bioengineered skeletal muscle tissue and gene expression, visualized through immunofluorescence staining. Where nuclei are blue, actin filaments are red, and the targeted protein (Desmin/ MyoG/ MHC) is green. Confocal images of Day 11 cultured (non)-pre differentiated iPSCs on different coatings.

Results

After 11 days of culture of iPSCs on Geltrex or Matrigel, there are no big differences observed in cell density, elongation, alignment and cell maturation. There are differences observed when comparing a rat tail collagen coating to geltrex and Matrigel. The cells seem to adhere less easily on Rat Tail Collagen. Thereby, is the maturation of cells (expression of MHC) mostly observed at the borders of the cell culture. The center of the cell sheets on the rat tail collagen were densely packed with layers of cells, which could influence the maturation of iPSCs, and thus the expression of MHC.

When comparing pre differentiated to non-pre differentiated cells on Matrigel, a better alignment, maturation and elongation is observed with pre-differentiated cells.

Conclusion

For the differentiation of iPSCs to myocytes, it is better to work with pre-differentiated cells, since these show better alignment, elongation and maturation. There is no significant difference in using Geltrex or Matrigel coatings. Cells do adhere better on Geltrex/Matrigel than on rat tail collagen coatings.

Appendix K.

Porosity and recovery test results

1.1. Porosity and recovery test values

	Diameter (mm)	Height (mm)	Weight after 24hrs PBS (g)	Weight after 30min drying	weight after 24hr PBS	Porosity (%)	Average Porosity	st dev	Recovery (%)	Average recovery	st dev
Bovine [3] PFA	15	8.4	1.579	0.066	1.466	95.82014	95.82014		92.84357		
Bovine [3] PFA	15	8	1.438	0.057	1.354	96.03616	96.03616		94.15855		
Bovine [3] PFA	15	8	1.494	0.063	1.41	95.78313	95.87981	0.136662	94.37751	93.79321	0.829667
Bovine [3] no PFA	15	8	1.403	0.055	0.247	96.07983			17.60513		
Bovine [3] no PFA	15	8.5	1.424	0.062	0.256	95.64607			17.97753		
Bovine [3] no PFA	15	7.5	1.36	0.058	0.255	95.73529	95.8204	0.229061	18.75	18.11089	0.583968
Rat [1.7] PFA	15	5.5	1.478	0.042	0.247	97.15832			16.71177		
Rat [1.7] PFA	15	7.5	1.19	0.032	0.208	97.31092			17.47899		
Rat [1.7] PFA	15	7.4	1.33	0.034	0.204	97.44361	97.30429	0.142759	15.33835	16.5097	1.084534
Rat[1.7] no PFA	15	7	1.198	0.122	0.76	89.81636			63.43907		
Rat[1.7] no PFA	15	8	1.355	0.121	0.704	91.07011			51.95572		
Rat[1.7] no PFA	15	8.5	1.493	0.138	0.847	90.75687	90.54778	0.652503	56.73141	57.3754	5.768695

Figure 27. Porosity test and recovery test values of fixed and non-fixed scaffolds made of Bovine collagen (3mg/mL) and rat tail collagen (1.7mg/mL).

1.2. Pictures of the porosity test

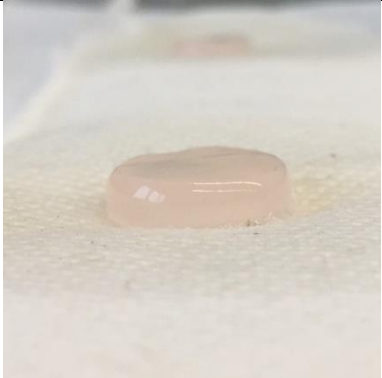
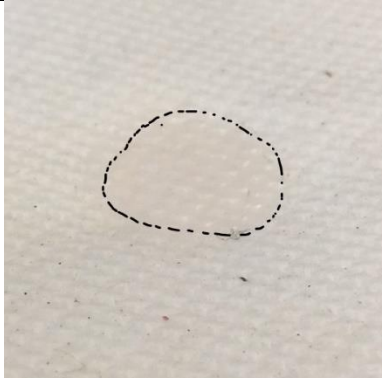






	Before dehydration	After 30min dehydration
Model A		
Rat tail collagen (1.7mg/mL) Fixed		
Rat tail collagen (1.7mg/mL) Non-fixed		
Model B		
Bovine collagen (3mg/mL) Fixed		
Bovine collagen (3mg/mL) Non-fixed		

Figure 28. Pictures of different hydrogel scaffolds before and after dehydration test - As described under Materials & Methods, the porosity of the scaffolds of Model A (base of rat tail collagen 1.7mg/mL) and Model B (base of bovine collagen 3mg/mL) measured as a percentage of weight loss after drying. The scaffolds were tested without cells.

Appendix L.

Rheometry setup and background information

Rheometry describes the strain (deformation) and flow behaviour of certain materials. Internal friction of the material and liquids can generate frictional heat and thus loss of energy. The storage modulus G' states the stored deformation energy, and the loss modulus G'' the dissipated deformation energy. Rheometry tests were performed at the DSM Food Applications and a rotational oscillation was used.



Figure 29. Rheometry measuring device with on the right a zoomed picture of the marked area where samples were placed before testing and a piece of steak placed on this area.

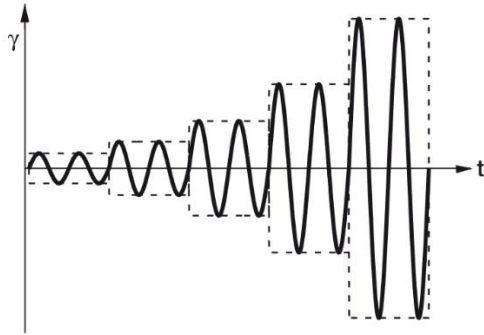


Figure 30. Amplitude sweep - An amplitude sweep describes the deformation behaviour without breaking the material.¹⁴

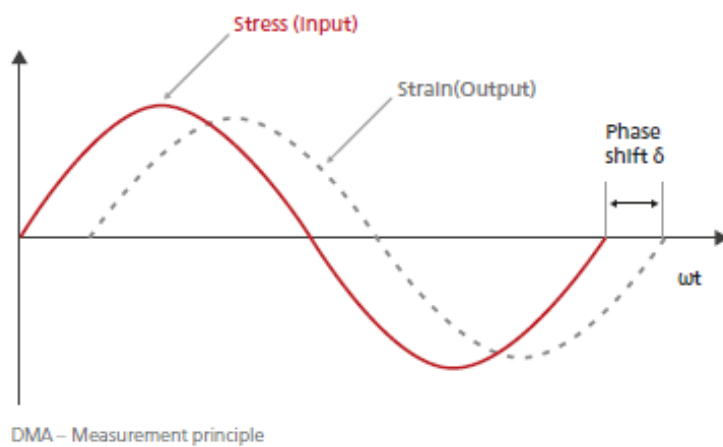


Figure 31. Measurement principle of Rheology where is visualised that the strain of the material lacks behind on the stress of the probe due to the viscoelastic behaviour of the material.¹⁵

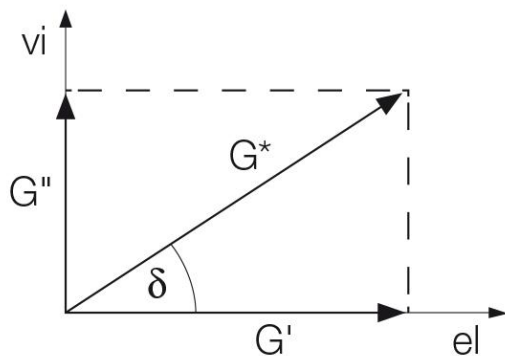


Figure 32. Dynamic Mechanical Analysis relationships – DMA uses the measured phase angle and amplitude of the signal to calculate a damping constant D . From these values, the storage and loss moduli are calculated. As the material becomes elastic, the phase angle becomes smaller, and G^* approaches G' .¹⁵

¹⁴ Anton Paar GmbH – e-learning course Basics of Rheology, 2010

¹⁵ Kevin P Menard - Dynamic Mechanical Analysis, A practical introduction – 1999